



National Library
of Canada

Bibliothèque nationale
du Canada

Canadian Theses Service

Service des thèses canadiennes

Ottawa, Canada
K1A 0N4

NOTICE

The quality of this microform is heavily dependent upon the quality of the original thesis submitted for microfilming. Every effort has been made to ensure the highest quality of reproduction possible.

If pages are missing, contact the university which granted the degree.

Some pages may have indistinct print especially if the original pages were typed with a poor typewriter ribbon or if the university sent us an inferior photocopy.

Reproduction in full or in part of this microform is governed by the Canadian Copyright Act, R.S.C. 1970, c. C-30, and subsequent amendments.

AVIS

La qualité de cette microforme dépend grandement de la qualité de la thèse soumise au microfilmage. Nous avons tout fait pour assurer une qualité supérieure de reproduction.

S'il manque des pages, veuillez communiquer avec l'université qui a conféré le grade.

La qualité d'impression de certaines pages peut laisser à désirer, surtout si les pages originales ont été dactylographiées à l'aide d'un ruban usé ou si l'université nous a fait parvenir une photocopie de qualité inférieure.

La reproduction, même partielle, de cette microforme est soumise à la Loi canadienne sur le droit d'auteur, SRC 1970, c. C-30, et ses amendements subséquents.

Control of Multiple Link Flexible Joint Robot Manipulators

Nagaratnam Rabindran

A Thesis

in

The Department

of

Electrical and Computer Engineering

**Presented in Partial Fulfilment of the Requirements
for the Degree of Master of Applied Science at
Concordia University
Montreal, Quebec, Canada**

September 1991

© Nagaratnam Rabindran, 1991



National Library
of Canada

Bibliothèque nationale
du Canada

Canadian Theses Service Service des thèses canadiennes

Ottawa, Canada
K1A 0N4

The author has granted an irrevocable non-exclusive licence allowing the National Library of Canada to reproduce, loan, distribute or sell copies of his/her thesis by any means and in any form or format, making this thesis available to interested persons.

The author retains ownership of the copyright in his/her thesis. Neither the thesis nor substantial extracts from it may be printed or otherwise reproduced without his/her permission.

L'auteur a accordé une licence irrévocable et non exclusive permettant à la Bibliothèque nationale du Canada de reproduire, prêter, distribuer ou vendre des copies de sa thèse de quelque manière et sous quelque forme que ce soit pour mettre des exemplaires de cette thèse à la disposition des personnes intéressées.

L'auteur conserve la propriété du droit d'auteur qui protège sa thèse. Ni la thèse ni des extraits substantiels de celle-ci ne doivent être imprimés ou autrement reproduits sans son autorisation.

ISBN 0-315-73689-5

Canada

ABSTRACT

Control of Multiple Link Flexible Joint Robot Manipulators

Nagaratnam Rabindran

The control problem for a robot manipulator with elastic joints is discussed. The equations of motion of the manipulator is derived based on the singular perturbation technique. This enables us to construct a reduced order "slow" subsystem of the full order model which is of the same order as the rigid model. A "fast" subsystem is then constructed to represent the effects of the fast dynamics due to joint elasticity which also represents the discrepancy between the full order model and the reduced order slow subsystem. A composite adaptive control scheme based on the reduced order slow and fast subsystem control laws is developed to robustly control the full order flexible system. Numerical comparisons between linear/ nonlinear, adaptive/ nonadaptive control strategies are included to illustrate the performance capabilities of the proposed controllers. Stability analysis of the full order system is also investigated, and bounds on the joint elasticity is obtained for robust adaptive control.

TO MY PARENTS
SAKUNTALA AND NAGARATNAM

ACKNOWLEDGEMENTS

First of all, I would like to express my thanks to my supervisor Dr. K. Khorasani, with whom I have been working for the past 2 years, and whose constant enthusiasm, friendly advise and encouragement contributed greatly to the success of my research.

I was helped by a friendly atmosphere at Concordia and for that I want to thank the graduate students with whom I interacted, with a special note to all colleagues at ER building.

My thanks are also due to T. Ramalingam, Sanjay Mazumdar and Sanjay Mawalkar for the fine hospitality shown to me during the fag end of the thesis. I am greatly indebted to my friends V. Kanthalingam, S. Amuthakumar and M. Muruganantham for providing a place to let my hair down!

Finally, I wish to thank my family, my parents, Sakuntala and Nagaratnam, and my brother, Radhakrishnan, who never ceased to encourage me.

TABLE OF CONTENTS

CHAPTER 1: INTRODUCTION	1
CHAPTER 2: DERIVATION OF SINGULAR PERTURBATION MODEL	6
CHAPTER 3: LINEAR CONTROL METHODS	19
3.a PD Nonadaptive Control Scheme for the Reduced Order System	20
3.b PD Adaptive Control Scheme for the Reduced Order System	28
CHAPTER 4: NONLINEAR CONTROL METHODS	39
4.a Feedback Linearization for the Reduced Order System	39
4.b Passivity Based Control Methods for the Reduced Order System	44
4.c Inverse Dynamics Method for the Reduced Order System	51
CHAPTER 5: NUMERICAL SIMULATION	57
5.a Reduced Order Model	57
5.b Full Order Model	69
5.c Comparison of Linear Control Methods	80
5.d Comparison of Nonlinear Control Methods	91
CHAPTER 6: STABILITY ANALYSIS OF ADAPTIVE SYSTEMS	95
6.a Slotine and Li's Scheme	96
6.b Craig, Hsu and Sastry's Scheme	106
CHAPTER 7: CONCLUSIONS AND DIRECTIONS FOR FUTURE WORK	110
7.a Conclusions	110
7.b Suggestions for Future Work	111
REFERENCES	113

LIST OF FIGURES

Figure 1	Single link manipulator with joint flexibility	12
Figure 2	Two link manipulator with joint flexibility	16
Figure 3	Linear control scheme	22
Figure 4	Alternate representation of linear control scheme	24
Figure 5	Adaptive linear control scheme	30
Figure 6	Model based control scheme	41
Figure 7	Passivity based adaptive control scheme	46
Figure 8	Inverse dynamics adaptive control scheme	53
Figure 9	The position response of the reduced order slow subsystem (single link flexible manipulator) using linear nonadaptive control of Seraji.	59
Figure 10	The position response of the reduced order slow subsystem (single link flexible manipulator) using linear nonadaptive control of Seraji. The uncertainty in the parameters is 20%.	59
Figure 11	The position response of the reduced order slow subsystem (two link flexible manipulator) using linear nonadaptive control of Seraji.	60
Figure 12	The velocity response of the reduced order slow subsystem (two link flexible manipulator) using linear nonadaptive control of Seraji.	60
Figure 13	The position response of the reduced order slow subsystem (two link flexible manipulator) using linear adaptive control of Seraji. The uncertainty in the parameters is 20%.	61
Figure 14	The velocity response of the reduced order slow subsystem (two link flexible manipulator) using linear adaptive control of Seraji. The uncertainty in the parameters is 20%.	61
Figure 15	The position response of the reduced order slow subsystem (two link flexible manipulator) using nonlinear nonadaptive controller (feedback linearization).	63
Figure 16	The velocity response of the reduced order slow subsystem (two link flexible manipulator) using nonlinear nonadaptive controller (feedback linearization).	63
Figure 17	The position response of the reduced order slow subsystem (two link flexible manipulator) using nonlinear nonadaptive controller (feedback linearization). The uncertainty in the parameters is 20%.	64
Figure 18	The velocity response of the reduced order slow subsystem (two link flexible manipulator) using nonlinear nonadaptive controller (feed-	

	back linearization). The uncertainty in the parameters is 20%.	64
Figure 19	The position response of the reduced order slow subsystem (two link flexible manipulator) using nonlinear passive adaptive control of Slotine and Li.	65
Figure 20	The velocity response of the reduced order slow subsystem (two link flexible manipulator) using nonlinear passive adaptive control of Slotine and Li.	65
Figure 21	The position response of the reduced order slow subsystem (two link flexible manipulator) using nonlinear passive adaptive control of Slotine and Li. The uncertainty in the parameters is 20%.	66
Figure 22	The velocity response of the reduced order slow subsystem (two link flexible manipulator) using nonlinear passive adaptive control of Slotine and Li. The uncertainty in the parameters is 20%.	66
Figure 23	The position response of the reduced order slow subsystem (two link flexible manipulator) using nonlinear adaptive control of Craig et al.	67
Figure 24	The velocity response of the reduced order slow subsystem (two link flexible manipulator) using nonlinear adaptive control of Craig et al.	67
Figure 25	The position response of the reduced order slow subsystem (two link flexible manipulator) using nonlinear adaptive control of Craig et al. The uncertainty in the parameters is 20%.	68
Figure 26	The velocity response of the reduced order slow subsystem (two link flexible manipulator) using nonlinear adaptive control of Craig et al. The uncertainty in the parameters is 20%.	68
Figure 27	The response of the fast variables (single link manipulator).	70
Figure 28	The position response of the full order system (two link flexible manipulator) using only the slow controller. The perturbation parameter is 0.1.	71
Figure 29	The velocity response of the full order system (two link flexible manipulator) using only the slow controller. The perturbation parameter is 0.1.	71
Figure 30	The position response of the full order system (two link flexible manipulator) using linear nonadaptive control of Seraji. The perturbation parameter is 0.1.	73
Figure 31	The velocity response of the full order system (two link flexible manipulator) using linear nonadaptive control of Seraji. The perturbation parameter is 0.1.	73
Figure 32	The position response of the full order system (single link flexible manipulator) using linear nonadaptive control of Seraji. The perturbation parameter is 0.1.	74
Figure 33	The velocity response of the full order system (single link flexible	

	manipulator) using linear nonadaptive control of Seraji. The perturbation parameter is 0.1.	74
Figure 34	The position response of the full order system (single link flexible manipulator) using linear nonadaptive control of Seraji. The perturbation parameter is 0.2.	75
Figure 35	The velocity response of the full order system (single link flexible manipulator) using linear nonadaptive control of Seraji. The perturbation parameter is 0.2.	75
Figure 36	The position response of the full order system (single link flexible manipulator) using linear nonadaptive control of Seraji. The uncertainty in the parameters is 20%. The perturbation parameter is 0.1.	76
Figure 37	The position response of the full order system (single link flexible manipulator) using linear nonadaptive control of Seraji. The uncertainty in the parameters is 20%. The perturbation parameter is 0.1.	76
Figure 38	The position response of the full order system (two link flexible manipulator) using linear adaptive control of Seraji. The perturbation parameter is 0.1.	77
Figure 39	The velocity response of the full order system (two link flexible manipulator) using linear adaptive control of Seraji. The perturbation parameter is 0.2.	77
Figure 40	The position response of the full order system (two link flexible manipulator) using linear adaptive control of Seraji. The perturbation parameter is 0.2.	78
Figure 41	The velocity response of the full order system (two link flexible manipulator) using linear adaptive control of Seraji. The perturbation parameter is 0.2.	78
Figure 42	The position response of the full order system (two link flexible manipulator) using linear adaptive control of Seraji. The uncertainty in the parameters is 20%. The perturbation parameter is 0.1.	79
Figure 43	The velocity response of the full order system (two link flexible manipulator) using linear adaptive control of Seraji. The uncertainty in the parameters is 20%. The perturbation parameter is 0.1.	79
Figure 44	The position response of the full order system (two link flexible manipulator) using nonlinear nonadaptive controller (feedback linearization). The perturbation parameter is 0.1.	81
Figure 45	The velocity response of the full order system (two link flexible manipulator) using nonlinear nonadaptive controller (feedback linearization). The perturbation parameter is 0.1.	81
Figure 46	The position response of the full order system (two link flexible	

	manipulator) using nonlinear nonadaptive controller (feedback linearization). The perturbation parameter is 0.1. The uncertainty in the parameters is 20%.	82
Figure 47	The velocity response of the full order system (two link flexible manipulator) using nonlinear nonadaptive controller (feedback linearization). The perturbation parameter is 0.1. The uncertainty in the parameters is 20%.	82
Figure 48	The position response of the full order system (two link flexible manipulator) using nonlinear nonadaptive controller (feedback linearization). The perturbation parameter is 0.2.	83
Figure 49	The velocity response of the full order system (two link flexible manipulator) using nonlinear nonadaptive controller (feedback linearization). The perturbation parameter is 0.2.	83
Figure 50	The position response of the full order system (two link flexible manipulator) using nonlinear passive adaptive control of Slotine and Li. The perturbation parameter is 0.1.	85
Figure 51	The velocity response of the full order system (two link flexible manipulator) using nonlinear passive adaptive control of Slotine and Li. The perturbation parameter is 0.1.	85
Figure 52	The position response of the full order system (two link flexible manipulator) using nonlinear passive adaptive control of Slotine and Li. The perturbation parameter is 0.1. The uncertainty in the parameters is 20%.	86
Figure 53	The velocity response of the full order system (two link flexible manipulator) using nonlinear passive adaptive control of Slotine and Li. The perturbation parameter is 0.1. The uncertainty in the parameters is 20%.	86
Figure 54	The position response of the full order system (two link flexible manipulator) using nonlinear passive adaptive control of Slotine and Li. The perturbation parameter is 0.2.	87
Figure 55	The velocity response of the full order system (two link flexible manipulator) using nonlinear passive adaptive control of Slotine and Li. The perturbation parameter is 0.2.	87
Figure 56	The position response of the full order system (two link flexible manipulator) using nonlinear adaptive control of Craig et al. The perturbation parameter is 0.1.	88
Figure 57	The velocity response of the full order system (two link flexible manipulator) using nonlinear adaptive control of Craig et al. The perturbation parameter is 0.1.	88
Figure 58	The position response of the full order system (two link flexible manipulator) using nonlinear adaptive control of Craig et al. The uncertainty in the parameters is 20%.	89
Figure 59	The velocity response of the full order system (two link flexible	

	manipulator) using nonlinear adaptive control of Craig et al. The uncertainty in the parameters is 20%.	89
Figure 60	The position response of the full order system (two link flexible manipulator) using nonlinear adaptive control of Craig et al. The perturbation parameter is 0.2.	90
Figure 61	The velocity response of the full order system (two link flexible manipulator) using nonlinear adaptive control of Craig et al. The perturbation parameter is 0.2.	90
Figure 62	The position response of the full order system (single link flexible manipulator) using nonlinear passive adaptive control of Slotine and Li. The perturbation parameter is 0.29.	92
Figure 63	The position response of the full order system (single link flexible manipulator) using nonlinear adaptive control of Craig et al. The perturbation parameter is 0.29.	92
Figure 64	The response of one of the parameter estimates for the full order system (single link flexible manipulator) using nonlinear passive adaptive control law of Slotine and Li.	93
Figure 65	Upper bounds of ϵ	103
Figure 66	Region b, $R_{\mu_m}^0$ and R_{μ_m}	105
Figure 67	Cross section of figure 66 showing region b, $R_{\mu_m}^0$ and R_{μ_m}	105

Chapter 1

Introduction

Robots used in the industry are programmable devices which manipulate and transport components in order to perform manufacturing tasks, which are physically demanding, or repetitive for human operators to perform efficiently. Manipulators have also been used extensively in hostile environments, such as nuclear power plant and waste handling, deep sea exploration and maintenance and in space. In these applications the manipulator is controlled by a remote human operator often referred to as the teleoperator. However, a control system is necessary to compute appropriate actuator commands to realize the desired motion. Continuous or intermittent feedback from the joint sensors which measure the joint angle is used to compute the required torque.

A non-sensory robot will move through approximately the same locations regardless of what is happening around it. Yet the objects on which the robot is working are not always of exactly the expected size or lie exactly in their expected positions. It is sometimes possible to cope with such uncertainties without recourse to sensors using compliance. For example consider the task of inserting a shaft into a chamfered hole- a peg-in-hole task. Even if the shaft is slightly dislocated, then a robot with compliance allows the forces between the shaft and the chamfer to deflect the end effector into the shaft. For compliance with external objects, flexibility is a desirable feature for a robot, although most robots are currently designed to be mechanically stiff and rigid because of the difficulty in controlling flexible members. It has been shown experimentally in [14] that, at least for a class of manipulators, the dominant source of compliance is due to torsional elasticity of the actuators. One of the main difficulties encountered when considering the control problem for robot manipulators with joint/ link elasticity is the mathematical

modeling. Singular perturbation, integral manifolds, feedback linearization and adaptive control are among the techniques used for modeling and control of flexible joint manipulators [6,9].

It has been shown in [13] that exact feedback linearization of the full order flexible system is not possible. The main drawback with using feedback linearization techniques is that the values of the parameters defining the actual system must be known precisely. This requirement is hardly ever satisfied in practice as parametric uncertainties can be present due to imprecise knowledge of the manipulator mass properties, unknown loads and uncertainty in the load position of the end-effector. Consequently perfect cancellations of the nonlinearities is not possible (due to imperfect modeling or inaccurate parameter estimates), which might lead to instability of the closed loop system.

Adaptive control strategies are used mainly to get over the difficulties arising from parametric and structural uncertainties that are invariably present in the actual flexible system. An advantage of the adaptive approach is that the accuracy of a manipulator carrying unknown loads improve with time as the adaptation mechanism keeps extracting parameter information from tracking errors. Since these adaptive schemes are based on rigid models, which is feedback linearizable and strictly passive, they cannot be applied directly to flexible joint manipulators which are neither feedback linearizable nor passive [6,9]. The presence of unmodeled high frequency dynamics due to joint elasticity can lead to severe stability problems for adaptive control algorithms that are designed based on models which have neglected the parasitic effects.

In this thesis using singular perturbation theory, a reduced order model of the flexible system is constructed which is indeed feedback linearizable. This facilitates the development of a composite controller [7], consisting of a slow adaptive controller based on the rigid robot model and a fast control designed to damp out the elastic oscillations at the joints. Ghorbel et al [7] use velocity feedback to provide the necessary damping of

the fast dynamics. We use state feedback controller to provide the required damping of the fast dynamics. It was found that a state feedback controller performed better than a fast adaptive controller in damping out the fast dynamics. Once the fast control law damps out the oscillations of the fast variables and the fast transients have decayed, the slow part of the system is close to the dynamics of the rigid robot, which can then be controlled by any technique. In short the controller takes the form

$$\text{composite controller} = \text{slow controller} + \text{fast controller}$$

This result is used in deriving a robust adaptive control law which takes into consideration both parametric and dynamic uncertainties keeping the overall complexity unchanged from that of a rigid control.

In this thesis, for the sake of analysis and simulation, the manipulator is modeled as set of n moving links connected in a serial chain with one end fixed on the ground and the other end free. The bodies are joined together with revolute joints with sensors incorporated in each joint to measure the position, velocity and acceleration. An actuator is provided at each joint to apply a torque on the neighboring link. The number of degrees of freedom is the number of independent joint position variables, usually equal to the number of joints. Euler- Lagrange formulation is used in modeling the dynamic behavior of the manipulator.

Comparisons between three adaptive control schemes and feedback linearization technique for a flexible joint manipulator have been presented. The first scheme is based on Seraji's [15,16] scheme. Here, the control action is generated in part by an adaptive feed forward controller which behaves as the inverse of the robot and is driven by the desired trajectory. An adaptive feedback controller and an auxiliary signal are used to enhance closed loop stability and to achieve faster adaptation. The parameters are updated according to a scheme developed based on Lyapunov stability theory.

The second scheme is based on Slotine and Li's [1,2] scheme. Though the flexible joint robot does not possess the required passivity property on which Slotine and Li's scheme is based on, the application of the composite controller reduces the full order system to a rigid system thereby allowing the passivity properties of the rigid robot dynamics to be utilized to guarantee certain desired performance specifications. This does not lead to a linear system in the closed loop even in the ideal case that all the parameters are known. The motivation for this scheme is that the regressor is independent of the joint acceleration. In [7], Slotine and Li's scheme has been applied to a single link manipulator presuming that the damping coefficients are known. We have modified the control law of Slotine and Li as it is directly not applicable to a single link manipulator as skew symmetry property does not hold in the case of a single link manipulator.

The third scheme is based on Craig et al's [4] scheme. This scheme also known as the computed torque method makes the closed loop system equivalent to a linear and decoupled controllable system even though the parameters of the robot are assumed to be unknown. This is accomplished by introducing a nonlinear controller in the feedback loop so as to cancel the nonlinear terms in the dynamic equations. A servo controller is then constructed for the linear model.

The main contents of each chapter are organized as follows:

Chapter 2 Derivation of Singular Perturbation Model

This chapter introduces the dynamical equations for a n link flexible joint manipulator. The Euler-Lagrange formulation of manipulator dynamics is given. The dynamics are then reformulated in terms of a singularly perturbed system with slow and fast dynamics. Single link and two link flexible joint manipulator examples are used to illustrate the concept of singular perturbation modeling.

Chapter 3 Linear Control Methods

This chapter introduces the basic concepts of linear control methods that are widely used in manipulator control. PD nonadaptive and adaptive control schemes based on Seraji's algorithm have been discussed. Controllers for a single link and a two link flexible joint manipulator are developed based on the schemes discussed.

Chapter 4 Nonlinear Control Methods

This chapter introduces the basic concepts of nonlinear and adaptive control methods. Feedback linearization, passivity based adaptive control methods and adaptive inverse dynamics methods have been discussed. Controllers for a single link and a two link flexible joint manipulator are developed based on the schemes discussed.

Chapter 5 Numerical Simulation

Simulation results for a single link and a two link flexible joint manipulator controlled by the algorithms described in Chapters 3 and 4 are presented in this chapter.

Chapter 6 Stability Analysis of Adaptive Schemes

Stability analysis for the two nonlinear adaptive control schemes developed in Chapter 4 are presented in this chapter.

Chapter 2

Derivation of Singular Perturbation Model

The flexible model that has been used in our study has $n+1$ rigid links connected by n flexible joints. Let q_i , $i=1,\dots,n$ denote the position of the i th link and q_{i+n} , $i=1,\dots,n$ denote the position of the i th actuator. It is assumed that the elasticity at the i th joint can be modeled as a linear torsional spring with spring constant K_i . The elastic force at the i th joint is represented by $Z_i := K_i (q_i - q_{i+n})$. When the joint is perfectly rigid, we have $q_i \equiv q_{i+n}$ for all i .

The equations of motion of the mechanical system can be derived from Euler-Lagrange equations and are defined by

$$M(\bar{q}) \ddot{\bar{q}} + h(\bar{q}, \dot{\bar{q}}) + e(\bar{q}) = P U^* \quad (2.1)$$

where $U^* = [U_1^*, \dots, U_n^*]^T$, U_i^* is the force delivered by the i th actuator,

$$\bar{q} = [\bar{q}_1, \dots, \bar{q}_{2n}]^T, e(\bar{q}) = [e_1(\bar{q}), \dots, e_{2n}(\bar{q})]^T, \quad e_i(\bar{q}) = \begin{cases} Z_i & 1 \leq i \leq n \\ -Z_{i-n} & n+1 \leq i \leq 2n \end{cases}, M(\bar{q}) \text{ is a}$$

symmetric positive definite $2n \times 2n$ inertia matrix, $h(\bar{q}, \dot{\bar{q}})$ is the vector of Coriolis, centripetal and gravitational forces and torques and $P := \begin{bmatrix} 0_{n \times n}^T & I_{n \times n}^T \end{bmatrix}^T$.

Due to the presence of joint elasticity there are now twice the number of degrees of freedom in the flexible system as compared to the rigid system. Hence there is no longer an independent control input for each degree of freedom. This means that it is not possible to cancel the nonlinearities of the system as in the computed torque scheme (described in chapter 4) for rigid robots. Moreover (2.1) does not possess the passivity properties of a rigid robot. As a result, standard control schemes in the literature cannot be directly applied to (2.1). However, when all the joints are rigid (2.1) reduces to a rigid

body equations

$$M_r(q_r) \ddot{q}_r + h_r(q_r, \dot{q}_r) = U^* \quad (2.2)$$

where $q_r = [q_1, \dots, q_n]^T$ and $M_r(q_r)$ is an $n \times n$ positive definite inertia matrix and $h_r(q_r, \dot{q}_r)$ is the vector of Coriolis, centripetal and gravitational forces.

Assuming that all the spring constants K_i are of the same order of magnitude, we can write $K_i := K \bar{K}_i$, $i=1, \dots, n$. Without loss of generality we take $\bar{K}_i = 1$ and $\mu := \frac{1}{K}$. It can be safely assumed that the joint stiffness is large relative to other parameters in the system. We realize this assumption of large joint stiffness by assuming that $K = \frac{1}{\epsilon^2}$ where ϵ is a parameter $\ll 1$. Proper scaling of parameters is essential for a successful implementation of singular perturbation technique. ϵ is therefore chosen so that the proportionality constant is in the same range as other parameters in the system- at the same time ϵ should be small enough to ensure that the settling time of the boundary layer dynamics is sufficiently rapid.

We partition matrix M and vector h as $M(\bar{q}) = \begin{bmatrix} M_1(\bar{q}) & M_2(\bar{q}) \\ M_2(\bar{q}) & M_3(\bar{q}) \end{bmatrix}$ and

$$h(\bar{q}, \dot{\bar{q}}) = \begin{bmatrix} h_1(\bar{q}, \dot{\bar{q}}) \\ h_2(\bar{q}, \dot{\bar{q}}) \end{bmatrix} \text{ where } M_i \in R^{n \times n}, i=1, \dots, 3 \text{ and } h_j \in R^n, j=1, 2. \text{ With the above}$$

definitions the equations of motion (2.1) may be written as

$$\begin{bmatrix} M_1(q, \mu Z) + M_2(q, \mu Z) \end{bmatrix} \ddot{q} - \mu M_2(q, \mu Z) \ddot{Z} + h_1(q, \dot{q}, \mu Z, \mu \dot{Z}) + Z = 0 \quad (2.3)$$

$$\begin{bmatrix} M_2(q, \mu Z) + M_3(q, \mu Z) \end{bmatrix} \ddot{q} - \mu M_3(q, \mu Z) \ddot{Z} + h_2(q, \dot{q}, \mu Z, \mu \dot{Z}) - Z = U^* \quad (2.4)$$

where $\bar{q} := \begin{bmatrix} q \\ q - \mu Z \end{bmatrix}$, $q \in R^n$ and $Z \in R^n$.

The joint displacement q are the slow variables and the elastic forces at the joints Z are the fast variables. This can be easily seen by expressing (2.3)-(2.4) in a standard state

space singularly perturbed form. We denote $M^{-1}(\bar{q})$ by $H(\bar{q})$ and write $H(\bar{q})$ as follows

$$M^{-1}(\bar{q}) = H(\bar{q}) = \begin{bmatrix} H_1(\bar{q}) & H_2(\bar{q}) \\ H_3(\bar{q}) & H_4(\bar{q}) \end{bmatrix}, \quad H_i \in R^{n \times n}, \quad i=1, \dots, 4 \quad \text{where } H_1 \text{ and } H_4 \text{ are non-}$$

singular matrices since the inertia matrix M is positive definite.

Equations (2.3)-(2.4) may be rewritten as

$$\ddot{\bar{q}} = -(H_1 h_1 + H_2 h_2) + (H_2 - H_1)Z + H_2 U^* \quad (2.5)$$

$$\mu \ddot{Z} = -((H_1 - H_3)h_1 + (H_2 - H_4)h_2) + (-H_1 + H_2 + H_3 - H_4)Z + (H_2 - H_4)U^* \quad (2.6)$$

which is in the standard singularly perturbed form. Both models (2.3)-(2.4) and (2.5)-(2.6) are well posed with respect to the perturbation parameter μ .

The rigid model is obtained by setting $\mu=0$ and by eliminating Z from (2.3)-(2.4) to give

$$(M_1 + 2M_2 + M_3)\ddot{\bar{q}} + (h_1 + h_2) = U^{*s} \quad (2.7)$$

which can also be written as

$$\ddot{\bar{q}} = (M_1 + 2M_2 + M_3)^{-1}(U^{*s} - h_1 - h_2) \quad (2.8a)$$

or from (2.5)-(2.6) by eliminating Z with $\mu=0$ to give

$$\begin{aligned} \ddot{\bar{q}} = & \left[-(H_2 - H_1)(-H_1 + H_2 + H_3 - H_4)^{-1}(H_2 - H_4) + H_2 \right] U^{*s} \\ & + \left[(H_2 - H_1)(-H_1 + H_2 + H_3 - H_4)^{-1}(H_1 - H_3) - H_1 \right] h_1 \\ & + \left[(H_2 - H_1)(-H_1 + H_2 + H_3 - H_4)^{-1}(H_2 - H_4) - H_2 \right] h_2. \end{aligned} \quad (2.8b)$$

Equations (2.5)-(2.6) represent a complex, highly nonlinear and coupled system. Given the complexity of the rigid model (2.8a) or (2.8b), the full order model (2.5)-(2.6) will not be easy to handle without simplification as far as control system design is concerned. However, the rigid model obtained from (2.5)-(2.6) does not accurately model the system if the joint flexibility is not negligible, and in fact, undesirable oscillations will occur using controllers designed based on only the rigid model.

To overcome these difficulties the full order system is broken down into two subsystems- the slow and fast subsystems. The slow subsystem is the same as the reduced order rigid model obtained earlier with $\mu = 0$ whereas the fast subsystem (to be derived later in this chapter) represents the discrepancy between the full order model and the reduced order rigid model due to the presence of joint flexibility. The lightly damped oscillations due to joint elasticity should initially be damped out by the control law designed for the fast subsystem.

The fact that the equations of motion appear as a singularly perturbed system means that standard results from singular perturbation theory can be used to derive and analyze reduced order models of (2.5)-(2.6) for which the controller design proves to be simple. We utilize the concept of composite control and choose the control input U^* of the form $U^* = U^{*s}(q, \dot{q}) + U^{*f}(\eta_1, \eta_2)$, where U^{*s} is the slow control and U^{*f} is the fast control. (η_1 and η_2 to be defined shortly). When this composite controller is applied to the full order system, the fast controller stabilizes the oscillations due to the joint flexibility thereby making the dynamics of the full order system equivalent to that of the reduced order system which can be controlled by any technique.

To this end we rewrite (2.6) in the configuration space with the transformations

$$Z^*_1 = Z \quad (2.9a)$$

and

$$Z^*_2 = \epsilon \dot{Z} \quad (2.9b)$$

to arrive at

$$\epsilon \dot{Z}^*_1 = Z^*_2 \quad (2.9c)$$

$$\epsilon \dot{Z}^*_2 = -((H_1 - H_3)h_1 + (H_2 - H_4)h_2) + (-H_1 + H_2 + H_3 - H_4)Z^*_1 + (H_2 - H_4)U^* \quad (2.9d)$$

Setting $\epsilon = 0$ in (2.9c)-(2.9d), corresponds to obtaining a "quasi steady state" (qss), for the fast variables Z^*_1 and Z^*_2 . The actual fast variables deviate from their qss values.

The difference of the fast variables from their quasi steady state is used to define new fast variables η_1 and η_2 . This is now used to represent the fast dynamics present due to torsional elasticity at the joints. We have

$$\eta_1 = \dot{Z}_1 - \dot{Z}_1^{qss}, \quad \eta_2 = \dot{Z}_2 - \dot{Z}_2^{qss} \quad (2.10)$$

or equivalently

$$\eta_1 = \dot{Z}_1 - \left[-H_1 + H_2 + H_3 - H_4 \right]^{-1} \left[((H_1 - H_3)h_1 + (H_2 - H_4)h_2) - (H_2 - H_4)U^{*s} \right] \\ \eta_2 = \dot{Z}_2 \quad (2.11)$$

where U^{*s} is the torque applied to the slow subsystem (rigid model). Computing the time derivative of η_1 and η_2 along the trajectories of the full order system (2.5)-(2.6) in the fast-time-scale $\tau = t/\epsilon$, we get

$$\frac{d\eta_1}{d\tau} = \epsilon \dot{\eta}_1 = \epsilon \dot{Z}_1 - \epsilon \frac{d}{dt}(\dot{Z}_1^{qss}) = \dot{Z}_2 - \epsilon \frac{d}{dt}(\dot{Z}_1^{qss}) = \eta_2 - \epsilon \frac{d}{dt}(\dot{Z}_1^{qss}) \quad (2.12a)$$

$$\frac{d\eta_2}{d\tau} = \epsilon \dot{\eta}_2 = -((H_1 - H_3)h_1 + (H_2 - H_4)h_2) + (-H_1 + H_2 + H_3 - H_4)\dot{Z}_1 + (H_2 - H_4)U^{*s} \\ = -((H_1 - H_3)h_1 + (H_2 - H_4)h_2) + (-H_1 + H_2 + H_3 - H_4)(\eta_1 + \dot{Z}_1^{qss}) + (H_2 - H_4)U^{*s} \quad (2.12b)$$

After simple algebraic manipulation and setting $\epsilon = 0$ in (2.12a)-(2.12b) we arrive at the fast subsystem which is expressed in the slow-time-scale

$$\epsilon \dot{\eta}_1 = \eta_2 \quad (2.13a)$$

$$\epsilon \dot{\eta}_2 = (-H_1 + H_2 + H_3 - H_4)\eta_1 + (H_2 - H_4)U^{*f}(\eta_1, \eta_2) \quad (2.13b)$$

where U^{*f} is the torque applied to the fast subsystem in order to stabilize the fast dynamics. Combining (2.13a) and (2.13b) we may alternatively express the fast subsystem as

$$\epsilon^2 \ddot{\eta}_1 + (H_1 - H_2 - H_3 + H_4)\eta_1 = (H_2 - H_4)U^{*f}(\eta_1, \eta_2). \quad (2.14)$$

For sufficiently small ϵ and shortly after $t=0$ the slow states q and \dot{q} more or less remain constant while the fast states \dot{Z}_1 and \dot{Z}_2 rapidly approach to their quasi steady states provided the fast subsystem is asymptotically stable. Therefore, we have to design

U^* such that $\eta_1 \rightarrow 0$ and $\eta_2 \rightarrow 0$ as $t \rightarrow \infty$, so that the quasi steady state is an attractive surface and the restriction of the full order system dynamics on this surface is meaningful. Consequently Z_1^* and Z_2^* approach their quasi steady states and therefore the rigid model dynamics become the dominant one.

In order to illustrate the concept of composite controller and its utility and to make comparisons between linear /nonlinear, adaptive/ nonadaptive controllers, two examples - a single link and a two link flexible joint manipulator are considered. Singular perturbation models are obtained in the next section, controllers are presented in Chapter 3 and 4 and numerical simulation results are presented in Chapter 5.

Example 1 Single link Manipulator

Refer to figure 1 for the setup and definitions of the variables. We have an actuator delivering a torque T_m to a motor shaft which is connected through a gear train to a link of length l (uniform bar), mass m and moment of inertia $1/3 ml^2$. For simplicity we model the elasticity at the joint as a linear torsional spring of stiffness K . The equations of motion are derived using Lagrangian formulation. The kinetic energy of the system is

$$KE = \frac{1}{6} ml^2 \dot{\theta}_l^2 + \frac{1}{2} J_m \dot{\theta}_m^2, \quad (2.15)$$

where J_m is the inertia of the motor. We assume that the rotor inertia is symmetric about its axis of rotation, therefore the gravitational potential is a function of only θ_l [9]. The total potential energy of the system is

$$PE = P_1(\theta_l) + P_2(\theta_l - \theta).$$

The second term in the above equation is due to the elastic potential of the spring and is given by

$$P_2 = \frac{1}{2} (\theta_l - \theta)^T K (\theta_l - \theta).$$

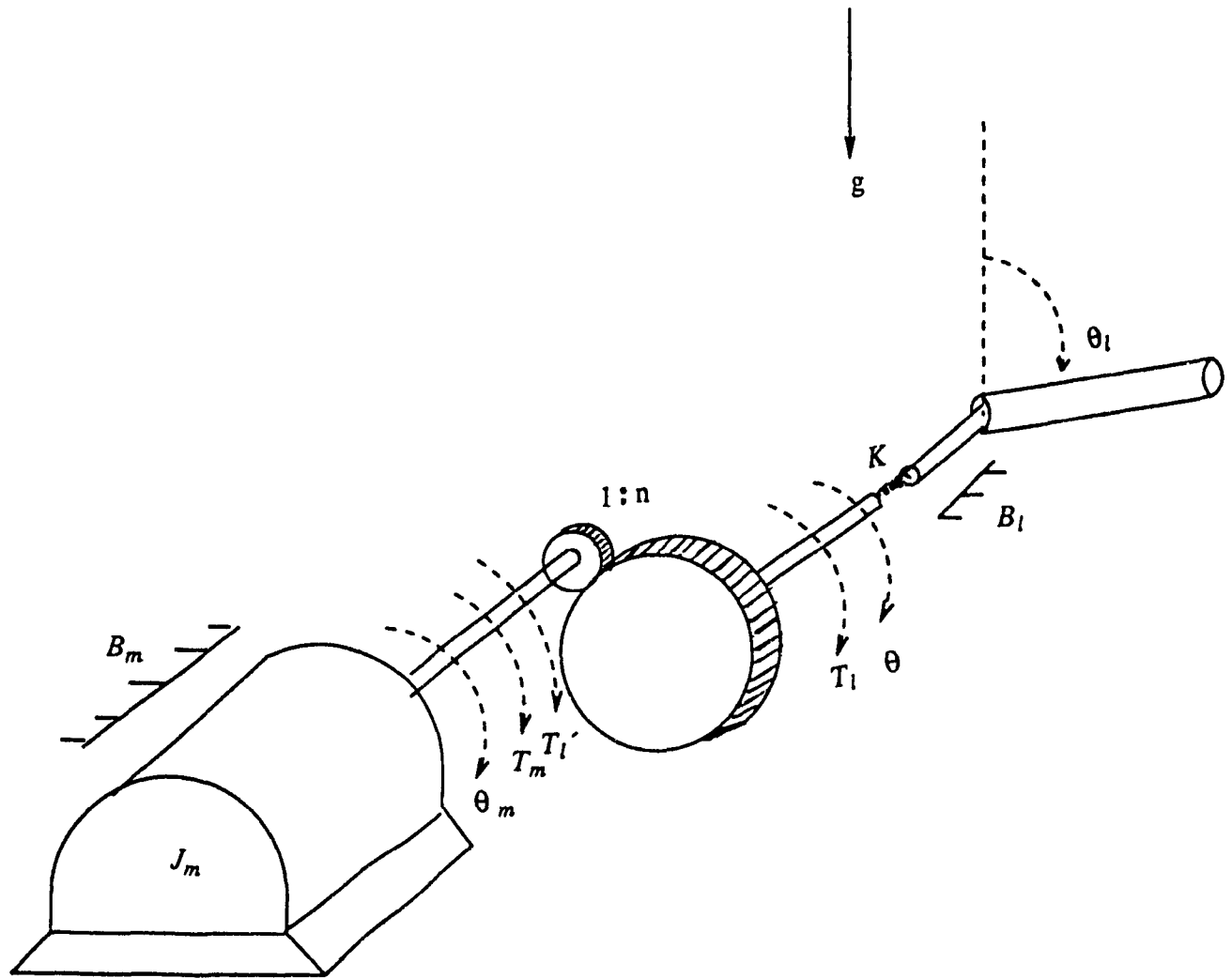


Figure 1. Single link manipulator with joint flexibility.

The Lagrangian L of the system is defined as $L = KE - PE$, which for our system becomes

$$L = \frac{1}{6}ml^2\dot{\theta}_l^2 + \frac{1}{2}J_m\dot{\theta}_m^2 + \frac{mgl}{2}(1 - \cos\theta_l) - \frac{1}{2}K(\theta_l - \theta)^2.$$

The equations of motion found from Euler-Lagrange equations are now governed by

$$\frac{1}{3}ml^2\ddot{\theta}_l + B_l\dot{\theta}_l + \frac{mgl}{2}\sin\theta_l + K(\theta_l - \theta) = 0 \quad (2.16)$$

$$J_m\ddot{\theta}_m + B_m\dot{\theta}_m = T_m + T_l', \quad (2.17)$$

where T_l' is the secondary side torque T_l of the gear mechanism (gear ratio n) reflected on the primary side and is given by

$$T_l' = -\frac{T_l}{n}, \quad T_l = K(\theta - \theta_l).$$

Incorporation of the effects of the joint elasticity renders it impossible for the application of conventional control schemes used to control rigid manipulators. However, by assuming that the joint stiffness is large a singularly perturbed model can be constructed, for which conventional control schemes may be developed through a model reduction scheme. To express the full order flexible system (2.16)-(2.17) in a standard singular perturbed form we let the elastic force at the joint be represented by

$$T_l = K(\theta_l - \theta) = Z. \quad (2.18)$$

Equations (2.16) and (2.17) may now be rewritten in terms of either θ_m and Z or θ_l and Z and using (2.18). In this thesis we choose to use θ_l and Z , as it is the link angle that one wishes to control. Letting $\epsilon^2 = 1/K$, $X_1 = \theta_l$, $X_2 = \dot{\theta}_l$, $Z_1 = Z$ and $Z_2 = \epsilon\dot{Z}_1$ and rewriting (2.16), (2.17) using (2.18) and the relationships between the primary side and secondary side of the gear mechanism, we arrive at

$$\dot{X}_1 = X_2 \quad (2.19a)$$

$$\dot{X}_2 = -3/ml^2 \left[B_l X_2 + \frac{mgl}{2} \sin X_1 + Z_1 \right] \quad (2.19b)$$

$$\epsilon \dot{Z}_1 = Z_2 \quad (2.19c)$$

$$\epsilon \dot{Z}_2 = \left[\frac{B_m}{J_m} - \frac{3B_l}{ml^2} \right] X_2 - \frac{3g \sin X_1}{2l} + \frac{T_m}{nJ_m} - \left[\frac{3}{ml^2} + \frac{1}{n^2 J_m} \right] Z_1 - \frac{B_m}{J_m} \epsilon Z_2. \quad (2.19d)$$

The rigid model or the slow subsystem is obtained by first setting $\epsilon = 0$ in (2.19c)-(2.19d) to get the quasi-steady-states

$$Z_1^{qss} = \frac{\left[\frac{B_m}{J_m} - \frac{3B_l}{ml^2} \right] X_2 - \frac{3g \sin X_1}{2l} + \frac{T_m^s}{nJ_m}}{\left[\frac{3}{ml^2} + \frac{1}{n^2 J_m} \right]}, \quad Z_2^{qss} = 0$$

which when substituted in (2.19b) and after simplification yields in the configuration space

$$\left[\frac{ml^2}{3n} + nJ_m \right] \ddot{\theta}_l + \left[nB_m + \frac{B_l}{n} \right] \dot{\theta}_l + \frac{mgl \sin \theta_l}{2n} = -T_m^s \quad (2.20)$$

where T_m^s is the torque for the slow subsystem. Note that the coefficient of T_m^s is negative as the equation is written in terms of the load side.

The fast subsystem is found by first defining a new fast variable η_1 and η_2 as the difference between the fast variables Z_1 and Z_2 from their quasi steady state values as $\eta_1 = Z_1 - Z_1^{qss}$, $\eta_2 = Z_2 - Z_2^{qss}$ and then computing their derivatives along the trajectories of the full order system to obtain

$$\epsilon^2 nJ_m \ddot{\eta}_1 + \left[\frac{3}{ml^2} + \frac{1}{n^2 J_m} \right] nJ_m \eta_1 = T_m^f \quad (2.21)$$

where T_m^f is the fast torque applied to (2.21) to stabilize the fast dynamics. The total con-

trol input is a composite controller consisting of a slow control and a fast control.

Example 2 Two link Manipulator

Refer to figure 2 for the setup and definitions of variables. The actuators are coupled to the links through linear torsional springs. The equations of motion are derived using the Euler- Lagrange formulation

$$m_{11}\ddot{q}_1 + m_{12}\ddot{q}_3 + c_{221}\dot{q}_3^2 + g_1 + K_1(q_1 - q_2) = 0 \quad (2.22a)$$

$$m_{21}\ddot{q}_1 + m_{22}\ddot{q}_3 + c_{112}\dot{q}_1^2 + g_2 + K_1(q_3 - q_4) = 0 \quad (2.22b)$$

$$n_1^2 J_1 \ddot{q}_2 - K_2(q_1 - q_2) = U_1 \quad (2.22c)$$

$$n_2^2 J_2 \ddot{q}_4 - K_2(q_3 - q_4) = U_2 \quad (2.22d)$$

where m_{ij} are the entries of the inertia matrix

$$M(q) = \begin{bmatrix} m_1 l_{c1}^2 + m_2 l_1^2 + I_1 & m_2 l_1 l_{c2} \cos(q_2 - q_1) \\ m_2 l_1 l_{c2} \cos(q_2 - q_1) & m_2 l_{c2}^2 + I_2 \end{bmatrix} \quad (2.23)$$

where m_i , I_i are the mass and moment of inertia of the i th link, l_i , l_{ci} are the length and distance to the center of mass of the i th link from the joint axis,

$$c_{221} = -m_2 l_1 l_{c2} \sin(q_2 - q_1)$$

$$c_{112} = m_2 l_1 l_{c2} \sin(q_2 - q_1)$$

$$g_1 = (m_1 l_{c1} + m_2 l_1) g \cos(q_1)$$

$$g_2 = m_2 l_{c2} g \cos(q_3)$$

g is the gravitational constant, K_i is the stiffness of the i th spring, J_i is the inertia of the actuators and n_i is the i th gear ratio. The input torque U_1 and U_2 are the control variables.

The equations of motion (2.22a)-(2.22d) may be rewritten in a singularly perturbed form of (2.3)-(2.4) by defining $\mu = \frac{1}{K_1} = \frac{1}{K_2} = \frac{1}{K}$ as the perturbation parameter and fast

variables Z_{11} and Z_{21} as $Z_{11} = K(q_1 - q_2)$ and $Z_{21} = K(q_3 - q_4)$.

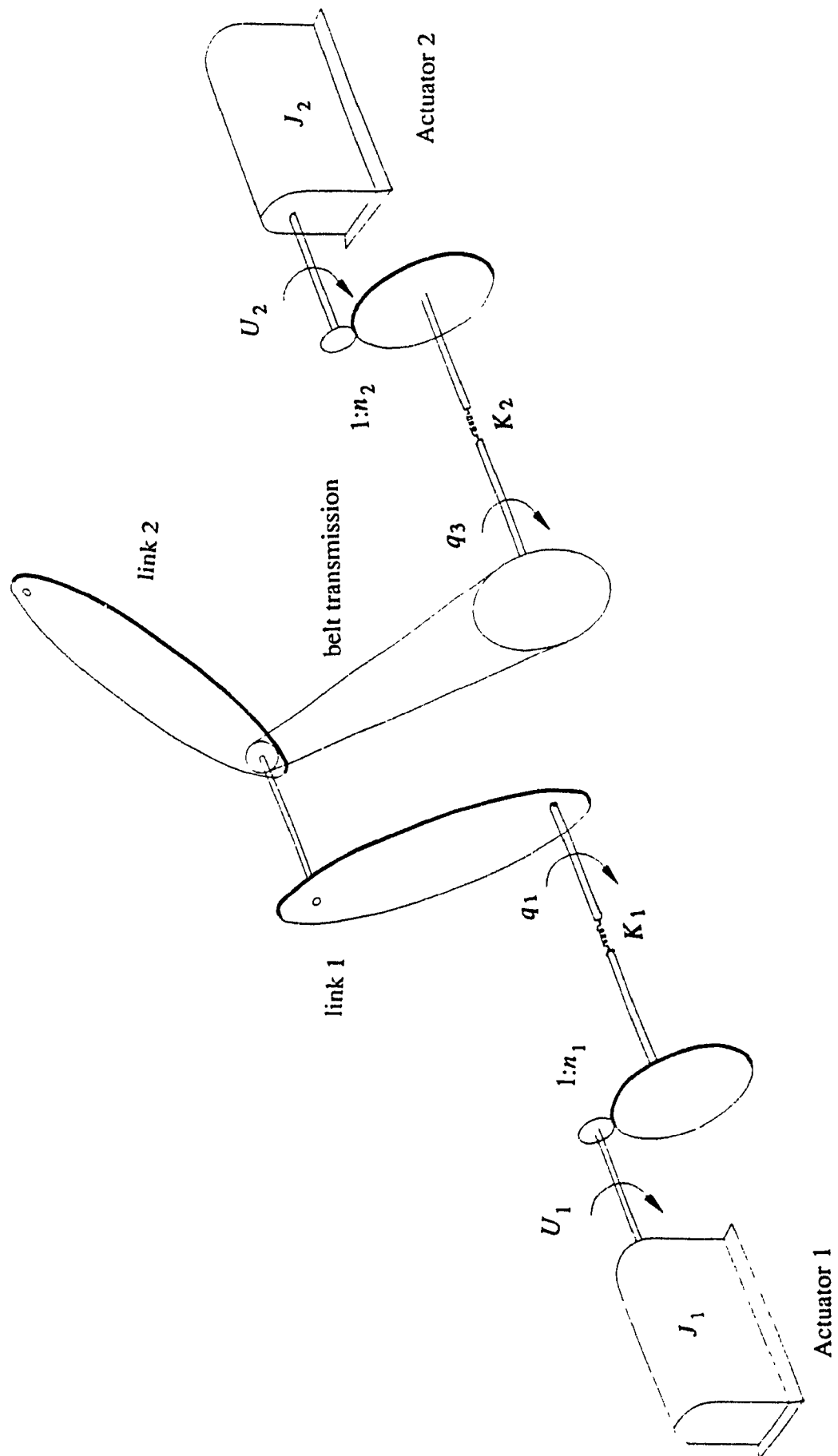


Figure 2. Two link manipulator with joint flexibility.

We get

$$\begin{bmatrix} m_{11} & m_{12} \\ m_{21} & m_{22} \end{bmatrix} \begin{bmatrix} \ddot{q}_1 \\ \ddot{q}_3 \end{bmatrix} + \begin{bmatrix} m_2 l_1 l_{c2} \sin(\mu Z_{11}) \dot{q}_3^2 + (m_1 l_{c1} + m_2 l_1) g \cos(q_1) \\ -m_2 l_1 l_{c2} \sin(\mu Z_{11}) \dot{q}_1^2 + m_2 l_{c2} g \cos(q_3) \end{bmatrix} + \begin{bmatrix} Z_{11} \\ Z_{21} \end{bmatrix} = 0 \quad (2.24)$$

$$\begin{bmatrix} n_1^2 J_1 & 0 \\ 0 & n_2^2 J_2 \end{bmatrix} \begin{bmatrix} \ddot{q}_1 \\ \ddot{q}_3 \end{bmatrix} - \mu \begin{bmatrix} n_1^2 J_1 \ddot{Z}_{11} \\ n_2^2 J_2 \ddot{Z}_{21} \end{bmatrix} - \begin{bmatrix} Z_{11} \\ Z_{21} \end{bmatrix} = \begin{bmatrix} U_1 \\ U_2 \end{bmatrix}. \quad (2.25)$$

The rigid model of the full order system is obtained by first setting $\mu = 0$ in (2.25) to get the quasi-steady states $Z_{11}^{qss} = n_1^2 J_1 \ddot{q}_1 - U_1^s$ and $Z_{21}^{qss} = n_2^2 J_2 \ddot{q}_3 - U_2^s$ which after substitution in (2.24) gives

$$\begin{bmatrix} m_{11} + n_1^2 J_1 & m_{12} \\ m_{21} & m_{22} + n_2^2 J_2 \end{bmatrix} \begin{bmatrix} \ddot{q}_1 \\ \ddot{q}_3 \end{bmatrix} + \begin{bmatrix} (m_1 l_{c1} + m_2 l_1) g \cos(q_1) \\ m_2 l_{c2} g \cos(q_3) \end{bmatrix} = \begin{bmatrix} U_1^s \\ U_2^s \end{bmatrix}. \quad (2.26)$$

The fast dynamics due to torsional elasticity at the joints is represented by the fast subsystem which is obtained by first defining new fast variables η_{11} and η_{21} , measuring the deviation of the original fast variables Z_{11} and Z_{21} from the quasi-steady states, specifically $\eta_{11} = Z_{11} - Z_{11}^{qss}$ and $\eta_{21} = Z_{21} - Z_{21}^{qss}$. Computing the time derivatives of η_{11} and η_{21} along the trajectories of the full order system (2.24)-(2.25) and defining a new fast time scale $\tau = \frac{t}{\sqrt{\mu}}$ and setting $\mu = 0$ we get

$$\frac{d^2 \eta_{11}}{d\tau^2} = \mu \frac{d^2 \eta_{11}}{dt^2} = -\eta_{11} - U_1^f(\eta_{11}) \quad (2.27)$$

$$\frac{d^2 \eta_{21}}{d\tau^2} = \mu \frac{d^2 \eta_{21}}{dt^2} = -\eta_{21} - U_2^f(\eta_{21}) \quad (2.28)$$

where U_1^f and U_2^f are the control inputs applied to the fast subsystem. The fast controls are inactive on the quasi steady state surface and are so designed that the equilibrium point $\eta_{11} = \eta_{21} = 0$ is asymptotically stable. The control input is a composite controller consisting of a slow control and a fast control.

In the next chapter, we present the basic concepts of linear control methods that have been widely used in manipulator control. PD nonadaptive and adaptive control schemes based on Seraji's algorithm are discussed. Controllers for a single link and a two link flexible joint manipulator are developed based on these schemes.

Chapter 3

Linear Control Methods

For a given nonlinear system local linearization may be employed to derive linear models which are approximations of the nonlinear equations in the neighborhood of an operating point. As the system moves the operating point is moved along and at each operating point a new linearization is performed. This results in a linear but time varying system.

Though the dynamic equations describing the manipulator motion are inherently nonlinear and highly coupled with each link exerting inertial, centripetal and Coriolis torques on all other links, linearization about an operating point presents an approximate but computationally simple solution to the manipulator control problem.

When designing a control law for the full order flexible system, the coupling effects between the slow and fast subsystems have to be included. The lightly damped oscillations due to joint elasticity should be completely damped out by the control law designed for the fast subsystem. These oscillations die at a faster rate than the rigid motion dynamics. Once these oscillations have decayed, the slow part of the system is identical to the dynamics of the rigid robot, which can be controlled by any control scheme that is discussed in the next sections.

The chosen control law for the fast subsystem is a state feedback controller designed to place the poles of the fast subsystem at desired locations in the complex plane away from the poles of the slow subsystem. The fast controller is given by

$$U^{*f} = K_{pf}\eta_1 + K_{vf}\eta_2 \quad (3.1)$$

where η_1 and η_2 are the new fast variables and K_{pf} and K_{vf} are the feedback gain constants. The subscript f denotes the fast subsystem.

A composite controller based on the reduced order slow and fast subsystem control laws is used to control the full order flexible system (2.5)-(2.6) which takes the form

$$U^* = U^{*s} + U^{*f}. \quad (3.2)$$

However the fast variables η_1 and η_2 should be expressed in terms of the original variables when the composite controller is applied to the full order system.

3.a PD Nonadaptive Control Scheme for the Reduced Order System

Here we present a simple solution to the manipulator control of the reduced order system based on linear multivariable theory. The control scheme described in [15] achieves tracking of any reference trajectory and also provides stability. The control scheme consists of multivariable feedforward and feedback controllers. The feedforward controller is the inverse of the linearized model of robot dynamics. This ensures that the manipulator joint angles track any reference trajectories. The feedback controller is of proportional-derivative (PD) type and achieves stability and pole placement.

The reduced order rigid body equation of the flexible joint manipulator is given by

$$M_r(q_r) \ddot{q}_r + h_r(q_r, \dot{q}_r) = U^{*s} \quad (3.3)$$

where $q_r = [q_1, \dots, q_n]^T$ and $M_r(q_r)$ is an $n \times n$ positive definite inertia matrix and $h_r(q_r, \dot{q}_r)$ is the vector of Coriolis, centripetal and gravitational forces. The elements of M_r and h_r are nonlinear functions of q_r and \dot{q}_r .

Suppose that the initial condition of the robot end effector corresponds to the angular position, velocity and acceleration vectors \hat{q}_r , $\dot{\hat{q}}_r$ and $\ddot{\hat{q}}_r$ in the joint space. Then the joint torque vector \hat{U}^{*s} required to produce this condition is given by (3.3) as

$$\hat{U}^{*s} = M_r(\hat{q}_r) \ddot{\hat{q}}_r + h_r(\hat{q}_r, \dot{\hat{q}}_r). \quad (3.4)$$

Let the operating point corresponding to the initial condition of the manipulator be denoted by $P = (\hat{q}_r, \dot{\hat{q}}_r)$. Now suppose that the joint torque vector is varied by ΔU^{*s} , that

is $U^{*s} = \dot{U}^{*s} + \Delta U^{*s}$, and let the resulting variations in the joint position and velocity be Q_r and \dot{Q}_r , i.e., $q_r(t) = \hat{q}_r(t) + Q_r$ and $\dot{q}_r(t) = \dot{\hat{q}}_r(t) + \dot{Q}_r$. Then assuming that the change in $M_r(q_r)$ is negligible, i.e. $M_r(\hat{q}_r + Q_r) = M_r(\hat{q}_r)$, from (3.3) we have

$$M_r(\hat{q}_r)(\ddot{\hat{q}}_r + \ddot{Q}_r) + h_r(\hat{q}_r + Q_r, \dot{\hat{q}}_r + \dot{Q}_r) = \dot{U}^{*s} + \Delta U^{*s}. \quad (3.5)$$

Expanding h_r about the operating point $P = (\hat{q}_r, \dot{\hat{q}}_r)$ using Taylor series expansion, we obtain

$$h_r(\hat{q}_r + Q_r, \dot{\hat{q}}_r + \dot{Q}_r) = h_r(\hat{q}_r, \dot{\hat{q}}_r) + \left[\frac{\partial h_r}{\partial q_r} \right]_P Q_r + \left[\frac{\partial h_r}{\partial \dot{q}_r} \right]_P \dot{Q}_r + \dots \quad (3.6)$$

When the variations Q_r and \dot{Q}_r are small, second and higher order terms in Q_r and \dot{Q}_r can be neglected in the above expansion and (3.5) can be written as

$$M_r(\hat{q}_r)\ddot{\hat{q}}_r + h_r(\hat{q}_r, \dot{\hat{q}}_r) + A\ddot{Q}_r + B\dot{Q}_r + CQ_r = \dot{U}^{*s} + \Delta U^{*s} \quad (3.7)$$

where the constant $n \times n$ matrices A , B and C are given by $A = \left[M_r(q_r) \right]_P$,

$$B_{ij} = \left[\frac{\partial h_{r_i}}{\partial \dot{q}_{r_j}} \right]_P, \quad C_{ij} = \left[\frac{\partial h_{r_i}}{\partial q_{r_j}} \right]_P. \quad \text{From (3.4) and (3.7) we obtain}$$

$$A\ddot{Q}_r + B\dot{Q}_r + CQ_r = \Delta U^{*s}. \quad (3.8)$$

Equation (3.8) gives a set of coupled linear time invariant differential equations which describe the incremental behavior of the robot dynamics for variations in the neighborhood of the operating point $P = (\hat{q}_r, \dot{\hat{q}}_r)$. The coefficient matrices appearing in the model (3.8) are dependent on the nominal operating point P . It can be shown that this linear model of the robot is both observable and controllable.

The control scheme is adopted as shown in figure 3 and consists of two separate controllers as follows:

- (1) Due to the controllability of the linear model of the manipulator, a state feedback control law may be designed to place the poles of the linear model at any desired

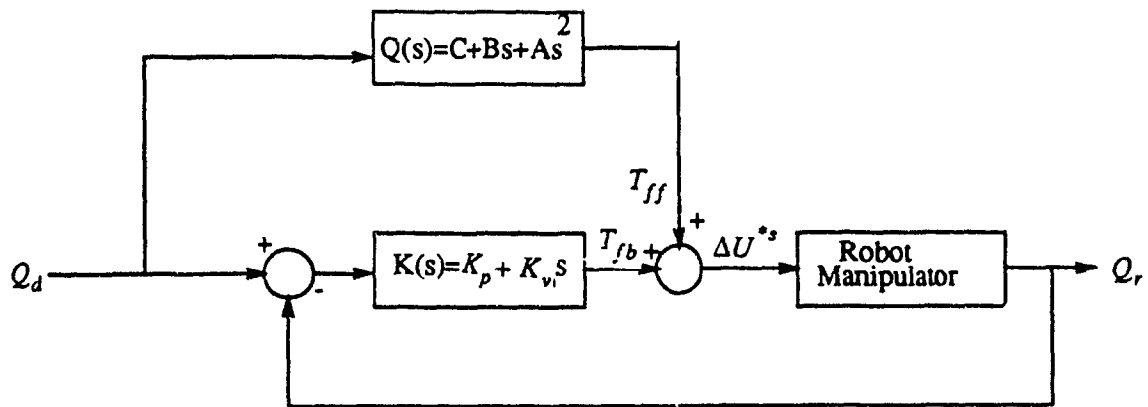


Figure 3. Linear Control Scheme.

location in the complex plane. We let the feedback controller be specified by

$$T_{fb} = K_p (Q_d(t) - Q_r(t)) + K_v (\dot{Q}_d(t) - \dot{Q}_r(t)). \quad (3.9)$$

(2) A feedforward controller is used to achieve tracking of any desired trajectory $Q_d(t)$. This controller is of the form

$$T_{ff} = A\ddot{Q}_d + B\dot{Q}_d + CQ_d. \quad (3.10)$$

Hence, the total control law is given by

$$\begin{aligned} \Delta U^{*s}(t) &= T_{fb}(t) + T_{ff}(t) \\ &= K_p(Q_d(t) - Q_r(t)) + K_v(\dot{Q}_d(t) - \dot{Q}_r(t)) + A\ddot{Q}_d(t) + B\dot{Q}_d(t) + CQ_d(t) \end{aligned} \quad (3.11)$$

which can be written as

$$\Delta U^{*s}(t) = K_p e(t) + K_v \dot{e}(t) + A\ddot{Q}_d(t) + B\dot{Q}_d(t) + CQ_d(t) \quad (3.12)$$

where $e(t) = Q_d(t) - Q_r(t)$ denotes the incremental position error in tracking. This alternate representation of the control law is shown in figure 4. Since the desired velocity $\dot{Q}_d(t)$ and acceleration $\ddot{Q}_d(t)$ and the actual velocity $\dot{Q}_r(t)$ are directly available, it is not necessary to perform numerical differentiation in order to implement the control law (3.12). When the "incremental" control law is applied to the manipulator model (3.3), the total control law is given by

$$\begin{aligned} U^{*s} &= \hat{U}^{*s} + \Delta U^{*s} \\ &= \hat{U}^{*s} + K_p e(t) + K_v \dot{e}(t) + A\ddot{Q}_d(t) + B\dot{Q}_d(t) + CQ_d(t). \end{aligned} \quad (3.13)$$

The total control law is the sum of two components- the first component is the value at the operating point P namely \hat{U}^{*s} and the second being the contribution due to incremental feedforward and feedback controllers. The total desired trajectory is $q_d = \hat{q}_d + Q_d$ and the total actual trajectory is $q_r = \hat{q}_r + Q_r$. Substituting these in (3.13) gives the total control law in terms of the total variables as

$$U^{*s} = K_p E(t) + K_v \dot{E}(t) + A\ddot{Q}_d(t) + B\dot{Q}_d(t) + CQ_d(t) + T(t) \quad (3.14)$$

where $T = \hat{U}^{*s} - K_p(\hat{q}_d - \hat{q}_r) - K_v(\dot{\hat{q}}_d - \dot{\hat{q}}_r) - A\ddot{\hat{q}}_d - B\dot{\hat{q}}_d - C\hat{q}_d$ reflects the effect of the operating point P in the total control law and $E(t) = q_d(t) - q_r(t)$.

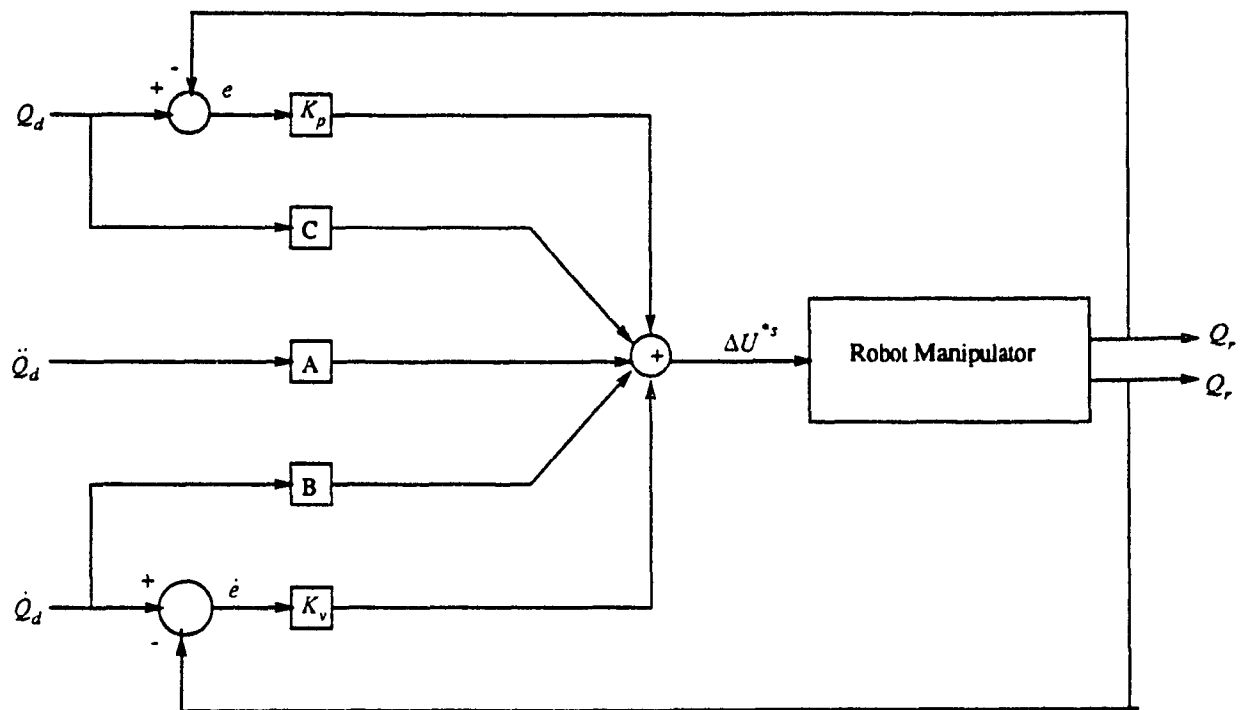


Figure 4. Alternate Representation of Linear Control Scheme.

When (3.14) is applied to the robot model given by (3.8), we obtain

$$A\ddot{Q}_r + B\dot{Q}_r + CQ_r = K_p e(t) + K_v \dot{e}(t) + A\ddot{Q}_d(t) + B\dot{Q}_d(t) + CQ_d(t).$$

This can be written as

$$A\ddot{e}(t) + (B + K_v)\dot{e}(t) + (C + K_p)e(t) = 0. \quad (3.15)$$

Equation (3.15) describes the dynamic behavior of the tracking error in terms of the feedback gains K_v and K_p . The solution of (3.15) is $e(t)=0$ for all t if the initial conditions $[Q_d(t), \dot{Q}_d(t)]$ and $[Q_r(t), \dot{Q}_r(t)]$ match exactly. However, in general the initial conditions are mismatched and $e(t)$ is a nonzero function of time. The gains K_p and K_v must be chosen in a manner that ensures the spectrum of (3.15) lie in the left half of the complex plane such that the tracking error $e(t) \rightarrow 0$ as $t \rightarrow \infty$. In fact by placing the poles at desired locations, the transient response of the tracking error can be shaped at discretion.

The feedforward controller does not affect the error characteristic polynomial. The role of T_{ff} is to ensure that the right hand side of the error differential equation (3.15) is equal to zero. If there is a mismatch between the robot model and the feedforward controller T_{ff} , (3.15) will have on its right hand side a forcing function which is a function of the desired trajectory. Therefore, the steady state value of the tracking error $e(t)$ is no longer zero but a time function of $Q_d(t)$. However, stability and transient response of $e(t)$ is unaffected by T_{ff} .

When the excursions of q_r and \dot{q}_r from the operating point $P=(\dot{q}_r, \ddot{q}_r)$ are large, it is necessary to adjust the gains of the feedforward controller T_{ff} to ensure good tracking. For this to be simple and efficient, it is assumed that $Q_r(t) = Q_d(t)$ and $\dot{Q}_r(t) = \dot{Q}_d(t)$ i.e any position and velocity errors $e(t) = Q_d(t) - Q_r(t)$ and $\dot{e}(t) = \dot{Q}_d(t) - \dot{Q}_r(t)$ are reduced to zero sufficiently fast by the feedback controller. Thus the gains A, B and C of the feedforward controller are evaluated on the basis of the desired trajectories instead of the actual trajectories $Q_r(t)$ and $\dot{Q}_r(t)$ and depend only on $Q_d(t)$ and $\dot{Q}_d(t)$ which are known in advance.

Suppose that the robot is required to track a preplanned position and velocity trajectory $q_d(t)$ and $\dot{q}_d(t)$ in time t_e . We discretize t_e into N instants of time $[t_1, \dots, t_N]$, which may or may not be equally spaced and are chosen on the basis of $q_d(t)$ and $\dot{q}_d(t)$. At each time $t = t_i$, the values of the desired position and velocity vectors are given by $Q_d(t_i)$ and $\dot{Q}_d(t_i)$ and are represented by the operating point $P_i = [Q_d(t_i), \dot{Q}_d(t_i)]$. At each P_i , a unique linear model with parameters $[A_i, B_i, C_i]$ describes the behavior of the manipulator and for each linear model, a particular feedforward controller is required for trajectory tracking.

Although the feedback controller can also be updated as the operating point P changes with time, this is not necessary for moderate excursions of P especially if it has been designed such that the poles are well inside the left half plane. This is justified by the fact that the feedback controller only determines the stability and transient response of the tracking error. As long as stability is ensured by proper placement of the poles, the error transient will eventually tend to zero as desired. However, when excessive excursions of the operating point P occurs, it is advisable to update the feedback controller gains to ensure stability and acceptable transient response.

The above control scheme is now developed for a single link and a two link flexible joint manipulator.

Example 1 Single link Manipulator

The reduced order slow subsystem is given by (2.20) as $a_1 \ddot{\theta}_l + a_2 \dot{\theta}_l + a_3 = -T_m^s$ where

$$a_1 = \left[\frac{ml^2}{3n} + nJ_m \right], a_2 = \left[nB_m + \frac{B_l}{n} \right] \text{ and } a_3 = \frac{mgl}{2n} \sin \theta_l. \text{ The problem we are addressing}$$

can be stated as follows: given the load desired position $\theta_d(t)$ and $\dot{\theta}_d(t)$ design a con-

trol law such that the load position $\theta_l(t)$ and load velocity $\dot{\theta}_l(t)$ track $\theta_d(t)$ and $\dot{\theta}_d(t)$ respectively.

There is only one nonlinear term present in the above equation. The feedforward controller T_{ff} then is given by

$$-T_{ff} = a_1 \ddot{Q}_d + a_2 \dot{Q}_d + CQ_d \quad (3.16)$$

where $C = \left[\frac{\partial a_3}{\partial \theta_d} \right]_P$ and P is the operating point on the trajectory about which the model

is linearized. The feedback controller is given by

$$-T_{fb} = K_p e(t) + K_v \dot{e}(t) \quad (3.17)$$

where K_p and K_v are feedback gains. The total control law is given by

$$-T_m^s = K_p e(t) + K_v \dot{e}(t) + a_1 \ddot{Q}_d + a_2 \dot{Q}_d + CQ_d \quad (3.18)$$

The fast subsystem is given by (2.21). The fast subsystem torque is chosen as

$$T_m^f = K_{pf} \eta_1 + K_{vf} \eta_2 \quad (3.19)$$

where η_1 and η_2 are the new fast variables defined by (2.10) and K_{pf} and K_{vf} are feedback gain constants. The composite controller used to control the full order system (2.19) takes the form $T_m = T_m^s + T_m^f$ with η_1 and η_2 expressed in terms of the slow variables θ_l and $\dot{\theta}_l$, and the original fast variables Z and \dot{Z} .

Example 2 Two link Manipulator

The reduced order slow subsystem is given by (2.26) as

$$M_r(q) \ddot{q} + h_r(q, \dot{q}) = U^s \quad (3.20)$$

where $M_r = \begin{bmatrix} m_{11} + n_1^2 J_1 & m_{12} \\ m_{21} & m_{22} + n_2^2 J_2 \end{bmatrix}$ and $h_r = \begin{bmatrix} (m_1 l_{c1} + m_2 l_1) g \cos(q_1) \\ m_2 l_{c2} g \cos(q_3) \end{bmatrix}$. The feedfor-

ward controller T_{ff} is given by

$$T_{ff} = A \ddot{Q}_d + CQ_d \quad (3.21)$$

where $A = \left[M_r(q_r) \right]_P$, $C_{ij} = \left[\frac{\partial h_{r_i}}{\partial q_{r_j}} \right]_P$ and P is the operating point on the trajectory

about which the model is linearized. The feedback controller is given by

$$T_{fb} = K_p e(t) + K_v \dot{e}(t) \quad (3.22)$$

where K_p and K_v are 2 x 2 feedback gain matrices. The total control law is given by

$$U^s = K_p e(t) + K_v \dot{e}(t) + A\ddot{Q}_d + CQ_d \quad (3.23)$$

The fast subsystem is given by (2.27)-(2.28). The fast subsystem torque is chosen as

$$U^f = K_{pf} \begin{bmatrix} \eta_{11} \\ \eta_{21} \end{bmatrix} + K_{vf} \begin{bmatrix} \dot{\eta}_{11} \\ \dot{\eta}_{21} \end{bmatrix} \quad (3.24)$$

where η_{11} and η_{21} are the fast variables and $\epsilon \dot{\eta}_{11} = \eta_{12}$, $\epsilon \dot{\eta}_{21} = \eta_{22}$ and K_{pf} and K_{vf} are 2 x 2 constant matrices. The composite controller used to control the full order system (2.24)-(2.25) is given by $U = U^s + U^f$ with η_{11} , η_{21} , η_{12} and η_{22} expressed in terms of the slow variables q_1 and q_3 and the original fast variables Z_{11} and Z_{21} .

Two position trajectories were tried in both the examples- a slowly time varying tra-

jectory $\theta_1^d = \frac{\pi}{4} \begin{bmatrix} 1 + 6e^{-\frac{t}{0.3}} - 8e^{-\frac{t}{0.4}} \end{bmatrix}$ which attains a constant value after some time and a

continuously time varying trajectory $\theta_1^d = \sin(t) - \cos(2t)$. The algorithm performs satisfactorily for the slow and fast subsystems considered separately. In some of the simulations, parameters were varied from their nominal values. The composite controller was applied to the full order system. The results of the simulations are discussed in Chapter 5.

3.b PD Adaptive Control Scheme for the Reduced Order System

The controller designed in the previous section is effective for motion of the manipulator in the neighborhood of the operating point P and when there is no mismatch between the robot model and the feedforward controller. However, during gross motion

of the manipulator, the operating point P and consequently the linearized model vary substantially with time. This will lead to steady state errors or even instability. To overcome this drawback the gains of the feedforward and feedback controllers are updated and an auxiliary signal is used to enhance closed loop stability and to achieve faster adaptation [16].

We have the reduced order rigid body equations of the manipulator as $M_r(q_r) \ddot{q}_r + h_r(q_r, \dot{q}_r) = U^{*s}$. This can be written as

$$A^*(q_r, \dot{q}_r) \ddot{q}_r + B^*(q_r, \dot{q}_r) \dot{q}_r + C^*(q_r, \dot{q}_r) q_r = U^{*s}. \quad (3.25)$$

In order to cope with changes of the operating point, the gains of the feedback and feedforward controllers in (3.1), are varied with time and a time varying auxiliary signal $F(t)$ corresponding to the operating point term $T(t)$ is included in the control law. The adaptive control law, the coefficients of which are updated by adaptive laws derived later in this chapter, is then given by

$$U^{*s} = F(t) + K_p(t)e(t) + K_v(t)\dot{e}(t) + A(t)\ddot{q}_d(t) + B(t)\dot{q}_d(t) + C(t)q_d(t). \quad (3.26)$$

Application of the adaptive control law (3.26) to the robot model (3.25) as shown in figure 5 yields

$$\begin{aligned} A^* \ddot{E}(t) + (B^* + K_v) \dot{E}(t) + (C^* + K_p) E(t) = & -F(t) + (A^* - A) \ddot{q}_d(t) \\ & + (B^* - B) \dot{q}_d(t) + (C^* - C) q_d(t). \end{aligned} \quad (3.27)$$

Defining the $2n \times 1$ position-velocity error vector as $E_{pv}(t) = \begin{bmatrix} E(t) \\ \dot{E}(t) \end{bmatrix}$, (3.27) can be

written as

$$\dot{E}_{pv}(t) = \begin{bmatrix} 0 & I_n \\ -\Delta_1 & -\Delta_2 \end{bmatrix} E_{pv}(t) + \begin{bmatrix} 0 \\ \Delta_0 \end{bmatrix} + \begin{bmatrix} 0 \\ \Delta_3 \end{bmatrix} q_d + \begin{bmatrix} 0 \\ \Delta_4 \end{bmatrix} \dot{q}_d + \begin{bmatrix} 0 \\ \Delta_5 \end{bmatrix} \ddot{q}_d \quad (3.28a)$$

where

$$\begin{aligned} \Delta_1 &= (A^*)^{-1} (C^* + K_p), \quad \Delta_2 = (A^*)^{-1} (B^* + K_v), \quad \Delta_0 = -(A^*)^{-1} (F) \\ \Delta_3 &= (A^*)^{-1} (C^* - C), \quad \Delta_4 = (A^*)^{-1} (B^* - B), \quad \Delta_5 = (A^*)^{-1} (A^* - A). \end{aligned} \quad (3.28b)$$

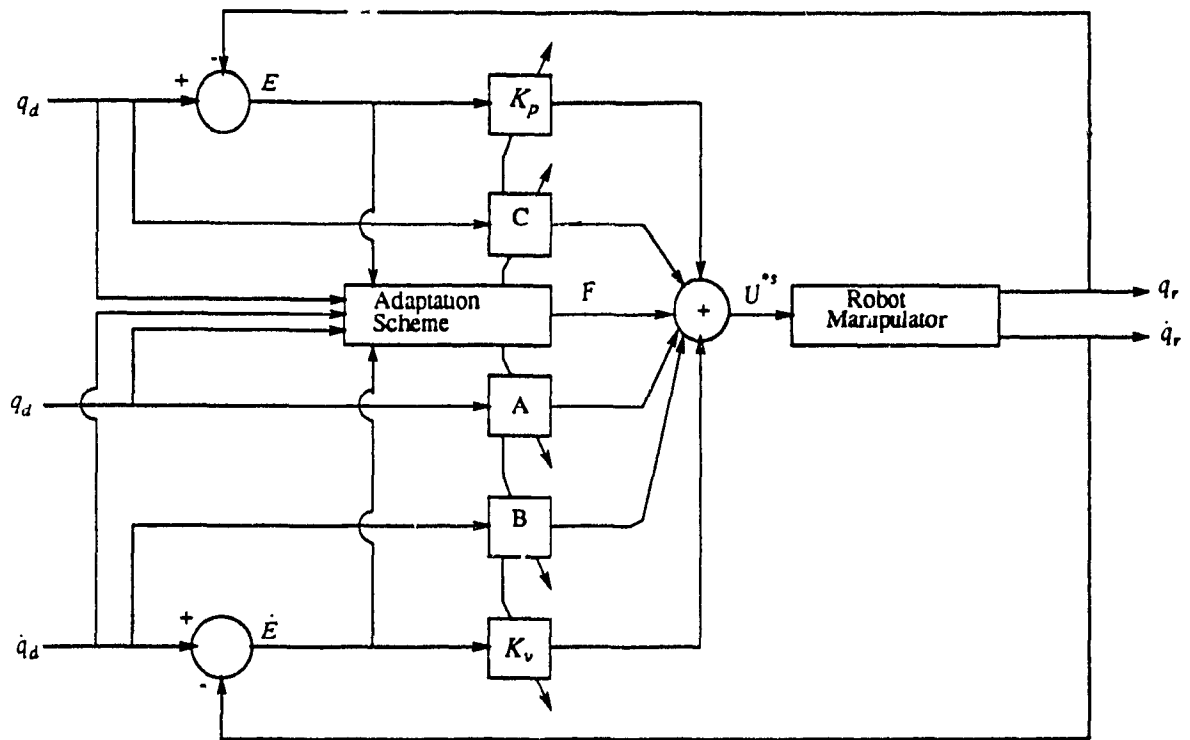


Figure 5. Adaptive Linear Control Scheme

We now define a "reference model" which reflects the desired performance (in terms of the tracking error $E(t)$). It is desired that each tracking error $E_i(t) = q_{id}(t) - q_{ir}(t)$ satisfy the second order differential equation

$$\ddot{E}_i(t) + 2\xi_i\omega_i\dot{E}_i(t) + \omega_i^2 E_i(t) = 0, \quad i = 1, \dots, n \quad (3.29)$$

where ξ_i and ω_i are the damping ratio and natural frequency to be chosen by the designer. Equation (3.29) can be written as

$$\dot{E}_{mpv}(t) = \begin{bmatrix} 0 & I_n \\ -D_1 & -D_2 \end{bmatrix} E_{mpv}(t) = DE_{mpv}(t) \quad (3.30)$$

where $D_1 = \text{diag}(\omega_i^2)$ and $D_2 = \text{diag}(2\xi_i\omega_i)$ are $n \times n$ constant diagonal matrices.

$E_{mpv}(t) = \begin{bmatrix} E_m \\ \dot{E}_m \end{bmatrix}$ is a $2n \times 1$ vector of desired position and velocity errors and the sub-

script m denotes the reference model. The solution of the homogeneous model (3.30) is

$$E_{mpv}(t) = e^{Dt} E_{mpv}(0) \quad (3.31)$$

where $E_{mpv}(0)$ is the initial state of the reference model. Since the initial values of the reference model and the actual trajectories are often the same, the initial error is actually zero; i.e. $E_{mpv}(0) = 0$. Hence from (3.31), $E_{mpv}(t) = 0$.

The problem is to adjust the controller terms $[K_p, K_v, A, B, C]$ so that for any $q_d(t)$ the system states $E_{pv}(t)$ approaches the model state $E_{mpv}(t)$ asymptotically i.e. $E_{pv}(t) \rightarrow E_{mpv}(t)$ as $t \rightarrow \infty$. Defining the adaptation error $e_a = E_{mpv}(t) - E_{pv}(t)$ and from (3.28) and (3.30) we obtain the error differential equation as

$$\begin{aligned} \dot{e}_a = & \begin{bmatrix} 0 & I_n \\ -D_1 & -D_2 \end{bmatrix} e_a + \begin{bmatrix} 0 & 0 \\ \Delta_1 - D_1 & \Delta_2 - D_2 \end{bmatrix} E_{pv} + \begin{bmatrix} 0 \\ -\Delta_0 \end{bmatrix} + \begin{bmatrix} 0 \\ -\Delta_3 \end{bmatrix} q_d \\ & + \begin{bmatrix} 0 \\ -\Delta_4 \end{bmatrix} \dot{q}_d + \begin{bmatrix} 0 \\ -\Delta_5 \end{bmatrix} \ddot{q}_d. \end{aligned} \quad (3.32)$$

The controller adaptation laws are derived by ensuring the stability of error dynamics (3.32). The Lyapunov function candidate is chosen as

$$\begin{aligned}
 V = e_a^T P e_a + (\Delta_0 - \Delta_0^*)^T Q_0 (\Delta_0 - \Delta_0^*) + \text{tr} \left\{ (\Delta_1 - D_1 - \Delta_1^*)^T Q_1 (\Delta_1 - D_1 - \Delta_1^*) \right\} + \\
 \text{tr} \left\{ (\Delta_2 - D_2 - \Delta_2^*)^T Q_2 (\Delta_2 - D_2 - \Delta_2^*) \right\} + \text{tr} \left\{ (\Delta_3 - \Delta_3^*)^T Q_3 (\Delta_3 - \Delta_3^*) \right\} + \\
 \text{tr} \left\{ (\Delta_4 - \Delta_4^*)^T Q_4 (\Delta_4 - \Delta_4^*) \right\} + \text{tr} \left\{ (\Delta_5 - \Delta_5^*)^T Q_5 (\Delta_5 - \Delta_5^*) \right\} \quad (3.33)
 \end{aligned}$$

where tr denotes the trace, $P = \begin{bmatrix} P_1 & P_2 \\ P_2 & P_3 \end{bmatrix}$ is a symmetric positive definite solution of the

Lyapunov equation

$$P D + D^T P = -Q \quad (3.34)$$

for a given symmetric positive definite $2n \times 2n$ constant matrix. $[Q_0, \dots, Q_5]$ are arbitrary symmetric positive definite constant $n \times n$ matrices. $[\Delta_0^*, \dots, \Delta_5^*]$ are functions of time which will be specified later.

The elements of P are found by substituting D and Q in (3.34), where

$$Q = \begin{bmatrix} -2Q_1 & 0 \\ 0 & -2Q_2 \end{bmatrix}, \text{ to yield}$$

$$P_1 = Q_1 D_2^{-1} + Q_1 D_1^{-1} D_2 + Q_2 D_2^{-1} D_1 \quad (3.35a)$$

$$P_2 = Q_1 D_1^{-1} \quad (3.35b)$$

$$P_3 = Q_2 D_2^{-1} + Q_1 D_1^{-1} D_2^{-1}. \quad (3.35c)$$

Different choices of Q_1 and Q_2 will result in different solutions for P . Letting

$Q_1 = G D_1^2 D_2$ and $Q_2 = (H - G) D_1 D_2$ where $G = \text{diag} (g_i)$ and $H = \text{diag} (h_i)$ with

$0 < g_i < h_i$ for $i=1, \dots, n$ we have

$$P = \begin{bmatrix} G D_1^2 D_2 + H D_1^2 & G D_1 D_2 \\ G D_1 D_2 & H D_1 \end{bmatrix}. \quad (3.36)$$

For $D_1 = \text{diag} (\omega_i^2)$ and $D_2 = \text{diag} (2\xi_i \omega_i)$, we obtain

$$P_2 = [\text{diag} (2\xi_i \omega_i^3 g_i)] , P_3 = [\text{diag} (\omega_i^2 h_i)]. \quad (3.37)$$

Differentiating V along the error trajectory (3.32), we have

$$\begin{aligned}
 \dot{V} = & -e_a^T Q e_a + 2\Delta_0^T \left[R + Q_0 \dot{\Delta}_0 - Q_0 \dot{\Delta}_0^* \right] - 2\Delta_0^{*T} Q_0 (\dot{\Delta}_0 - \dot{\Delta}_0^*) + \\
 & 2 \operatorname{tr} \left\{ (\Delta_1 - D_1)^T \left[-R E^T + Q_1 \dot{\Delta}_1 - Q_1 \dot{\Delta}_1^* \right] - \Delta_1^{*T} Q_1 (\dot{\Delta}_1 - \Delta_1^{*T}) \right\} + \\
 & 2 \operatorname{tr} \left\{ (\Delta_2 - D_2)^T \left[-R \dot{E}^T + Q_2 \dot{\Delta}_2 - Q_2 \dot{\Delta}_2^* \right] - \Delta_2^{*T} Q_2 (\dot{\Delta}_2 - \Delta_2^{*T}) \right\} + \\
 & 2 \operatorname{tr} \left\{ \Delta_3^T \left[R q_d^T + Q_3 \dot{\Delta}_3 - Q_3 \dot{\Delta}_3^* \right] - \Delta_3^{*T} Q_3 [\dot{\Delta}_3 - \dot{\Delta}_3^*] \right\} + \\
 & 2 \operatorname{tr} \left\{ \Delta_4^T \left[R \dot{q}_d^T + Q_4 \dot{\Delta}_4 - Q_4 \dot{\Delta}_4^* \right] - \Delta_4^{*T} Q_4 [\dot{\Delta}_4 - \dot{\Delta}_4^*] \right\} + \\
 & 2 \operatorname{tr} \left\{ \Delta_5^T \left[R \ddot{q}_d^T + Q_5 \dot{\Delta}_5 - Q_5 \dot{\Delta}_5^* \right] - \Delta_5^{*T} Q_5 [\dot{\Delta}_5 - \dot{\Delta}_5^*] \right\} \quad (3.38)
 \end{aligned}$$

where R is a $n \times 1$ weighted error vector defined as

$$\begin{aligned}
 R = & - \begin{bmatrix} P_2 & P_3 \end{bmatrix} e_a = \begin{bmatrix} P_2 & P_3 \end{bmatrix} E_{pv} \\
 = & P_2 E(t) + P_3 \dot{E}(t). \quad (3.39)
 \end{aligned}$$

As $E_{mpv} = 0$ and $e_a = -E_{pv}$. For the adaptation error $e_a(t)$ to vanish asymptotically \dot{V} must be negative definite. Letting

$$Q_0 [\dot{\Delta}_0 - \dot{\Delta}_0^*] = -R \quad (3.40a)$$

$$Q_1 [\dot{\Delta}_1 - \dot{\Delta}_1^*] = R E^T \quad (3.40b)$$

$$Q_2 [\dot{\Delta}_2 - \dot{\Delta}_2^*] = R \dot{E}^T \quad (3.40c)$$

$$Q_3 [\dot{\Delta}_3 - \dot{\Delta}_3^*] = -R q_d^T \quad (3.40d)$$

$$Q_4 [\dot{\Delta}_4 - \dot{\Delta}_4^*] = -R \dot{q}_d^T \quad (3.40e)$$

$$Q_5 [\dot{\Delta}_5 - \dot{\Delta}_5^*] = -R \ddot{q}_d^T, \quad (3.40f)$$

\dot{V} then reduces to

$$\begin{aligned}
 \dot{V} = & -e_a^T Q e_a + 2\Delta_0^{*T} R - 2 \operatorname{tr} [\Delta_1^{*T} R E^T] - 2 \operatorname{tr} [\Delta_2^{*T} R \dot{E}^T] \\
 & + 2 \operatorname{tr} [\Delta_3^{*T} R q_d^T] + 2 \operatorname{tr} [\Delta_4^{*T} R \dot{q}_d^T] + 2 \operatorname{tr} [\Delta_5^{*T} R \ddot{q}_d^T]. \quad (3.41)
 \end{aligned}$$

Choosing

$$\Delta_0^* = -Q_0^* R \quad (3.42a)$$

$$\Delta_1^* = Q_1^* R E^T \quad (3.42b)$$

$$\Delta_2^* = Q_2^* R \dot{E}^T \quad (3.42c)$$

$$\Delta_3^* = -Q_3^* R q_d^T \quad (3.42d)$$

$$\Delta_4^* = -Q_4^* R \dot{q}_d^T \quad (3.42e)$$

$$\Delta_5^* = -Q_5^* R \ddot{q}_d^T \quad (3.42f)$$

where $[Q_0^*, \dots, Q_5^*]$ are symmetric positive semi definite constant $n \times n$ matrices, (3.41)

simplifies to

$$\begin{aligned} \dot{V} = & -e_a^T Q e_a - 2R^T Q_0^* R - 2(R^T R) E^T Q_1^* E - 2(R^T R) \dot{E}^T Q_2^* \dot{E} \\ & - 2(R^T R) q_d^T Q_3^* q_d - 2(R^T R) \dot{q}_d^T Q_4^* \dot{q}_d - 2(R^T R) \ddot{q}_d^T Q_5^* \ddot{q}_d \end{aligned} \quad (3.43)$$

which is a negative definite function of e_a . Consequently the error differential equation (3.32) is asymptotically stable; i.e. $e_a(t) \rightarrow 0$ or $E_{pv}(t) \rightarrow E_{mpv}(t)$ as $t \rightarrow \infty$. From (3.40a)-(3.40f) and (3.42a)-(3.42f) the adaptation laws are found to be

$$\dot{\Delta}_0 = -Q_0^{-1} R - Q_0^* \dot{R} \quad (3.44a)$$

$$\dot{\Delta}_1 = Q_1^{-1} [R E^T] + Q_1^* \frac{d}{dt} (R E^T) \quad (3.44b)$$

$$\dot{\Delta}_2 = Q_2^{-1} [R \dot{E}^T] + Q_2^* \frac{d}{dt} (R \dot{E}^T) \quad (3.44c)$$

$$\dot{\Delta}_3 = -Q_3^{-1} [R q_d^T] - Q_3^* \frac{d}{dt} (R q_d^T) \quad (3.44d)$$

$$\dot{\Delta}_4 = -Q_4^{-1} [R \dot{q}_d^T] - Q_4^* \frac{d}{dt} (R \dot{q}_d^T) \quad (3.44e)$$

$$\dot{\Delta}_5 = -Q_5^{-1} [R \ddot{q}_d^T] - Q_5^* \frac{d}{dt} (R \ddot{q}_d^T). \quad (3.44f)$$

It is assumed that the change of the robot model matrices A^* , B^* and C^* in each sampling interval is much smaller than that of the controller gains which implies that A^* , B^* and C^* can be treated as unknown and slowly time varying compared with the controller gains. That is for instance $\frac{dA^*}{dt} \ll \frac{dA}{dt}$. This assumption is justified in practice

since the robot model changes significantly in the 1/10 sec. time scale whereas significant changes in the controller gains occur in the 1/1000 sec. time scale of sampling interval. Using these assumptions on differentiating (3.28b) yields,

$$\dot{\Delta}_0 = - \left[A^* \right]^{-1} \dot{F} \quad (3.45a)$$

$$\dot{\Delta}_1 = \left[A^* \right]^{-1} \dot{K}_p \quad (3.45b)$$

$$\dot{\Delta}_2 = \left[A^* \right]^{-1} \dot{K}_v \quad (3.45c)$$

$$\dot{\Delta}_3 = - \left[A^* \right]^{-1} \dot{C} \quad (3.45d)$$

$$\dot{\Delta}_4 = - \left[A^* \right]^{-1} \dot{B} \quad (3.45e)$$

$$\dot{\Delta}_5 = - \left[A^* \right]^{-1} \dot{A} \quad (3.45f)$$

In order to make the adaptation laws independent of the robot matrix A^* the matrices in (3.44a)-(3.44f) are chosen as

$$\begin{aligned} Q_0 &= \frac{1}{\delta_1} A^*, \quad Q_0^* = \delta_2 \left[A^* \right]^{-1} \\ Q_1 &= \frac{1}{\alpha_1} A^*, \quad Q_1^* = \alpha_2 \left[A^* \right]^{-1} \\ Q_2 &= \frac{1}{\beta_1} A^*, \quad Q_2^* = \beta_2 \left[A^* \right]^{-1} \\ Q_3 &= \frac{1}{\mu_1} A^*, \quad Q_3^* = \mu_2 \left[A^* \right]^{-1} \\ Q_4 &= \frac{1}{\gamma_1} A^*, \quad Q_4^* = \gamma_2 \left[A^* \right]^{-1} \\ Q_5 &= \frac{1}{\lambda_1} A^*, \quad Q_5^* = \lambda_2 \left[A^* \right]^{-1} \end{aligned} \quad (3.46)$$

where $\left[\delta_1, \alpha_1, \beta_1, \mu_1, \gamma_1, \lambda_1 \right]$ and $\left[\delta_2, \alpha_2, \beta_2, \mu_2, \gamma_2, \lambda_2 \right]$ are positive scalars. From (3.44a)-(3.44f) and (3.46) the controller adaptation laws are obtained as

$$\dot{F} = \delta_1 R + \delta_2 \dot{R} \quad (3.47a)$$

$$\dot{K}_p = \alpha_1 \left[RE^T \right] + \alpha_2 \frac{d}{dt} (RE^T) \quad (3.47b)$$

$$\dot{K}_v = \beta_1 \left[R \dot{E}^T \right] + \beta_2 \frac{d}{dt} (R \dot{E}^T) \quad (3.47c)$$

$$\dot{C} = \mu_1 \left[R q_d^T \right] + \mu_2 \frac{d}{dt} (R q_d^T) \quad (3.47d)$$

$$\dot{B} = \gamma_1 \left[R \dot{q}_d^T \right] + \gamma_2 \frac{d}{dt} (R \dot{q}_d^T) \quad (3.47e)$$

$$\dot{A} = \lambda_1 \left[R \ddot{q}_d^T \right] + \lambda_2 \frac{d}{dt} (R \ddot{q}_d^T) \quad (3.47f)$$

Substituting for P_2 and P_3 from (3.37) in (3.39) we obtain

$$R(t) = W_p D_1 D_2 E(t) + W_v D_1 \dot{E}(t) \quad (3.48)$$

where $W_p = \text{diag} (w_{p_i})$ and $W_v = \text{diag} (w_{v_i})$ are chosen to reflect the significance of the position and velocity errors E and \dot{E} .

From (3.47) the required auxiliary signal and controller gains are

$$F(t) = F(0) + \delta_2 R(t) + \delta_1 \int_0^t R(t) dt \quad (3.49a)$$

$$K_p(t) = K_p(0) + \alpha_2 R(t) E^T(t) + \alpha_1 \int_0^t R(t) E^T(t) dt \quad (3.49b)$$

$$K_v(t) = K_v(0) + \beta_2 R(t) \dot{E}^T(t) + \beta_1 \int_0^t R(t) \dot{E}^T(t) dt \quad (3.49c)$$

$$C(t) = C(0) + \mu_2 R(t) q_d^T(t) + \mu_1 \int_0^t R(t) q_d^T(t) dt \quad (3.49d)$$

$$B(t) = B(0) + \gamma_2 R(t) \dot{q}_d^T(t) + \gamma_1 \int_0^t R(t) \dot{q}_d^T(t) dt \quad (3.49e)$$

$$A(t) = A(0) + \lambda_2 R(t) \ddot{q}_d^T(t) + \lambda_1 \int_0^t R(t) \ddot{q}_d^T(t) dt \quad (3.49f)$$

and the control law is given by (3.26). The reference model (3.30) is reflected only on the weighted error $R(t)$.

Example 1 Single link Manipulator

The reduced order slow subsystem is given as $a_1 \ddot{\theta}_l + a_2 \dot{\theta}_l + a_3 = -T_m^s$ where

$$a_1 = \left[\frac{ml^2}{3n} + nJ_m \right], a_2 = \left[nB_m + \frac{B_l}{n} \right] \text{ and } a_3 = \frac{mgl}{2n} \sin \theta_l. \text{ The parameters of the refer-}$$

ence model which reflect the desired performance of the joint angles are chosen to be $\omega_1 = 10$ rad/sec and $\xi_1 = 1$ which yield a reference model $D_1 = 100$ and $D_2 = 20$ and $R(t) = 0.6 D_1 D_2 E(t) + 3.2 D_1 \dot{E}(t)$. The feedforward and feedback controllers are as given in (3.16) and (3.17) respectively. The total control law in addition to T_{ff} and T_{fb} has an auxiliary signal $F(t)$ that is given by

$$-T_m^s = F(t) + K_p e(t) + K_v \dot{e}(t) + a_1 \ddot{Q}_d + a_2 \dot{Q}_d + CQ_d$$

where $F(t)$ and the controller gains are given by (3.49a)-(3.49f).

The fast subsystem control law was unchanged from (3.19). The composite controller is given as $T_m = T_m^s + T_m^f$.

Example 2 Two link Manipulator

The reduced order slow subsystem is given in (2.26) as $M_r(q) \ddot{q} + h_r(q, \dot{q}) = U^s$. For sake of simplicity, we assume that n_1, n_2, J_1 and J_2 are known and $n_1^2 J_1 = n_2^2 J_2 = 1$. The parameters of the reference model which reflect the desired performance of the joint angles are chosen to be $\omega_1 = \omega_2 = 10$ rad/sec and $\xi_1 = \xi_2 = 1$ which yield a reference model $D_1 = 100 I_2$ and $D_2 = 20 I_2$ and $R(t) = 0.6 D_1 D_2 E(t) + 3.2 D_1 \dot{E}(t)$. The feedforward and feedback controllers are as given in (3.21) and (3.22), respectively. The total control law in addition to T_{ff} and T_{fb} has an auxiliary signal $F(t)$ that is given by

$$U^s = F(t) + K_p e(t) + K_v \dot{e}(t) + A \ddot{Q}_d + CQ_d$$

where $F(t)$ and the controller gains are given by (3.49a-3.49f).

The fast subsystem control law was unchanged from (3.24). The composite controller is given as $U^* = U^{*s} + U^{*f}$.

The two position trajectories that were tried in the previous (Single link and Two link Manipulators) section were used in this instance too. The algorithm performs satisfactorily for the slow and fast subsystems considered separately. When the composite controller was applied to the full order system the adaptation gains had to be reduced by nearly ten fold from their corresponding values for the reduced order slow subsystem. In some of the simulations, parameters were varied from their nominal values. The results of the simulations are discussed in Chapter 5.

In the next chapter, we present the basic concepts of nonlinear and adaptive control methods. Feedback linearization, passivity based adaptive control method (Slotine and Li) and adaptive inverse dynamics method (Craig, Hsu and Sastry) are discussed. Controllers for a single link and a two link flexible joint manipulator are developed based on these schemes.

Chapter 4

Nonlinear Control Methods

In the preceding chapter, we dealt with linear control methods. In this chapter, we will deal with the nonlinear equations of motion directly and will not try to linearize in deriving the controller. Essentially the nonlinear term in the control law in some sense would cancel the nonlinearity present in the system such that the overall closed loop system is linear.

As in the preceding chapter a fast control law is designed to damp out the lightly damped oscillations due to joint elasticity. The chosen fast control law is a state feedback controller and is given as in (3.1).

A composite controller based on the reduced order slow and fast subsystem control laws is used to control the full order flexible system (2.5)-(2.6), defined by

$$U^* = U^{*s} + U^{*f}$$

where the fast variables η_1 and η_2 are expressed in terms of the slow variables and original fast variables when implementing the fast controller U^{*f} .

4.a Feedback Linearization for the Reduced Order System

The controller will reduce the system to a purely inertial system with unit mass. The controller has two parts. The first part is model based and it makes use of the parameters of the system to be controlled. The second part is error driven. It forms error signals based on the desired and actual trajectories. Since the model based portion of the control law has the effect of making the system appear as a unit mass inertial system, servo portion is designed as if the system is purely inertial (i.e no friction).

The reduced order rigid body equations of the flexible joint manipulator are given by (2.2) as

$$M_r(q_r) \ddot{q}_r + h_r(q_r, \dot{q}_r) = U^{*s} \quad (4.1)$$

where $M_r(q_r)$ represents the inertia matrix and $h_r(q_r, \dot{q}_r)$ represents Coriolis, centripetal and gravitational forces. The model based portion of the controller takes the form

$$U^{*s} = \alpha U_m^{*s} + \beta \quad (4.2)$$

where α and β are functions so chosen that when U_m^{*s} is taken as the new input to the system the closed loop system appears to be an inertial system with unit mass. Letting $\alpha = M_r(q_r)$ and $\beta = h_r(q_r, \dot{q}_r)$ and applying (4.2) to (4.1) we have the system equations as

$$\ddot{q}_r = U_m^{*s}. \quad (4.3)$$

Equation (4.3) is similar in form to a double integrator system as it represents n decoupled double integrators. The nonlinear control law (4.2) is called the inverse dynamics control or computed torque and makes the new system linear and decoupled. Each input $U_{m_i}^{*s}$ can be designed to control a second order linear system. Assuming that $U_{m_i}^{*s}$ is a function only of q_{r_i} and its derivatives, then $U_{m_i}^{*s}$ will affect the q_{r_i} independently of the motion of the other links. U_m^{*s} is a function of errors as

$$U_m^{*s} = \ddot{q}_d + K_v \dot{e} + K_p e \quad (4.4)$$

where $e = q_d - q_r$, K_v and K_p are the feedback gains. From (4.3) and (4.4), we have the error dynamics as

$$\ddot{e} + K_v \dot{e} + K_p e = 0 \quad (4.5)$$

Figure 6 shows the block diagram of the decoupling and linearizing control system. An obvious choice for the gain matrices K_v and K_p are

$$K_p = \text{diag}[\omega_1^2, \dots, \omega_n^2], \quad K_v = \text{diag}[2\omega_1, \dots, 2\omega_n] \quad (4.6)$$

which results in a closed loop system with each joint response equal to the response of a

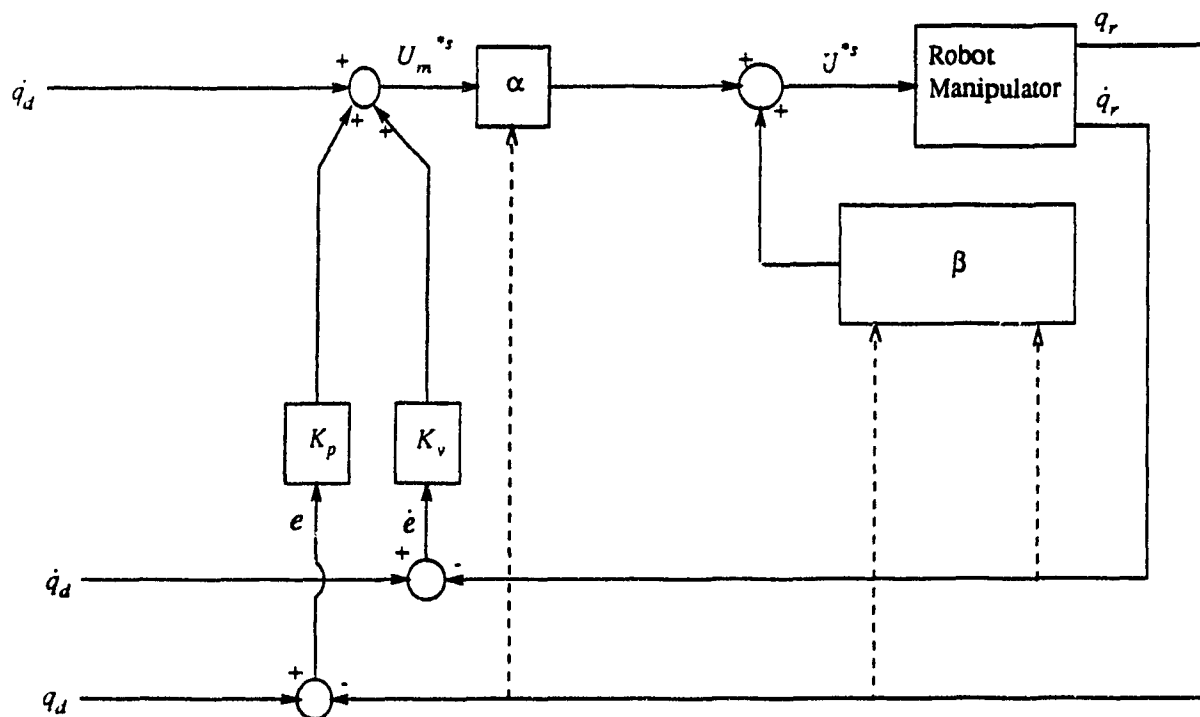


Figure 6. Model Based Control Scheme.

critically damped second order linear system with natural frequency ω_1 .

In a sense, the linearizing control law is an inverse model of the system being controlled. The nonlinearities in the system cancel those in the inverse model and this together with the servo control law results in a linear closed loop system.

The control law (4.2) requires that the parameters in the dynamic model be known precisely. However, in any physical system there is a degree of uncertainty regarding the values of various parameters, more so in the case of a robot carrying unknown loads. Therefore it is more reasonable to assume that the nonlinear controller is of the form

$$U^{*s} = \alpha U_m^{*s} + \beta \quad (4.7)$$

where $\alpha = \hat{M}_r(q_r)$, $\beta = \hat{h}_r(q_r, \dot{q}_r)$ and \hat{M}_r and \hat{h}_r represent the nominal or computed versions of M_r and h_r respectively. The uncertainty in the modeling is given by

$$\Delta M = \hat{M}_r(q_r) - M_r(q_r), \quad \Delta h = \hat{h}_r(q_r, \dot{q}_r) - h_r(q_r, \dot{q}_r). \quad (4.8)$$

With the nonlinear control law (4.7) the system reduces to

$$M_r \ddot{q}_r + h_r = \hat{M}_r U_m^{*s} + \hat{h}_r$$

that can be expressed as

$$\ddot{q}_r = I U_m^{*s} + (M_r^{-1} \hat{M}_r - I) U_m^{*s} + M_r^{-1} \Delta h. \quad (4.9)$$

Defining $M^* = (M_r^{-1} \hat{M}_r - I)$ and letting $U_m^{*s} = \ddot{q}_d + K_v \dot{e} + K_p e$ as in (4.4), we have the error dynamics as

$$\ddot{e} + K_v \dot{e} + K_p e = -M^* U_m^{*s} - M_r^{-1} \Delta h. \quad (4.10)$$

Equation (4.10) is a coupled nonlinear system and therefore it is not obvious that the system is stable. Changing the gains is not one of the options as the right hand side of the error dynamic equation (4.10) is a nonlinear function of U_m^{*s} . By adapting the controller gains the mismatch in modeling can be overcome, thus reducing equation (4.10) to a homogeneous one. Two adaptive nonlinear control schemes are discussed in the next two sections to remedy these difficulties. First we apply the results so far to a single link and a two link flexible joint manipulator.

Example 1 Single link Manipulator

The reduced order slow subsystem is given by (2.20) as

$$a_1 \ddot{\theta}_l + a_2 \dot{\theta}_l + a_3 = -T_m^s \quad (4.11)$$

where $a_1 = \left[\frac{ml^2}{3n} + nJ_m \right]$, $a_2 = \left[nB_m + \frac{B_l}{n} \right]$ and $a_3 = \frac{mgl}{2n} \sin \theta_l$. The controller is chosen

as

$$-T_m^s = \alpha T_{mm}^s + \beta \quad (4.12)$$

where $\alpha = a_1$, $\beta = a_2 \dot{\theta}_l + a_3$, $T_{mm}^s = \ddot{\theta}_d + K_v \dot{e} + K_p e$ and $e = \theta_d - \theta_l$. K_p and K_v are the feedback gains.

The fast subsystem is given by (2.21). The fast subsystem torque is chosen as

$$T_m^f = K_{pf} \eta_1 + K_{vf} \eta_2 \quad (4.13)$$

where η_1 and η_2 are the new fast variables defined by (2.10) and K_{pf} and K_{vf} are constant gains. The composite controller used to control the full order system is given by $T_m = T_m^s + T_m^f$ with the necessary substitutions made for η_1 and η_2 in terms of θ_l and $\dot{\theta}_l$ as described in the previous chapter.

Example 2 Two link Manipulator

The reduced order slow subsystem is given by (3.20). The controller is chosen as

$$U^s = \alpha U_m^s + \beta \quad (4.14)$$

where $\alpha = M_r$, $\beta = h_r$, $U_m^s = \ddot{q}_d + K_v \dot{e} + K_p e$ and $e = q_d - q$. K_p and K_v are 2×2 feedback gain matrices.

The fast subsystem is given by (2.27)-(2.28). The fast subsystem torque is chosen as

$$U^f = K_{pf} \begin{bmatrix} \eta_{11} \\ \eta_{21} \end{bmatrix} + K_{vf} \begin{bmatrix} \eta_{12} \\ \eta_{22} \end{bmatrix} \quad (4.15)$$

where η_{11} and η_{21} are the fast variables and $\epsilon\dot{\eta}_{11} = \eta_{12}$, $\dot{\eta}_{21} = \eta_{22}$ and K_{pf} and K_{vf} are 2×2 constant matrices. The composite controller used to control the full order system is given by $U = U^s + U^f$.

Two position trajectories were tried in both examples- a slowly time varying

$$\theta_1^d = \frac{\pi}{4} \begin{bmatrix} 1+6e^{-\frac{t}{0.3}} & -\frac{t}{0.4} \end{bmatrix} \text{ which attains a constant value after some time and a continu-}$$

ously time varying trajectory $\theta_1^d = \sin(t) - \cos(2t)$. The algorithm performs satisfactorily for the slow and fast subsystems considered separately. In some of the simulations, parameters were varied from their nominal values. The composite controller was then applied to the full order flexible system and the results are discussed in chapter 5.

4.b Passivity Based Control Methods for the Reduced Order System

In this section we present, the algorithm of Slotine and Li [1,2] that exploits the skew symmetry property of the robot equations of motion matrices and vectors. Unlike the feedback linearization scheme discussed in the previous section, this algorithm does not lead to a closed loop linear system even in the ideal case when all parameters are known exactly. The main motivation for this scheme as will be shown is that it does not require measurement of the manipulator acceleration nor does it require inversion of the inertia matrix.

The dynamics of the reduced order rigid manipulator is given by (2.2) as

$$M_r(q_r) \ddot{q}_r + h_r(q_r, \dot{q}_r) = U^{*s}$$

where h_r represents the Coriolis, centripetal and gravitational torques. We write h_r as

$$h_r(q_r, \dot{q}_r) = C_r(q_r, \dot{q}_r) \dot{q}_r + g_r(q_r) \quad (4.16)$$

where $C_r(q_r, \dot{q}_r) \dot{q}_r$ represents the Coriolis and centripetal torques and $g_r(q_r)$ represents gravitational torques. Hence the reduced order model is now given by

$$M_r(q_r) \ddot{q}_r + C_r(q_r, \dot{q}_r) \dot{q}_r + g_r(q_r) = U^{*s} \quad (4.17)$$

It is possible to define C_r (though the centripetal and Coriolis vector is uniquely defined) such that the matrix $\dot{M}_r - 2C$ is skew symmetric [1,2].

Let P_s be a constant m dimensional vector containing the unknown parameters and \hat{P}_s be its time varying estimate. Let \hat{M}_r , \hat{C}_r and \hat{g}_r be the estimates of M_r , C_r and g_r . Because of the linear parametrizability of the nonlinear functions characterizing the robot equations of motion, we have

$$\tilde{M}_r(q_r) \ddot{q}_r + \tilde{C}_r(q_r, \dot{q}_r) \dot{q}_r + \tilde{g}_r(q_r) = Y(q_r, \dot{q}_r, \dot{q}_r^r, \ddot{q}_r^r) \tilde{P}_s \quad (4.18)$$

where $\tilde{P}_s = \hat{P}_s - P_s$ is the parameter estimation error and Y is a $n \times m$ matrix independent of the parameters called the regressor. \dot{q}_r^r is defined in terms of the desired velocity and is introduced to guarantee the convergence of the tracking errors to zero and is given by

$$\dot{q}_r^r = \dot{q}_d - \Lambda_s \tilde{q}_r \quad (4.19)$$

with Λ_s being a positive definite matrix, and \tilde{q}_r , the position tracking error is defined by

$$\tilde{q}_r = q_r - q_d. \quad (4.20)$$

The control law for (4.17) is now chosen as

$$U^{*s} = \hat{M}_r \ddot{q}_r^r + \hat{C}_r \dot{q}_r^r + \hat{g}_r - K_{ds} S_s \quad (4.21)$$

where K_{ds} is a positive definite matrix and S_s is a measure of tracking accuracy defined by

$$S_s = \dot{q}_r - \dot{q}_r^r. \quad (4.22)$$

Figure 7 shows the structure of the controller. Substituting (4.21) in (4.17) and calculating \ddot{q}_r in terms of \dot{S}_s we have

$$M_r \dot{S}_s + C_r S_s + K_{ds} S_s = (\hat{M}_r - M_r) \ddot{q}_r + (\hat{C}_r - C_r) \dot{q}_r + (\hat{g}_r - g_r) \quad (4.23)$$

which on using (4.18) reduces to

$$M_r \dot{S}_s + C_r S_s + K_{ds} S_s = Y \tilde{P}_s. \quad (4.24)$$

The update law for adjusting the parameters may now be obtained by selecting the Lyapunov function candidate as

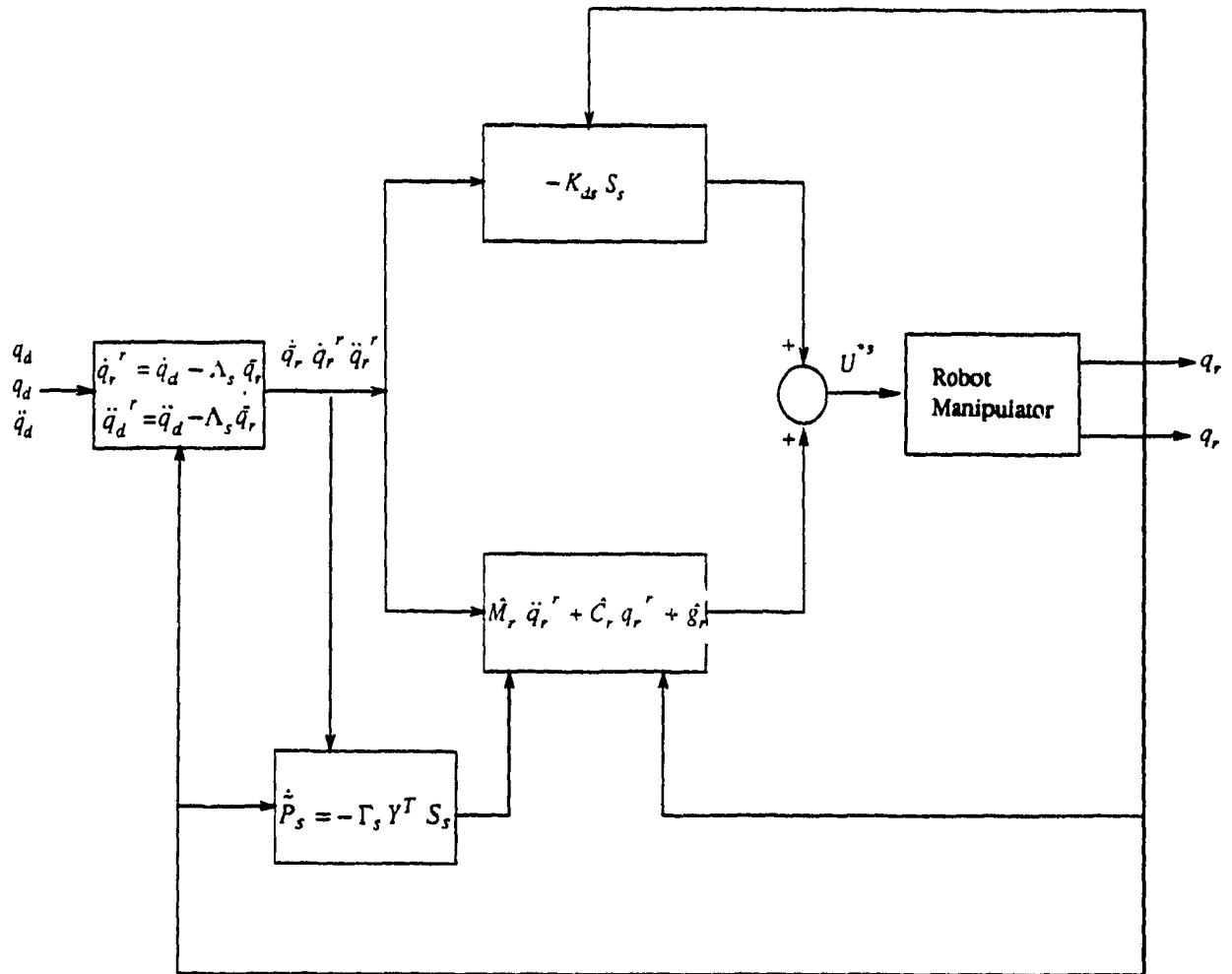


Figure 7. Passivity Based Adaptive Control Scheme.

$$V(t) = \frac{1}{2} S_s^T M_r S_s + \frac{1}{2} \bar{P}_s^T \Gamma_s^{-1} \bar{P}_s. \quad (4.25)$$

Differentiating $V(t)$ along the trajectories of (4.17) yields

$$\dot{V}(t) = S_s^T \dot{M}_r S_s + \frac{1}{2} S_s^T \dot{M}_r S_s + \bar{P}_s^T \Gamma_s^{-1} \dot{\bar{P}}_s. \quad (4.26)$$

Substituting for $\dot{M}_r S_s$ from (4.24), we have

$$\dot{V}(t) = S_s^T \left[Y \bar{P}_s - C_r S_s - K_{ds} S_s \right] + \frac{1}{2} S_s^T \dot{M}_r S_s + \bar{P}_s^T \Gamma_s^{-1} \dot{\bar{P}}_s. \quad (4.27)$$

Rearranging and using the skew symmetry property $\dot{M}_r - 2C_r = 0$, we get

$$\dot{V}(t) = -S_s^T K_{ds} S_s + \bar{P}_s^T \left[\Gamma_s^{-1} \dot{\bar{P}}_s + Y^T S_s \right] \quad (4.28)$$

where Γ_s is a constant positive definite matrix. Letting

$$\dot{\bar{P}}_s = -\Gamma_s Y^T S_s \quad (4.29)$$

(4.28) reduces to

$$\dot{V}(t) = -S_s^T K_{ds} S_s. \quad (4.30)$$

$V(t)$ is lower bounded by zero and $\dot{V}(t) \leq 0$. Equation (4.30) implies that S_s is bounded and converges to zero as $t \rightarrow \infty$. Therefore, as long as the desired trajectories q_d , \dot{q}_d and \ddot{q}_d are bounded, the tracking errors must converge to zero.

Example 1 Single link Manipulator

The reduced order slow subsystem is given by (4.11). Since the coefficients of (4.11) are all constants, skew symmetry property cannot be used to prove stability. Hence the control law for (4.11) is chosen as

$$T_m^s = - \left[d_1 \ddot{\theta}_r + d_2 \dot{\theta}_r + d_3 \sin \theta_l - K_{ds} S_s \right] \quad (4.31)$$

instead of

$$T_m^s = - \left[d_1 \ddot{\theta}_r + d_2 \dot{\theta}_r + d_3 \sin \theta_l - K_{ds} S_s \right] \quad (4.32)$$

as suggested by (4.21), where $\hat{P}_s := [\hat{a}_1 \ \hat{a}_2 \ \hat{a}_3]^T$ is the estimate of the parameter vector $P_s := [a_1 \ a_2 \ a_3]^T$, K_d is a positive constant gain and S_s is a measure of tracking accuracy defined by

$$S_s = \dot{\theta}_l - \dot{\theta}_r. \quad (4.33)$$

$\dot{\theta}_r$ is defined in terms of the reference velocity and is introduced to guarantee the convergence of the tracking errors to zero and is given by

$$\dot{\theta}_r = \dot{\theta}_d - \Lambda_s \theta_l. \quad (4.34)$$

with Λ_s a positive constant and the position tracking error is defined by

$$\theta_l = \theta_l - \theta_d.$$

Substituting (4.31) in (4.11) and calculating $\ddot{\theta}_l$ in terms of \dot{S}_s we have

$$a_1 \dot{S}_s + K_d S_s = \begin{bmatrix} \ddot{\theta}_r & \dot{\theta}_l & \sin \theta_l \end{bmatrix} \begin{bmatrix} \hat{a}_1 - a_1 \\ \hat{a}_2 - a_2 \\ \hat{a}_3 - a_3 \end{bmatrix} \quad (4.35)$$

The update law for adjusting the parameters may now be obtained by selecting the Lyapunov function candidate as

$$V(t) = \frac{1}{2} S_s a_1 S_s + \frac{1}{2} \begin{bmatrix} \hat{a}_1 - a_1 & \hat{a}_2 - a_2 & \hat{a}_3 - a_3 \end{bmatrix} \Gamma_s \begin{bmatrix} \hat{a}_1 - a_1 \\ \hat{a}_2 - a_2 \\ \hat{a}_3 - a_3 \end{bmatrix} \quad (4.36)$$

where Γ_s is a constant positive definite matrix. Differentiating V along the trajectories of (4.11) yields

$$\dot{V} = a_1 S_s \dot{S}_s + \begin{bmatrix} \dot{\hat{a}}_1 & \dot{\hat{a}}_2 & \dot{\hat{a}}_3 \end{bmatrix} \Gamma_s \begin{bmatrix} \hat{a}_1 - a_1 \\ \hat{a}_2 - a_2 \\ \hat{a}_3 - a_3 \end{bmatrix}$$

By substituting for $a_1 \dot{S}_s$ from (4.35) and selecting

$$\dot{a}_1 = -\Gamma_{s1}^{-1} S_s \ddot{\theta}_1$$

$$\dot{a}_2 = -\Gamma_{s2}^{-1} S_s \dot{\theta}_1$$

$$\dot{a}_3 = -\Gamma_{s3}^{-1} S_s \sin \theta_1$$

we have $\dot{V} = -S_s K_d S_s \leq 0$. $V(t)$ is lower bounded by zero, and $\dot{V}(t) \leq 0$. Proceeding in a similar manner as in the previous section it can be shown that as long as the desired trajectories $\theta_d, \dot{\theta}_d$ and $\ddot{\theta}_d$ are bounded, tracking errors must converge to zero.

As in the preceding chapter a fast controller is designed to damp out the lightly damped oscillations due to the joint elasticity. Instead of a state feedback controller, an adaptive fast controller is designed for the fast subsystem identical in approach to the slow subsystem. The Lyapunov function candidate for the fast subsystem is chosen as

$$W(t) = \frac{1}{2} S_f b_1 S_f + \frac{1}{2} \begin{bmatrix} \hat{b}_1 - b_1 & \hat{b}_2 - b_2 \end{bmatrix} \Gamma_f \begin{bmatrix} \hat{b}_1 - b_1 \\ \hat{b}_2 - b_2 \end{bmatrix} \quad (4.37)$$

where $b_1 = \epsilon^2 n J_m$, $b_2 = \left[\frac{3}{ml^2} + \frac{1}{n^2 J_m} \right] n J_m$ and Γ_f is a constant positive definite

matrix. Choosing the control as

$$T_m^f = \left[\hat{b}_1 \ddot{\eta}_{r1} + \hat{b}_2 \eta_1 - K_{df} S_f \right] \quad (4.38)$$

and the adaptation laws to be

$$\dot{\hat{b}}_1 = -\Gamma_{f1}^{-1} S_f \ddot{\eta}_{r1}$$

$$\dot{\hat{b}}_2 = -\Gamma_{f2}^{-1} S_f \eta_1$$

we have $\dot{W} = -S_f (K_{df}) S_f \leq 0$ where K_{df} is a positive constant gain, $S_f = \dot{\eta}_1 - \dot{\eta}_{r1}$, $\dot{\eta}_{r1} = \dot{\eta}_{d1} - \Lambda_f \eta_1$ and $\eta_1 = \eta_1 - \eta_{d1}$. Since $W(t)$ is lower bounded by zero, and $\dot{W}(t) \leq 0$ and as long as the desired trajectories $\eta_{d1}, \dot{\eta}_{d1}$ and $\ddot{\eta}_{d1}$ are bounded, using the same arguments as earlier it can be shown that tracking error measures must converge to zero.

The composite controller used to control the full order system is in the form of $T_m = T_m^s + T_m^f$ with the required substitutions made for η_1 and η_2 in terms of the slow variables and fast variables.

Example 2 Two link Manipulator

The reduced order slow subsystem is given by (2.26) as $M_r(q)\ddot{q} + h_r(q, \dot{q}) = U^s$. This can be rewritten as

$$M_r(q)\ddot{q} + C_r(q, \dot{q})\dot{q} + g_r(q) = U^s \quad (4.39)$$

where

$$M_r = \begin{bmatrix} m_{11} + n_1^2 J_1 & m_{12} \\ m_{21} & m_{22} + n_2^2 J_2 \end{bmatrix}, \quad C_r = 0, \\ g_r = \begin{bmatrix} (m_1 l_{c1} + m_2 l_1)g \cos(q_1) \\ m_2 l_{c2}g \cos(q_3) \end{bmatrix}, \quad q = \begin{bmatrix} q_1 \\ q_3 \end{bmatrix} \quad (4.40)$$

The skew symmetry property $\dot{M}_r - 2C_r = 0$ holds in this case. We assume for the sake of simplicity that n_1, n_2, J_1 and J_2 are known and $n_1^2 J_1 = n_2^2 J_2 = 1$. Substituting these values in (4.40), we have \hat{M}_r and \hat{g}_r which are the estimated values of M_r and g_r as

$$\hat{M}_r = \begin{bmatrix} 1 + P_1 & P_2 \\ P_2 & 1 + P_3 \end{bmatrix} \quad \text{and} \quad \hat{g}_r = \begin{bmatrix} P_4 \cos(q_1) \\ P_5 \cos(q_3) \end{bmatrix} \quad \text{where } P_s^T = [P_1, \dots, P_5] \text{ is the vector of}$$

estimated parameters. The controller is now chosen as

$$U^s = \begin{bmatrix} U_1^s \\ U_2^s \end{bmatrix} = \begin{bmatrix} 1 + P_1 & P_2 \\ P_2 & 1 + P_3 \end{bmatrix} \ddot{q}^r + \begin{bmatrix} P_4 \cos(q_1) \\ P_5 \cos(q_3) \end{bmatrix} - K_d S_s \quad (4.41)$$

where $\ddot{q}^r = \ddot{q}_d - \Lambda_s (\dot{q} - \dot{q}_d)$ and $S_s = \dot{q} - \dot{q}_d + \Lambda_s (q - q_d)$. K_d is a positive definite matrix and $\Lambda_s = \text{diag}(\lambda_1, \lambda_2) > 0$. The parameters are adjusted according to the adaptation law (4.29) which is given by

$$\dot{\hat{P}} = -\Gamma_s Y^T S_s \quad (4.42)$$

where $Y = \begin{bmatrix} \ddot{q}_1^r & \ddot{q}_3^r & 0 & \cos(q_1) & 0 \\ 0 & \ddot{q}_1^r & \ddot{q}_3^r & 0 & \cos(q_3) \end{bmatrix}$ with Γ_s a symmetric positive definite matrix.

In the control of a single link flexible joint manipulator, numerical simulations suggest that a feedback fast controller is less susceptible to changes in ϵ when compared to an adaptive fast controller. Hence for the two link flexible manipulator we chose a feedback fast controller instead of an adaptive fast controller. The fast subsystem is given by (2.27)-(2.28). The fast subsystem torque is chosen as

$$U^f = K_{pf} \begin{bmatrix} \eta_{11} \\ \eta_{21} \end{bmatrix} + K_{vf} \begin{bmatrix} \eta_{12} \\ \eta_{22} \end{bmatrix} \quad (4.43)$$

where η_{11} and η_{21} are the fast variables and $\epsilon \dot{\eta}_{11} = \eta_{12}$, $\epsilon \dot{\eta}_{21} = \eta_{22}$ and K_{pf} and K_{vf} are 2×2 constant matrices. The composite controller used to control the full order system is given by $U = U^s + U^f$.

The two position trajectories that were used to simulate the system using feedback linearization controller were tried here too. The algorithm was found to perform satisfactorily for the slow and fast subsystems considered separately. In some of the simulations, parameters were varied from their nominal values. Then the composite controller was applied to the full order flexible system. The simulation results are discussed in Chapter 5.

4.c Inverse Dynamics Method for the Reduced Order System

In this section we present, the algorithm of Craig, Hsu and Sastry [3,4]. Unlike the algorithm of Slotine and Li discussed in the previous section, this method requires the measurement of the manipulator acceleration and inversion of the inertia matrix. The acceleration can be usually estimated from the velocity.

The reduced order rigid body equations of the flexible joint manipulator are given by (4.1). To control the manipulator, the following control law is chosen

$$U^{*s} = \hat{M}_r(q_r) \ddot{q}_r^* + \hat{h}_r(q_r, \dot{q}_r) \quad (4.44)$$

where $\hat{P}_s := [\hat{M}_r \quad \hat{h}_r]^T$ is estimate of $P_s := [M_r \quad h_r]^T$ and \ddot{q}_r^* is defined as

$$\ddot{q}_r^* = \ddot{q}_d + K_v \dot{E} + K_p E \quad (4.45)$$

where E is the position error defined as $E = q_d - q_r$ and K_v and K_p are positive diagonal gain matrices that are chosen to give desired transient characteristics. Figure 8 shows the structure of the controller. This control strategy requires (as does the feedback linearization and Slotine and Li's control methods) that the desired trajectory be twice continuously differentiable. Substituting (4.44)-(4.45) in (4.1) and after simple algebraic manipulation yields

$$\ddot{E} + K_v \dot{E} + K_p E = \hat{M}_r^{-1} [\bar{M}_r \ddot{q}_r + \bar{h}_r] \quad (4.46)$$

where $\bar{M}_r = M_r - \hat{M}_r$ and $\bar{h}_r = h_r - \hat{h}_r$ represent the errors in the parameters estimates of (4.1). Equation (4.46) may be written as

$$\ddot{E} + K_v \dot{E} + K_p E = \hat{M}_r^{-1} Y \bar{P}_s \quad (4.47)$$

where Y is a matrix of functions known as regressor and $\bar{P}_s = P_s - \hat{P}_s$ is a vector containing the parameter estimation error. From the right hand side of (4.47) it follows that \hat{M}_r must remain nonzero during the adaptation interval. The adaptive law will essentially compute the appropriate changes in parameter estimates as a function of a filtered servo error which is given by $E_1 = \dot{E} + \phi E$ where $\phi = \text{diag}(\phi_1, \dots, \phi_n)$ and is chosen such that the

transfer function $\frac{s + \phi_j}{s^2 + K_{v,j} s + K_{p,j}}$ is strictly positive real. The filtered error equation for

the entire system in state space can be obtained as

$$\begin{aligned} \dot{\underline{X}} &= A \underline{X} + B \hat{M}_r^{-1} Y \bar{P}_s \\ E_1 &= C^T \underline{X} \end{aligned} \quad (4.48)$$

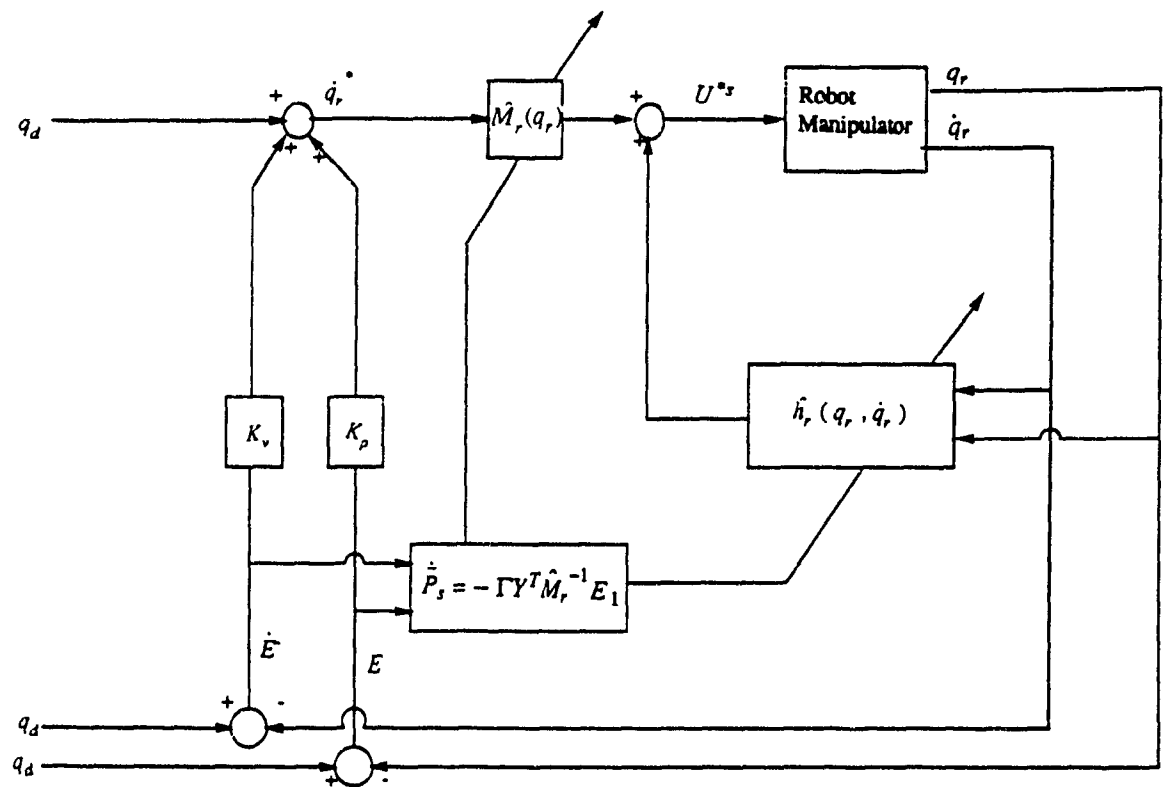


Figure 8. Inverse Dynamics Adaptive Control Scheme.

where

$$\underline{X} = \begin{bmatrix} \underline{E} \\ \underline{\dot{E}} \end{bmatrix}, A = \begin{bmatrix} 0 & I \\ -K_p & -K_v \end{bmatrix}, B = \begin{bmatrix} 0 \\ I_n \end{bmatrix}, C = \begin{bmatrix} 0 \\ I_n \end{bmatrix}.$$

We now choose the Lyapunov function candidate as

$$V(\underline{X}, \tilde{P}_s) = \underline{X}^T \rho \underline{X} + \tilde{P}_s^T \Gamma^{-1} \tilde{P}_s \quad (4.49)$$

with $\Gamma = \text{diag}(\Gamma_1, \dots, \Gamma_n)$, $\Gamma_i > 0$ and where $\rho = \text{diag}(\rho_1, \dots, \rho_n)$, $\rho_i > 0$ is the positive definite solution of the Lyapunov equation

$$A^T \rho + \rho A = -Q \quad (4.50)$$

for a given positive definite matrix $Q = \text{diag}(Q_1, \dots, Q_n)$. Differentiating V with respect to time along the trajectories of (4.46) gives

$$\dot{V} = \underline{\dot{X}}^T \rho \underline{X} + \underline{X}^T \rho \underline{\dot{X}} + \tilde{P}_s^T \Gamma^{-1} \dot{\tilde{P}}_s + \tilde{P}_s^T \Gamma^{-1} \dot{\tilde{P}}_s. \quad (4.51)$$

Substituting for $\underline{\dot{X}}$ from (4.47), we have

$$\dot{V} = \underline{X}^T (A^T \rho + \rho A) \underline{X} + 2\tilde{P}_s^T \Gamma^{-1} \dot{\tilde{P}}_s + 2\tilde{P}_s^T Y^T \hat{M}_r^{-1} E_1. \quad (4.52)$$

Substituting for $(A^T \rho + \rho A)$ from (4.50), we have

$$\dot{V} = -\underline{X}^T Q \underline{X} + 2\tilde{P}_s^T \left[\Gamma^{-1} \dot{\tilde{P}}_s + Y^T \hat{M}_r^{-1} E_1 \right]. \quad (4.53)$$

Letting

$$\dot{\tilde{P}}_s = -\Gamma Y^T \hat{M}_r^{-1} E_1, \quad (4.54)$$

Equation (4.53) reduces to $\dot{V} = -\underline{X}^T Q \underline{X}$ which is negative semi definite. Since $V(t)$ is lower bounded by zero and $\dot{V}(t) \leq 0$, both the position and velocity tracking errors must converge to zero. Since $\tilde{P}_s = P_s - \hat{P}_s$, we now have $\dot{\tilde{P}}_s = -\dot{\hat{P}}_s$, and so the adaptation law may be expressed as

$$\dot{\hat{P}}_s = \Gamma Y^T \hat{M}_r^{-1} E_1. \quad (4.55)$$

Example 1 Single link Manipulator

The reduced order slow subsystem is given by (4.11). The controller is chosen as

$$-T_m^s = \hat{d}_1 \ddot{\theta}_l^* + \hat{d}_2 \dot{\theta}_l + \hat{d}_3 \sin \theta_l \quad (4.56)$$

where $\hat{P} := [\hat{d}_1 \ \hat{d}_2 \ \hat{d}_3]^T$ is estimate of $P := [a_1 \ a_2 \ a_3]^T$ and $\ddot{\theta}_l^*$ is defined as

$$\ddot{\theta}_l^* = \ddot{\theta}_d + K_v \dot{E} + K_p E.$$

E is the position error defined as $E = \theta_d - \theta_l$ and K_v and K_p are constants that are chosen to give desired transient characteristics. The adaptation laws are given by

$$\dot{\hat{P}}_s = \Gamma Y^T \hat{d}_1^{-1} E_1 \quad (4.57a)$$

where

$$Y = \begin{bmatrix} \ddot{\theta}_l^* \\ \dot{\theta}_l \\ \sin(\theta_l) \end{bmatrix}. \quad (4.57b)$$

E_1 is the filtered servo error defined as

$$E_1 = \dot{E} + \phi E \quad (4.57c)$$

where ϕ is so chosen such that the transfer function $\frac{s + \phi}{s^2 + K_v s + K_p}$ is strictly positive real.

An adaptive fast subsystem torque is designed based on this scheme as was done for the passivity based scheme. The composite controller used to control the full order system is given by $T_m = T_m^s + T_m^f$.

Example 2 Two link Manipulator

The reduced order slow subsystem is given by (4.39). As in the previous section, we assume for the sake of simplicity that n_1, n_2, J_1 and J_2 are known and $n_1 J_1^2 = n_2 J_2^2 = 1$

and substituting these values in (4.40), we have \hat{M}_r and \hat{g}_r which are the estimated values of M_r and g_r as $\hat{M}_r = \begin{bmatrix} 1 + P_1 & P_2 \\ P_2 & 1 + P_3 \end{bmatrix}$ and $\hat{g}_r = \begin{bmatrix} P_4 \cos(q_1) \\ P_5 \cos(q_3) \end{bmatrix}$ where $P_s^T = [P_1, \dots, P_5]$ is the vector of estimated parameters. The controller is now chosen as

$$U^s = \begin{bmatrix} U_1^s \\ U_2^s \end{bmatrix} = \begin{bmatrix} 1 + P_1 & P_2 \\ P_2 & 1 + P_3 \end{bmatrix} \ddot{q}^* + \begin{bmatrix} P_4 \cos(q_1) \\ P_5 \cos(q_3) \end{bmatrix} \quad (4.58)$$

where $\ddot{q}^* = \ddot{q}_d + K_v \dot{E} + K_p E$ with $q = \begin{bmatrix} q_1 \\ q_3 \end{bmatrix}$ and position error E is given by $E = q_d - q$.

The adaptation law is given by

$$\dot{P}_s = \Gamma Y^T \hat{M}_r^{-1} E_1 \quad (4.59)$$

where $Y = \begin{bmatrix} \ddot{q}_1 & \ddot{q}_3 & 0 & \cos(q_1) & 0 \\ 0 & \ddot{q}_1 & \ddot{q}_3 & 0 & \cos(q_3) \end{bmatrix}$ with Γ_s a symmetric positive definite matrix and E_1 is given by (4.57c).

The fast subsystem is given by (2.27)-(2.28). The fast subsystem torque is chosen as

$$U^f = K_{pf} \begin{bmatrix} \eta_{11} \\ \eta_{21} \end{bmatrix} + K_{vf} \begin{bmatrix} \eta_{12} \\ \eta_{22} \end{bmatrix} \quad (4.60)$$

where η_{11} and η_{21} are the fast variables and $\dot{\eta}_{11} = \eta_{12}$, $\dot{\eta}_{21} = \eta_{22}$, η_{12} and η_{22} are their derivatives respectively and K_{pf} and K_{vf} are 2×2 constant matrices. The composite controller used to control the full order system is given by $U = U^s + U^f$.

In the simulation the same trajectories as in the previous instances were tried here. After verifying that the algorithms performed satisfactorily for the reduced order systems considered separately, the composite controller was applied to the full order flexible system. The simulation results are discussed in Chapter 5.

In the next chapter, we present the simulation results for a single link and a two link flexible joint manipulator controlled by the algorithms presented in Chapters 3 and 4.

Chapter 5

Numerical Simulation

Two position trajectories were used in our simulations. The first one being an exponential slowly time varying trajectory $\theta_1^d = \frac{\pi}{4} \left[1 + 6e^{-t/0.3} - 8e^{-t/0.4} \right]$ which attains a constant value after some time. The second is a continuously time varying faster trajectory $\theta_1^d = \sin(t) - \cos(2t)$ when compared with the first one.

The nominal values used in the simulation of the single link flexible joint manipulator are: $m = 10 \text{ kg}$, $l = 3 \text{ meter}$, $B_m = 0.015 \text{ N.m/rad.sec}^{-1}$, $B_l = 36 \text{ N.m/rad.sec}^{-1}$, $J_m = 0.04 \text{ kg-m}^2$, $n=100$, $\mu = \epsilon^2 = 0.01$ and $g = 9.8 \text{ m/sec}^2$.

The nominal values used in the simulation of the two link flexible joint manipulator are: $m_1 = m_2 = 1 \text{ kg}$, $I_1 = I_2 = 1 \text{ kg-m}^2$, $n_1^2 J_1 = n_2^2 J_2 = 1 \text{ kg-m}^2$, $l_1 = l_2 = 1 \text{ meter}$, $l_{c1} = l_{c2} = 0.5 \text{ meter}$, $K_1 = K_2 = 100$ and $g = 9.8 \text{ m/sec}^2$.

5.a Reduced Order Model

Linear Control Methods

PD Nonadaptive Control Scheme

This scheme was discussed in Section 3.a. Though the equations of motion describing the robot motion are nonlinear and coupled, this local linearization scheme provides an approximate and simple solution to the robot control problem that can be easily implemented in practice.

The reduced order models of a single link manipulator given by (2.20) and a two link manipulator given by (2.26) were simulated using the nominal values given earlier with control laws given by (3.18) and (3.23) respectively. The steady state position and

velocity errors were reduced to zero, the position response of which is as shown in figure 9. However when the parameters of the system were changed from their nominal values by 20% (that is the uncertainty in the system parameters were assumed to be 20%), the steady state position error did not converge to zero though the system remained stable as shown in figure 10. This error is due to the mismatch in the controller and system parameters.

PD Adaptive Control Scheme

This scheme was discussed in Section 3.b. In this case though the same controller is used as in the previous case, the coefficients of the controller are updated by the adaptive laws given by (3.49a)-(3.49f).

On simulating the reduced order models of a single link and a two link flexible joint manipulator using the nominal values, the steady state position and velocity errors were reduced to zero as shown in figures 11 and 12. The difference in performance between the adaptive and the nonadaptive schemes is that when the parameters of the system were changed from their nominal values by 20% the steady state position and velocity errors are reduced to zero for the adaptive scheme as shown in figures 13 and 14.

Nonlinear Control Methods

Feedback Linearization Scheme

As was described in Section 4.a, this nonlinear feedback linearization scheme globally linearizes the nonlinear equations of motion by cancelling the nonlinearities such that the overall closed loop system is linear.

The reduced order models of the single link flexible joint manipulator given by (2.20) and the two link flexible joint manipulator given by (2.26) were simulated using the nominal values given earlier with control laws given by (4.12) and (4.14) respec-

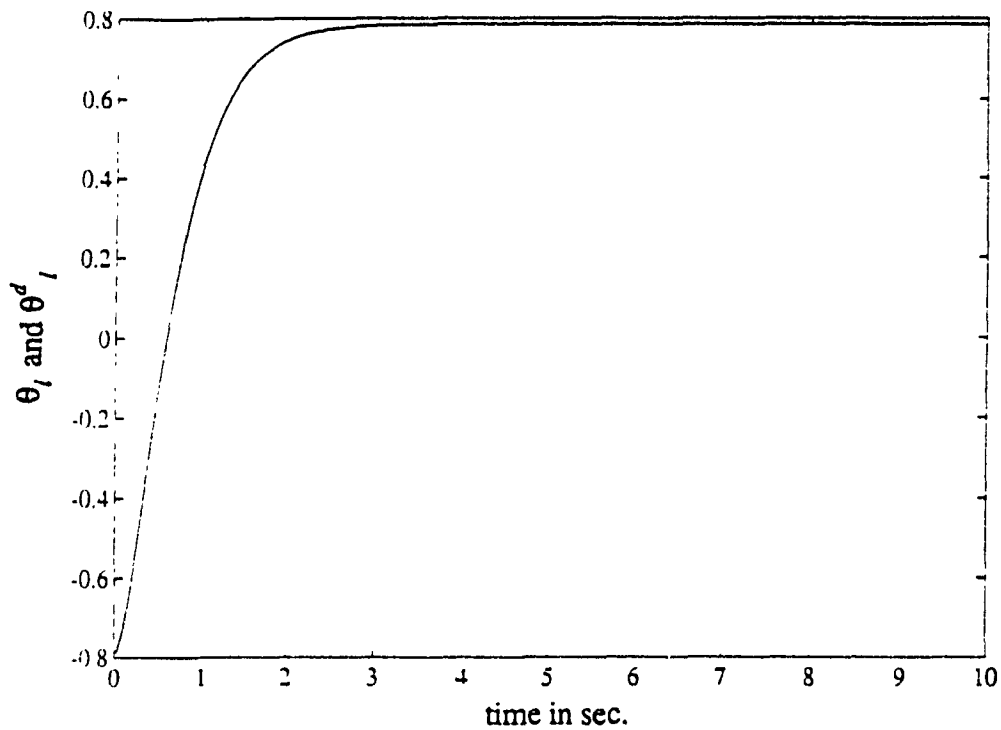


Figure 9. The position response of the reduced order slow subsystem (single link flexible manipulator) using linear non-adaptive control of Seraji. — denotes the desired trajectory and - - denotes the actual trajectory.

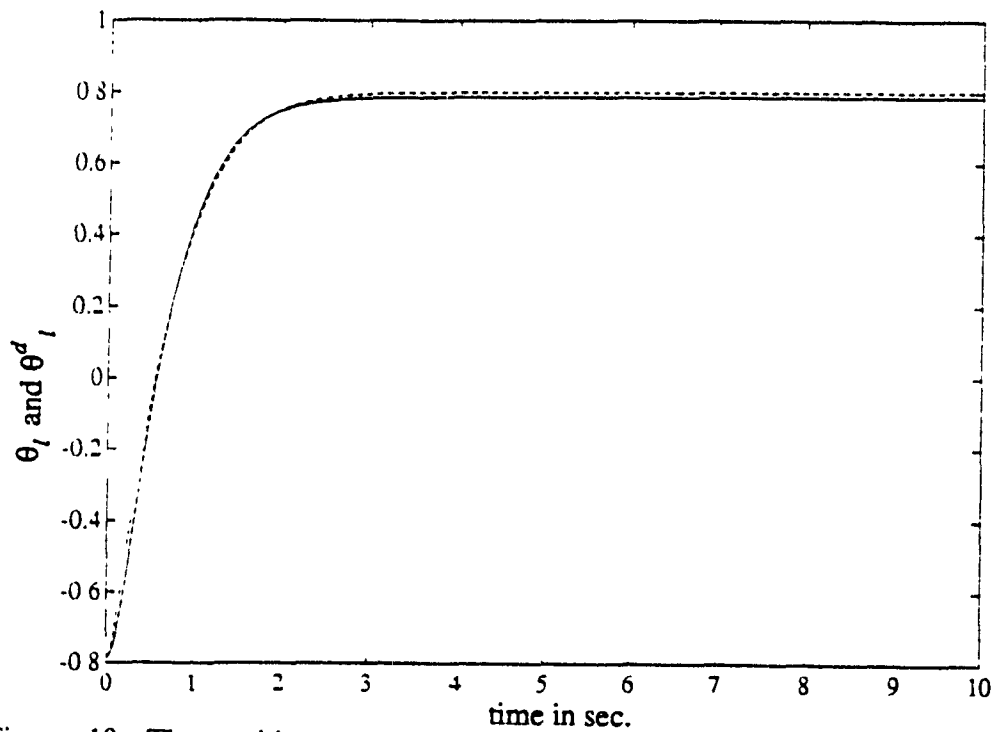


Figure 10. The position response of the reduced order slow subsystem (single link flexible manipulator) using linear non-adaptive control of Seraji. The uncertainty in the parameters is 20%. — denotes the desired trajectory and - - denotes the actual trajectory.

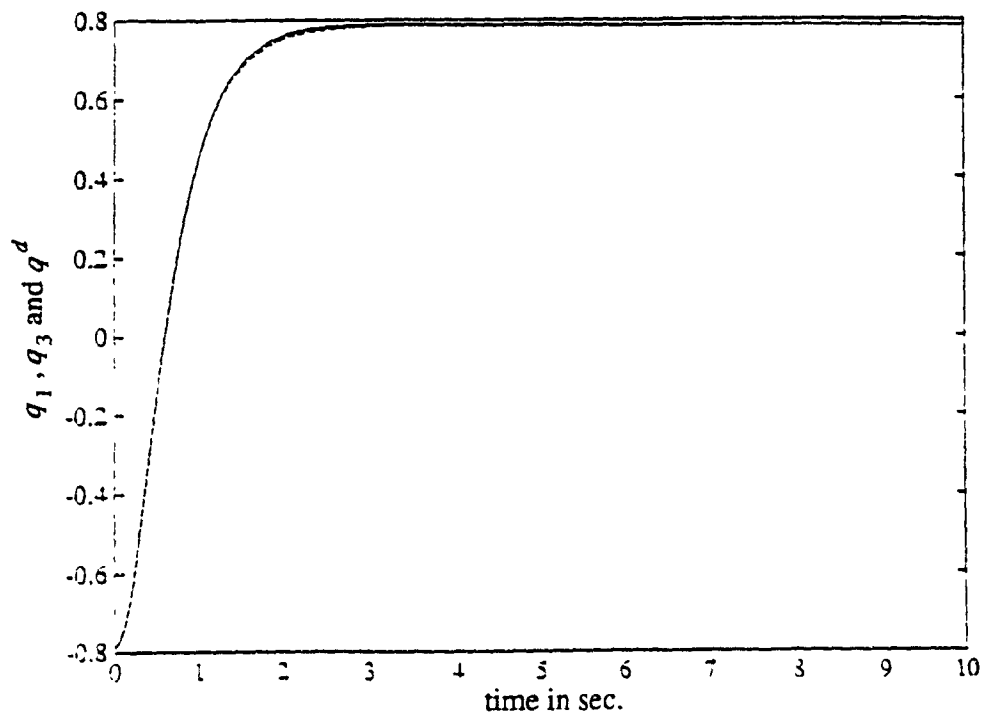


Figure 11. The position response of the reduced order slow subsystem (two link flexible manipulator) using linear non-adaptive control of Seraji. — denotes the desired trajectory, - - denotes the response of the first link and ... denotes that of the second link.

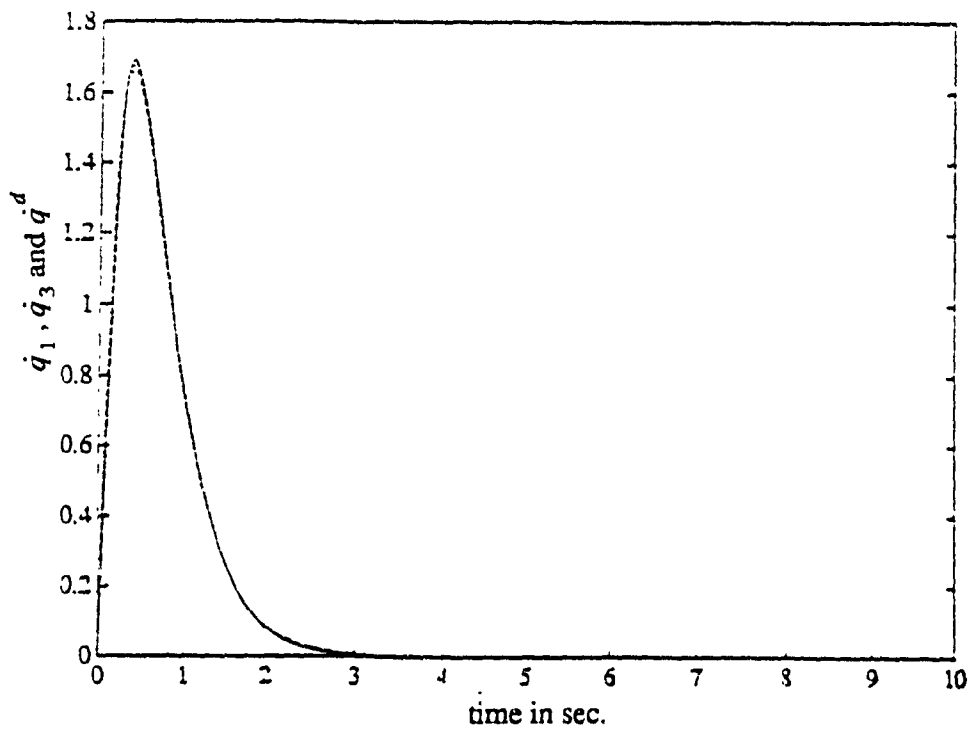


Figure 12. The velocity response of the reduced order slow subsystem (two link flexible manipulator) using linear non-adaptive control of Seraji. — denotes the desired trajectory, - - denotes the response of the first link and ... denotes that of the second link.

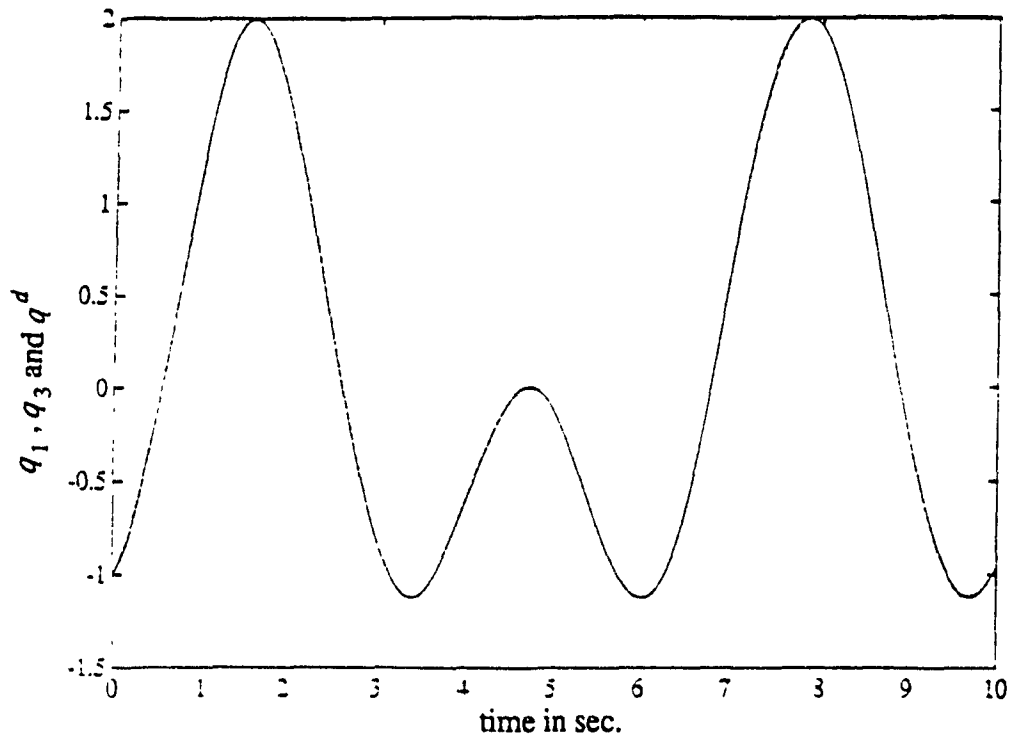


Figure 13. The position response of the reduced order slow subsystem (two link flexible manipulator) using linear adaptive control of Seraji. The uncertainty in the parameters is 20%. — denotes the desired trajectory, - - denotes the response of the first link and ... denotes that of the second link.

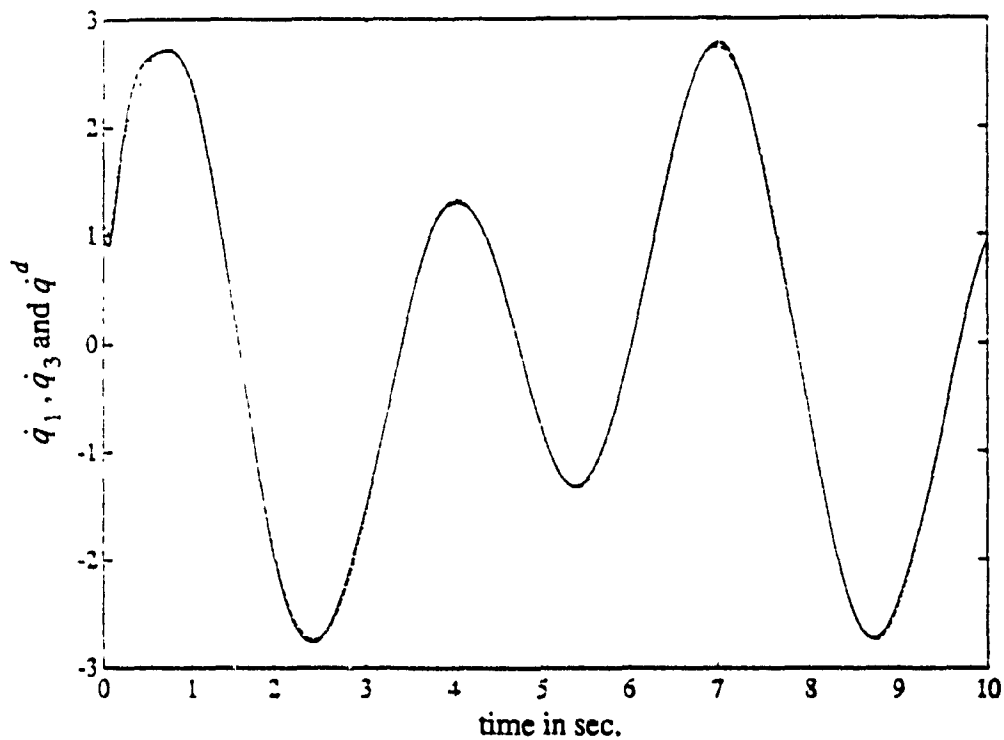


Figure 14. The velocity response of the reduced order slow subsystem (two link flexible manipulator) using linear adaptive control of Seraji. The uncertainty in the parameters is 20%. — denotes the desired trajectory, - - denotes the response of the first link and ... denotes that of the second link.

tively. The steady state position and velocity errors were reduced to zero as shown in figures 15 and 16. However when the uncertainty in the parameters of the system were assumed to be 20%, the steady state position error did not converge to zero though the system remained stable as shown in figures 17 and 18. This error is due to the mismatch in the controller and system parameters.

Passivity Based Control Methods

This scheme described in section 4.b, exploits the skew symmetry property of the robot dynamics and does not lead to a closed loop linear system. The main advantage of this scheme over other schemes is that it does not require measurement of manipulator acceleration or inversion of inertia matrix.

The control laws for the reduced order single link and two link flexible joint manipulators are given by (4.32) and (4.41) respectively. On application of these control laws to the reduced order models obtained with nominal values the steady state position and velocity errors were reduced to zero as shown in figures 19 and 20. When the control laws were applied to the models whose parameter uncertainty was assumed to be 20%, the steady state position and velocity errors were reduced to zero due to the adaptation process as shown in figures 21 and 22.

Inverse Dynamics Method

Unlike the nonlinear passivity based adaptive control scheme, this method requires the measurement of the manipulator acceleration and inversion of inertia matrix.

The control laws for the reduced order single link and two link flexible joint manipulators are given by (4.56) and (4.58). When these control laws were applied to the "nominal" reduced order models, the steady state position and velocity errors were reduced to zero as shown in figures 23 and 24. They were equally effective when applied to models with 20% parameter uncertainty as can be seen from figures 25 and 26.

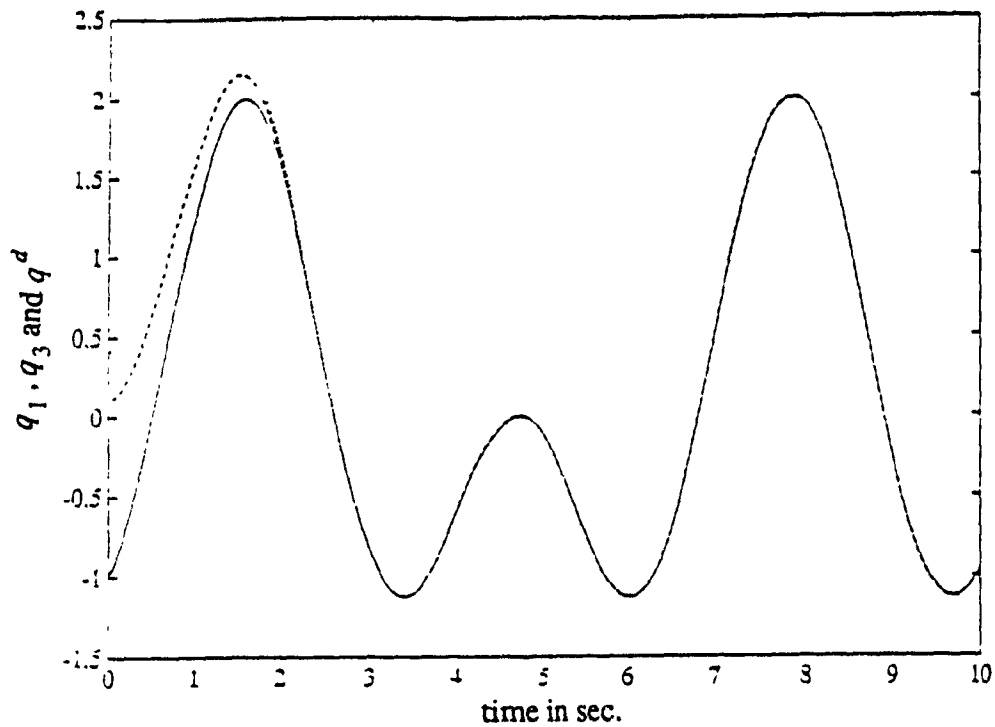


Figure 15. The position response of the reduced order slow subsystem (two link flexible manipulator) using non-linear non-adaptive controller (feedback linearization). — denotes the desired trajectory, - - denotes the response of the first link and ... denotes that of the second link.

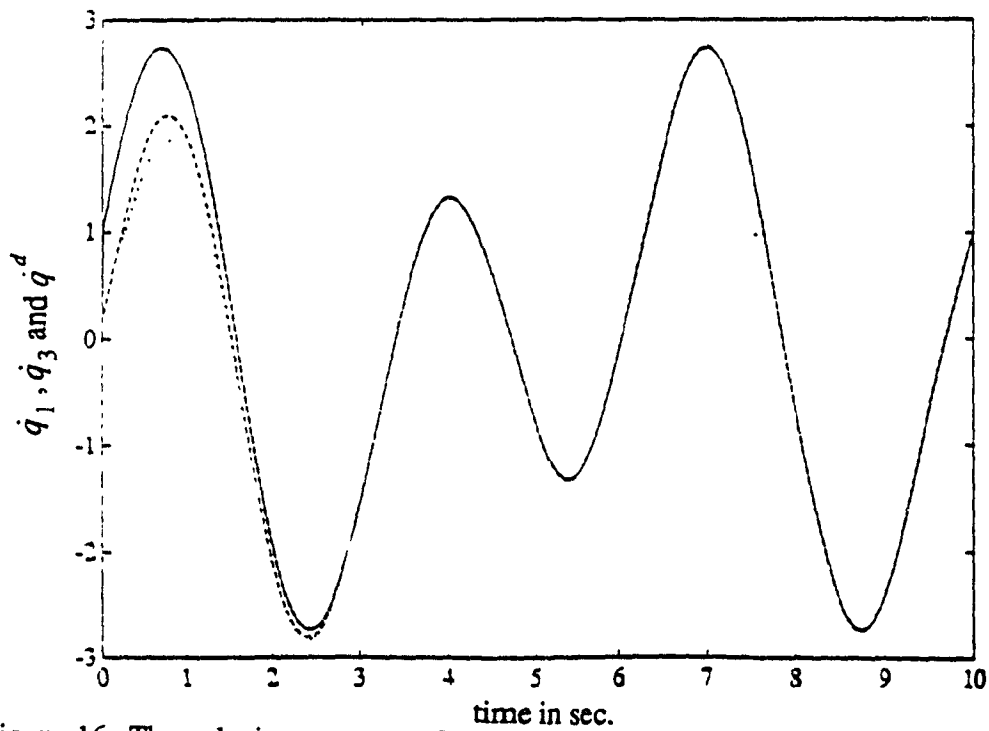


Figure 16. The velocity response of the reduced order slow subsystem (two link flexible manipulator) using non-linear non-adaptive controller (feedback linearization). — denotes the desired trajectory, - - denotes the response of the first link and ... denotes that of the second link.

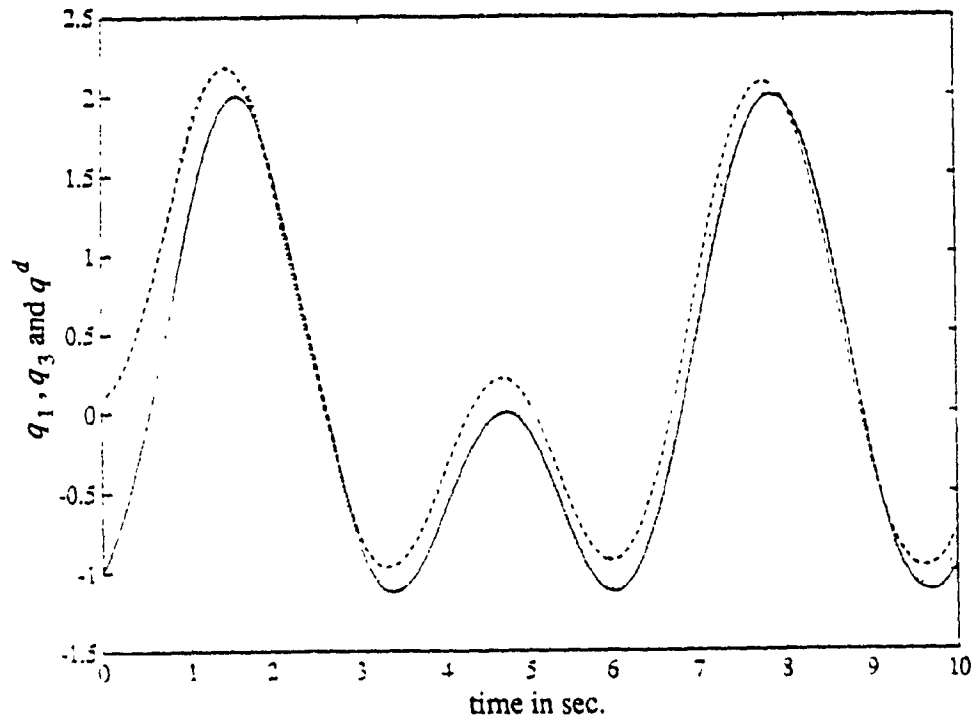


Figure 17. The position response of the reduced order slow subsystem (two link flexible manipulator) using non-linear non-adaptive controller (feedback linearization). The uncertainty in the parameters is 20%. — denotes the desired trajectory, - - denotes the response of the first link and ... denotes that of the second link.

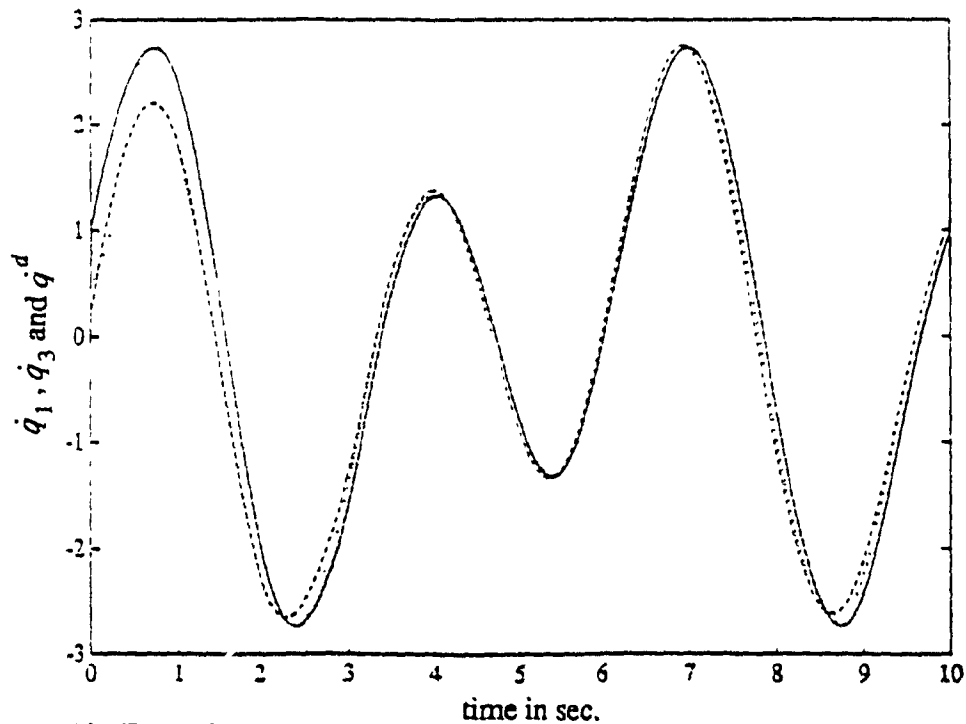


Figure 18. The velocity response of the reduced order slow subsystem (two link flexible manipulator) using non-linear non-adaptive controller (feedback linearization). The uncertainty in the parameters is 20%. — denotes the desired trajectory, - - denotes the response of the first link and ... denotes that of the second link.

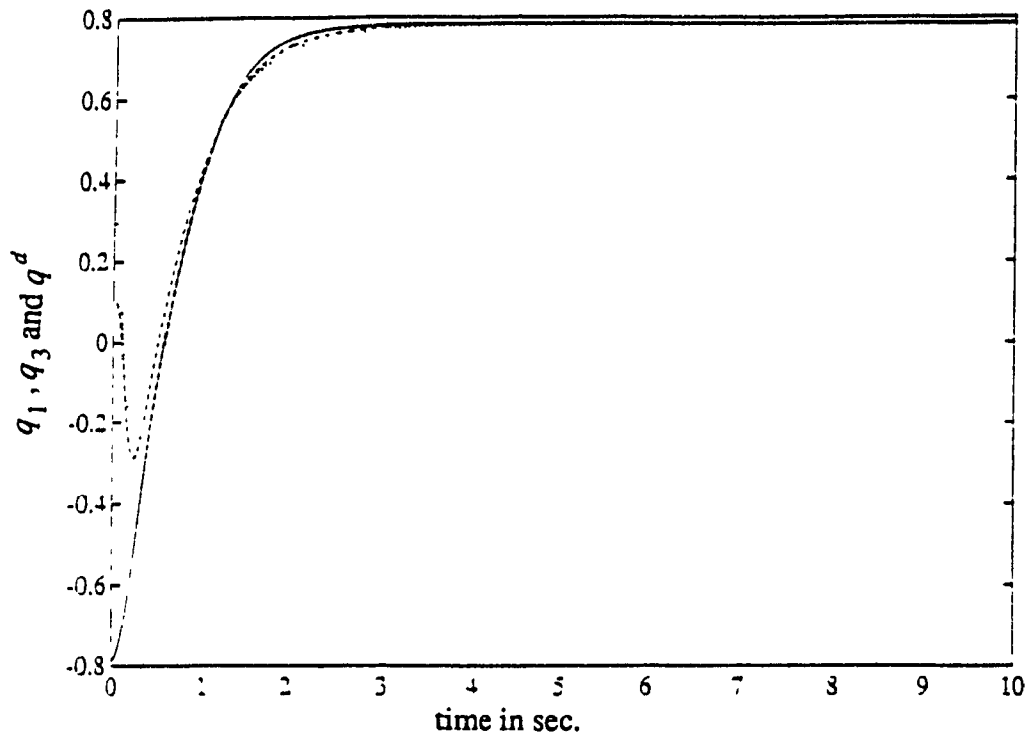


Figure 19. The position response of the reduced order slow subsystem (two link flexible manipulator) using non-linear passive adaptive control of Slotine and Li. — denotes the desired trajectory, - - denotes the response of the first link and ... denotes that of the second link.

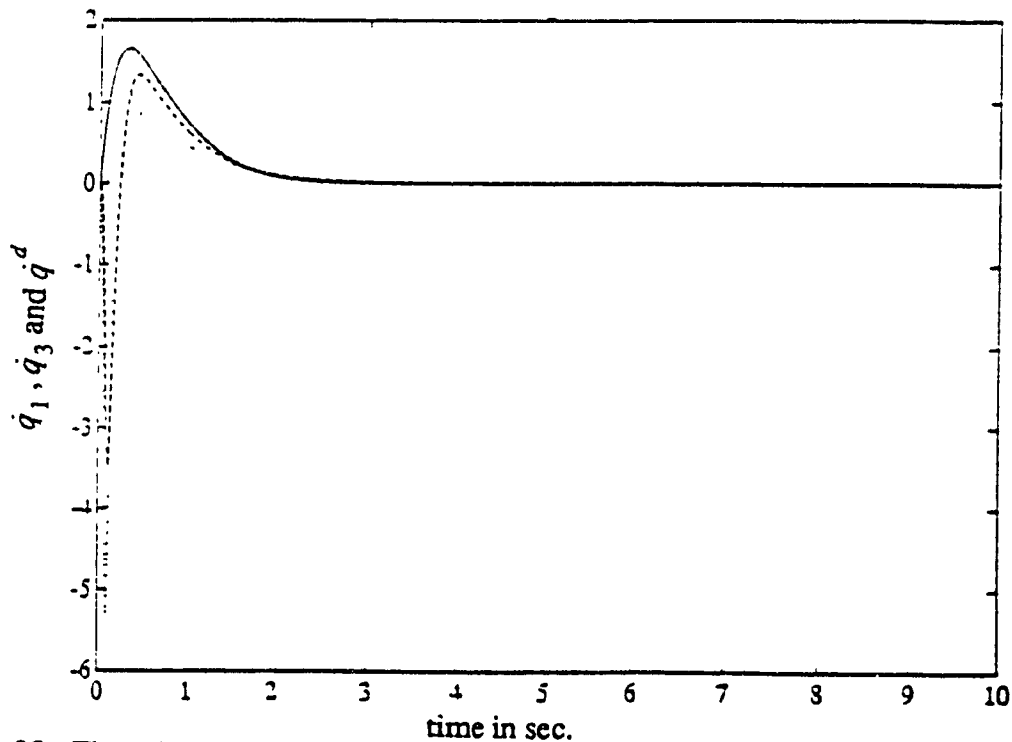


Figure 20. The velocity response of the reduced order slow subsystem (two link flexible manipulator) using non-linear passive adaptive control of Slotine and Li. — denotes the desired trajectory, - - denotes the response of the first link and ... denotes that of the second link.

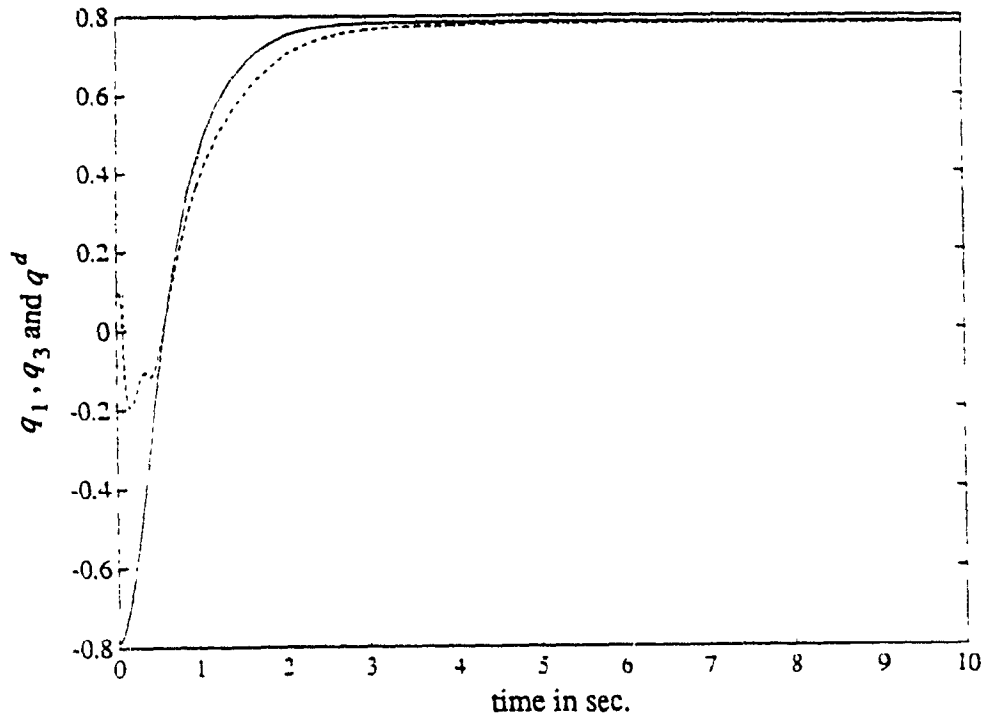


Figure 21. The position response of the reduced order slow subsystem (two link flexible manipulator) using non-linear passive adaptive control of Slotine and Li. The uncertainty in the parameters is 20%. — denotes the desired trajectory, - - denotes the response of the first link and ... denotes that of the second link.

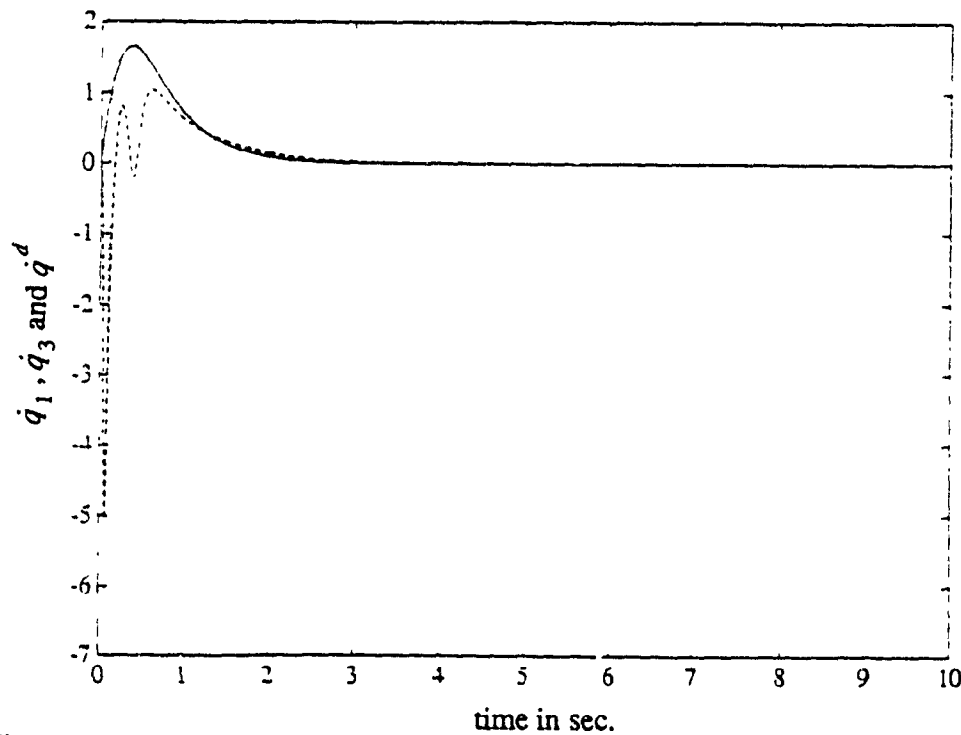


Figure 22. The velocity response of the reduced order slow subsystem (two link flexible manipulator) using non-linear passive adaptive control of Slotine and Li. The uncertainty in the parameters is 20%. — denotes the desired trajectory, - - denotes the response of the first link and ... denotes that of the second link.

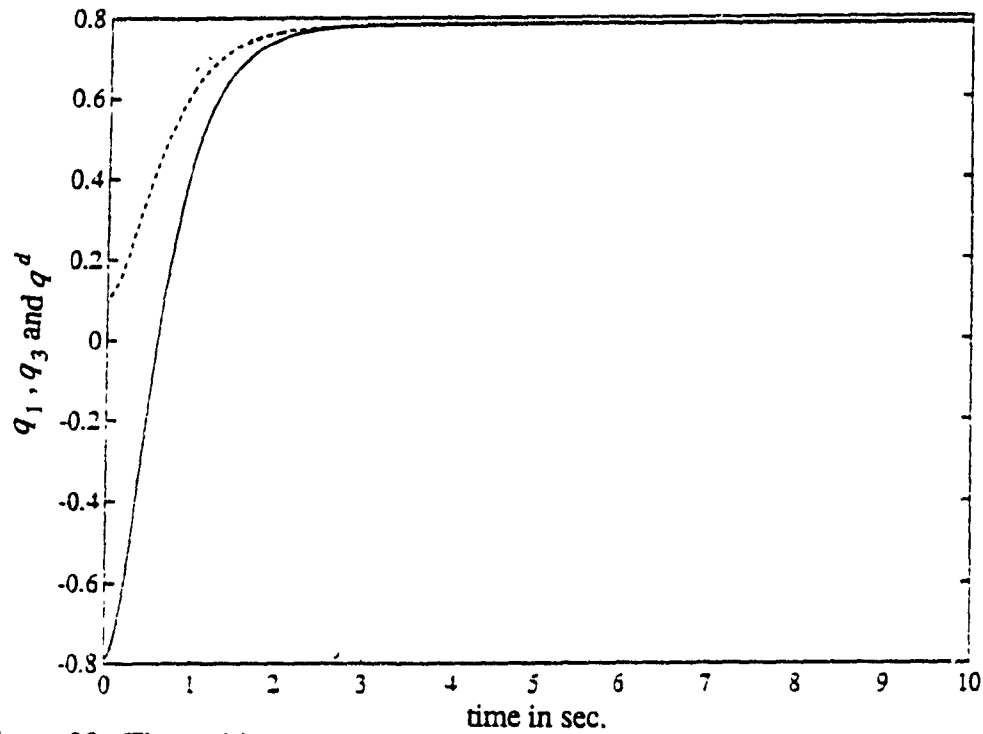


Figure 23. The position response of the reduced order slow subsystem (two link flexible manipulator) using non-linear adaptive control of Craig et al. — denotes the desired trajectory, - - denotes the response of the first link and ... denotes that of the second link.

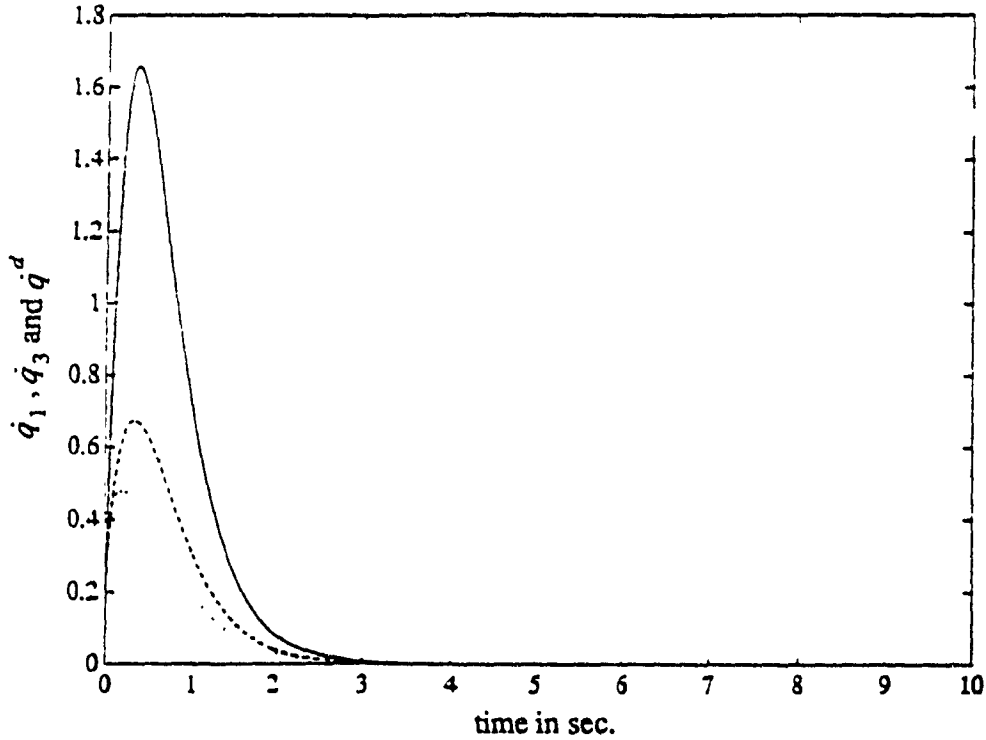


Figure 24. The velocity response of the reduced order slow subsystem (two link flexible manipulator) using non-linear adaptive control of Craig et al. — denotes the desired trajectory, - - denotes the response of the first link and ... denotes that of the second link.

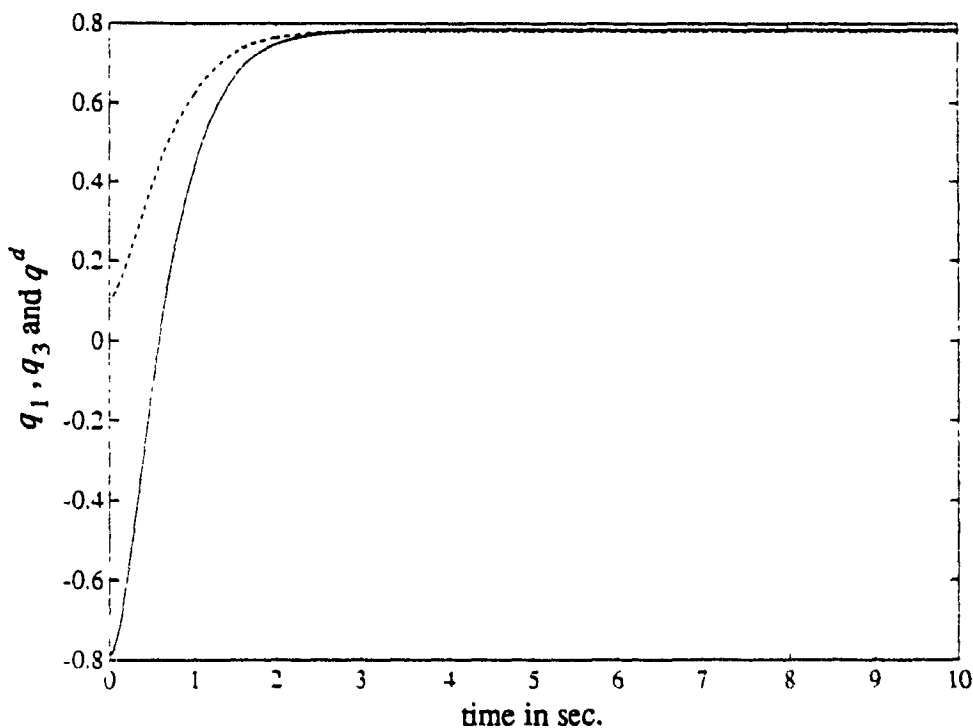


Figure 25. The position response of the reduced order slow subsystem (two link flexible manipulator) using non-linear adaptive control of Craig et al. The uncertainty in the parameters is 20%. — denotes the desired trajectory, - - denotes the response of the first link and ... denotes that of the second link.

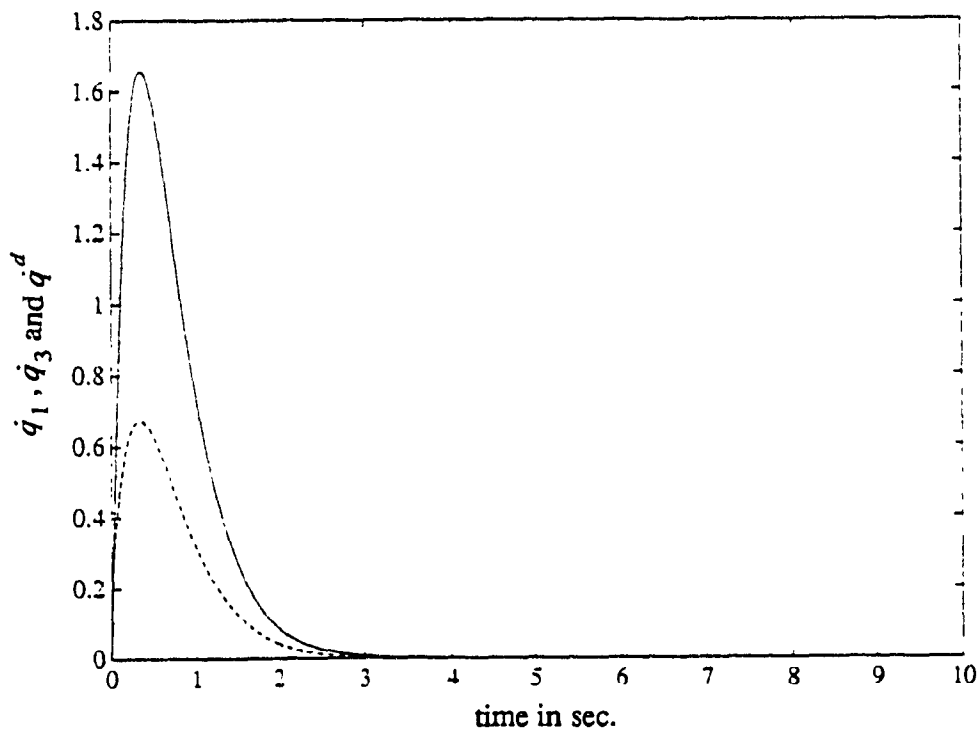


Figure 26. The velocity response of the reduced order slow subsystem (two link flexible manipulator) using non-linear adaptive control of Craig et al. The uncertainty in the parameters is 20%. — denotes the desired trajectory, - - denotes the response of the first link and ... denotes that of the second link.

The fast subsystem was simulated and found to be stable as shown in figure 27. In all simulations involving the two link flexible joint manipulator, we assumed for the sake of simplicity that the gear ratio and actuator inertia are known and $n_1^2 J_1 = n_2^2 J_2 = 1$.

5.b Full Order Model

When the rigid control laws (linear/ nonlinear, nonadaptive/ adaptive) that were developed in Chapters 3 and 4 based on the reduced order model were applied to the full order system, it resulted in instability. As can be seen from figures 28 and 29, the flexible system is unstable. Therefore a fast controller is added to the rigid controller to ensure asymptotic stability of the full order system. A state feedback fast controller was used to damp out the oscillations due to joint flexibility. The motivation for using a state feedback controller instead of an adaptive control is that as the perturbation parameter ϵ was increased from the nominal value of $\epsilon = 0.1$, it was found that with a state feedback fast controller stability of the full order system was possible at a higher value of ϵ whereas stability was not possible with an adaptive fast controller. A composite controller is designed based on the reduced order slow and fast subsystem control laws to control the full order flexible system (2.5)-(2.6) that takes the form

$$U = U^s(q, \dot{q}) + U^f(\eta_1, \eta_2).$$

The rigid body dynamics were easily simulated using MATLAB. However the full order system dynamics could not be simulated on MATLAB because they were too stiff. Hence the simulations were carried out on VAX/VMS computer using IMSL subroutines.

Linear Control Methods

PD Nonadaptive Control Scheme

The full order models of single link manipulator given by (2.19a)-(2.19d) and a two link flexible joint manipulator given by (2.24)-(2.25) were simulated with composite con-

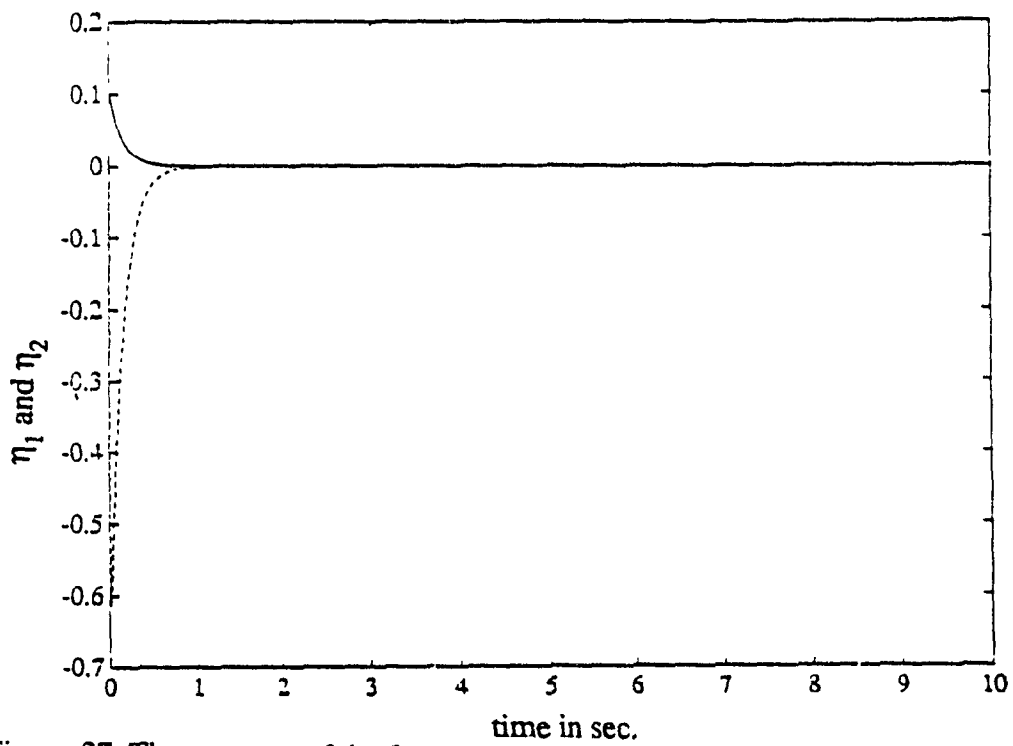


Figure 27. The response of the fast variables (single link manipulator).

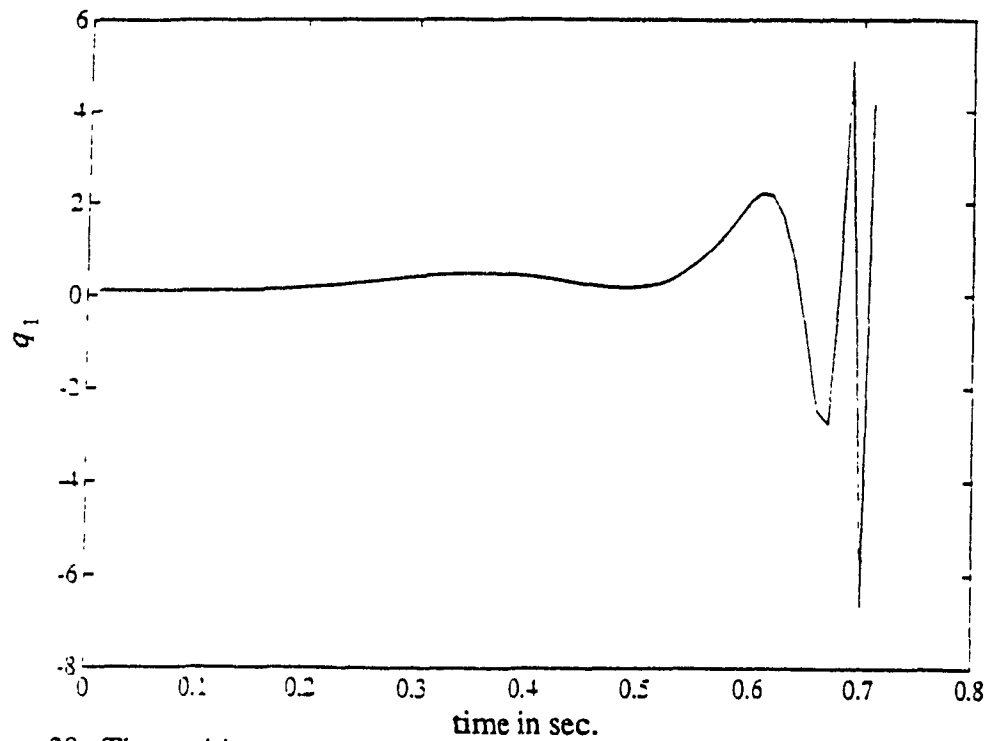


Figure 28. The position response of the full order system (two link flexible manipulator) using only the slow controller. The perturbation parameter is 0.1.

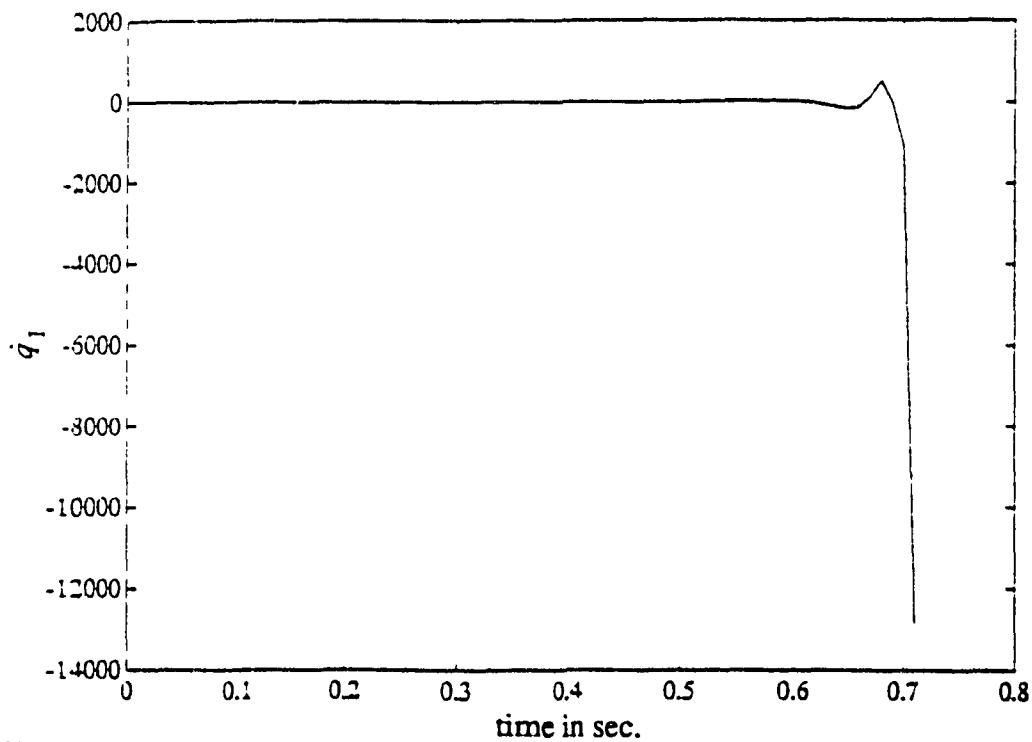


Figure 29. The velocity response of the full order system (two link flexible manipulator) using only the slow controller. The perturbation parameter is 0.1.

trol laws using the nominal values given earlier. The slow component of the composite controller for the single link manipulator is given by (3.18) and the fast component by (3.19). For the two link manipulator the slow component is given by (3.23) and the fast component by (3.24). Figures 30 and 31 show the unstable position and velocity response for the two link flexible joint manipulator. However when the single link flexible joint manipulator was simulated using the same control laws, the steady state position and velocity errors were reduced to zero as shown in figures 32 and 33. The explanation for this behavior is that the dynamics of the two link manipulator is more nonlinear when compared to that of the single link manipulator. Figures 34 and 35 show the response of the single link flexible joint manipulator when ϵ was increased to 0.2 from its nominal value of 0.1. When the parameters of the system (single link manipulator) were changed from their nominal values by 20% the steady state position error did not converge to zero though the system remained stable as shown in figures 36 and 37. This error is due to the mismatch in the controller and system parameters.

PD Adaptive Control Scheme

In order to overcome the drawback due to the mismatch between the controller and system parameters, keeping the controller the same as in the previous case, we update the coefficients of the controller by the adaptive laws given by (3.49a)-(3.49f). The gains associated with the adaptive laws had to be reduced by nearly ten fold from their corresponding values for the reduced order model for successful tracking. On simulating the "nominal" full order models of the single link and two link flexible joint manipulators, the steady state position and velocity errors were reduced to zero as shown in figures 38 and 39. Figure 40 and 41 show the response of the two link flexible joint manipulator when ϵ was increased to 0.2 from its nominal value of 0.1. Due to the adaptation process, the system responds equally well when the parameters of the system have been changed by 20% as shown in figures 42 and 43.

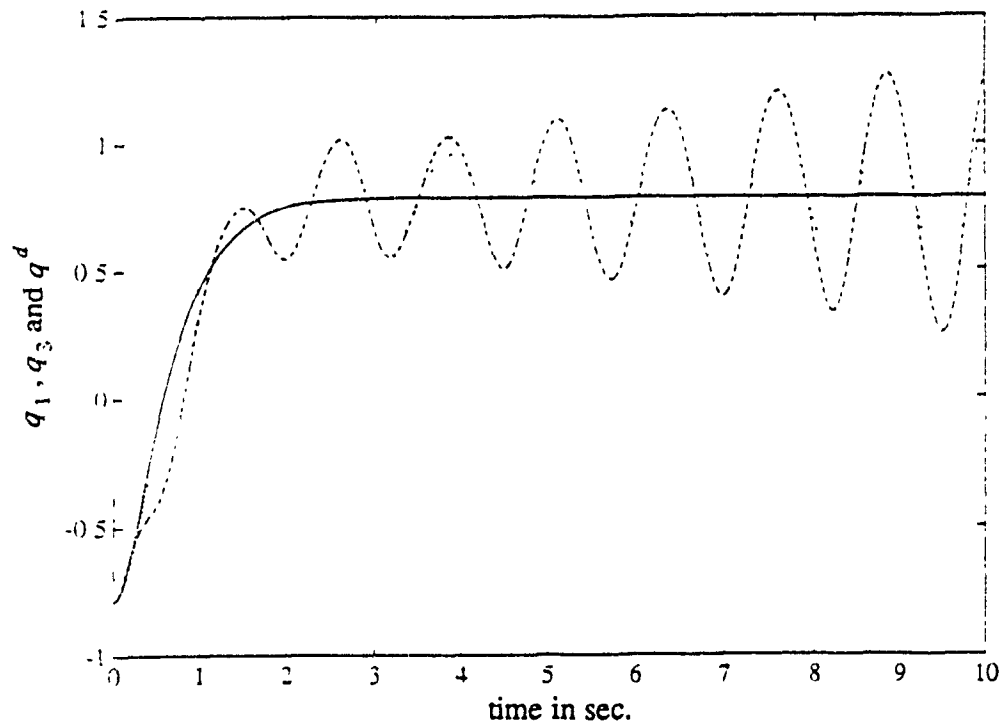


Figure 30. The position response of the full order system (two link flexible manipulator) using linear non-adaptive control of Seraji. The perturbation parameter is 0.1. — denotes the desired trajectory, - - denotes the response of the first link and ... denotes that of the second link.

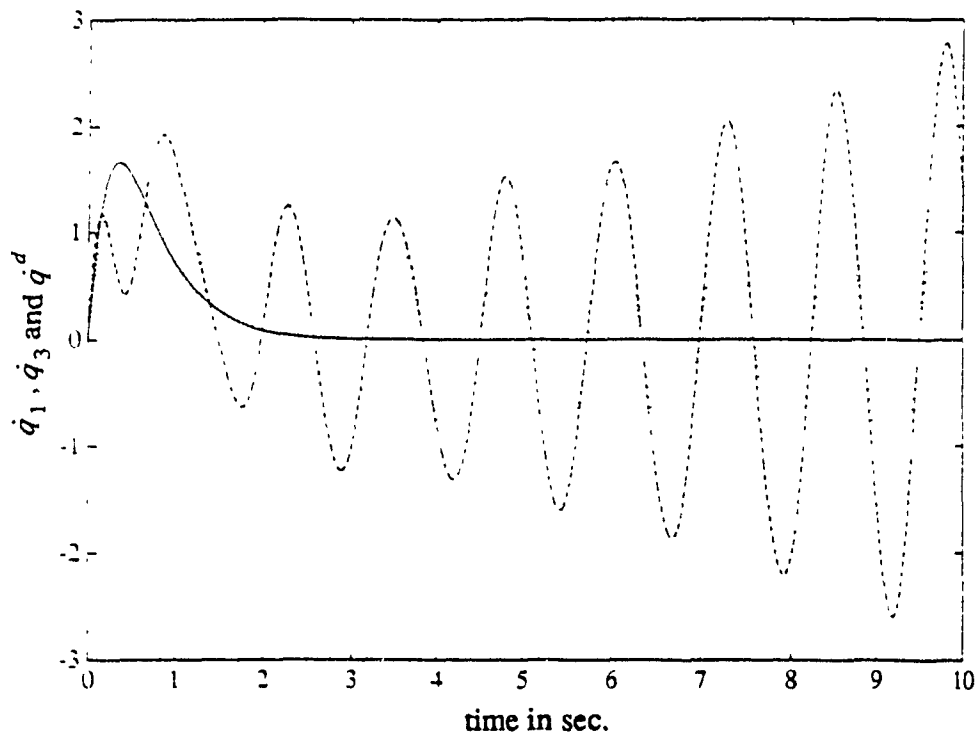


Figure 31. The velocity response of the full order system (two link flexible manipulator) using linear non-adaptive control of Seraji. The perturbation parameter is 0.1. — denotes the desired trajectory, - - denotes the response of the first link and ... denotes that of the second link.

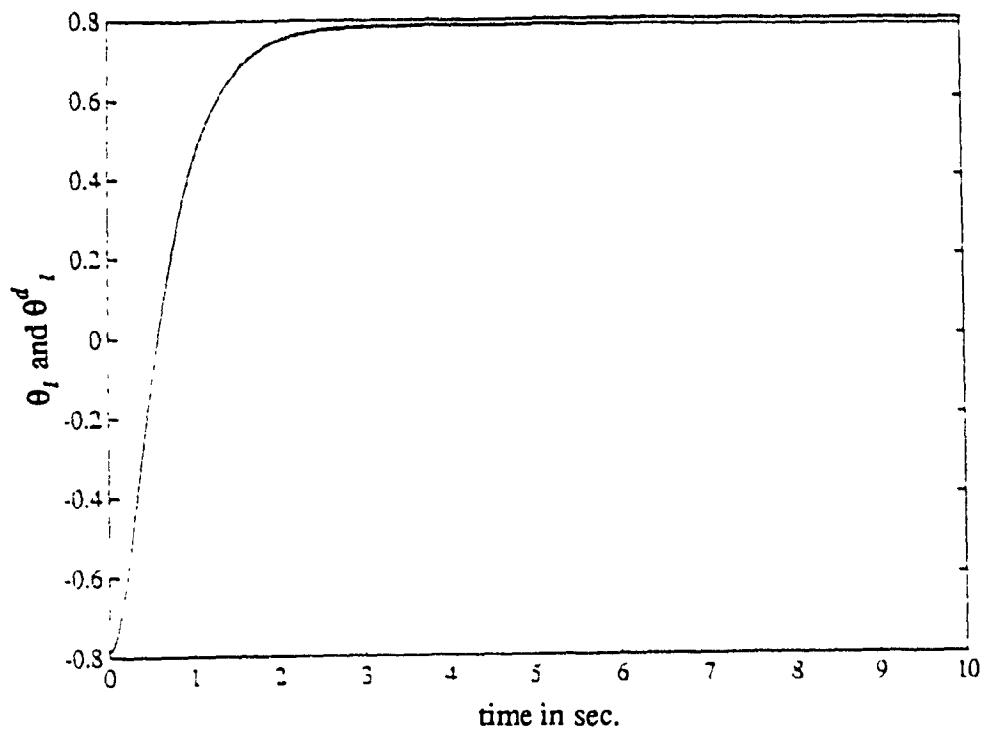


Figure 32. The position response of the full order system (single link flexible manipulator) using linear non-adaptive control of Seraji. The perturbation parameter is 0.1. — denotes the desired trajectory and - - denotes the actual trajectory.

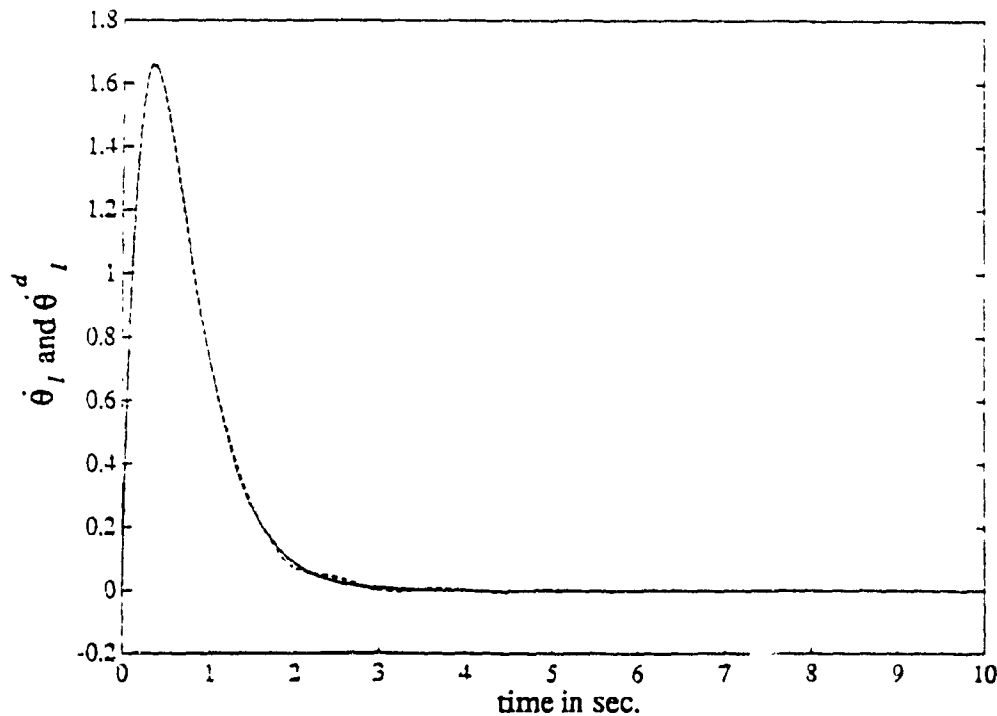


Figure 33. The velocity response of the full order system (single link flexible manipulator) using linear non-adaptive control of Seraji. The perturbation parameter is 0.1. — denotes the desired trajectory and - - denotes the actual trajectory.

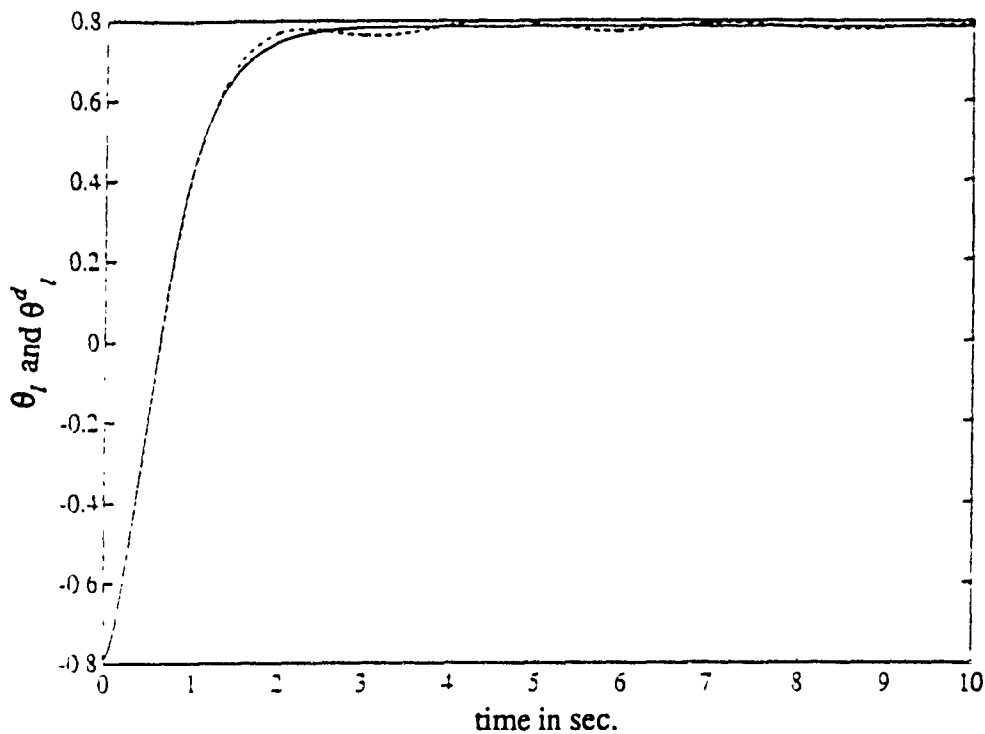


Figure 34. The position response of the full order system (single link flexible manipulator) using linear non-adaptive control of Seraji. The perturbation parameter is 0.2. — denotes the desired trajectory and - - denotes the actual trajectory.

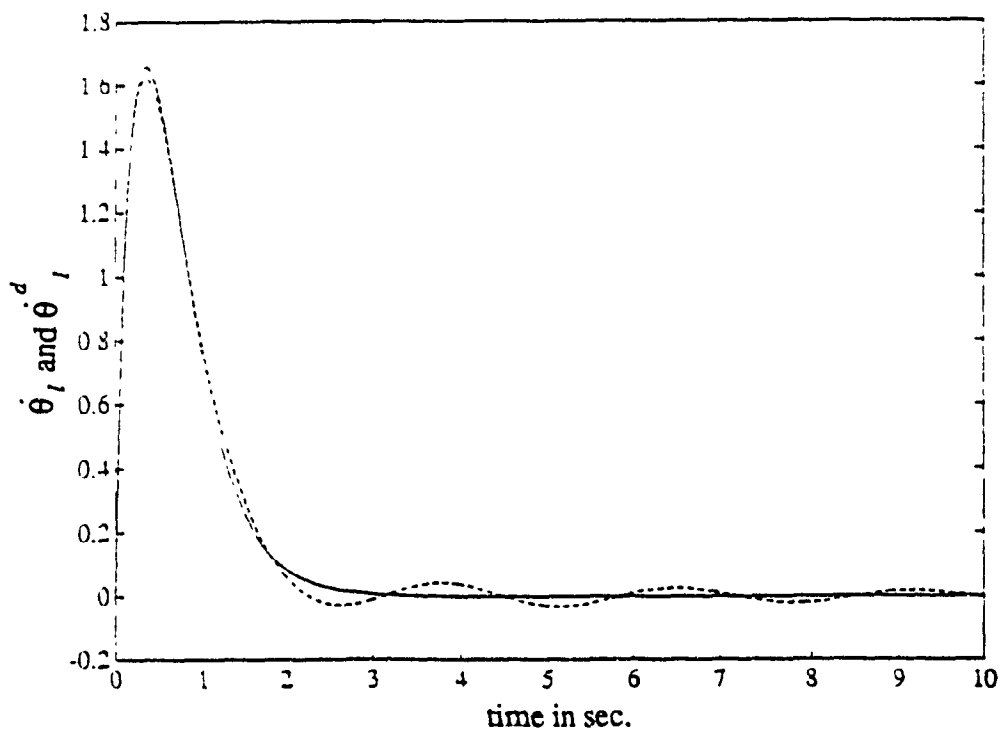


Figure 35. The velocity response of the full order system (single link flexible manipulator) using linear non-adaptive control of Seraji. The perturbation parameter is 0.2. — denotes the desired trajectory and - - denotes the actual trajectory

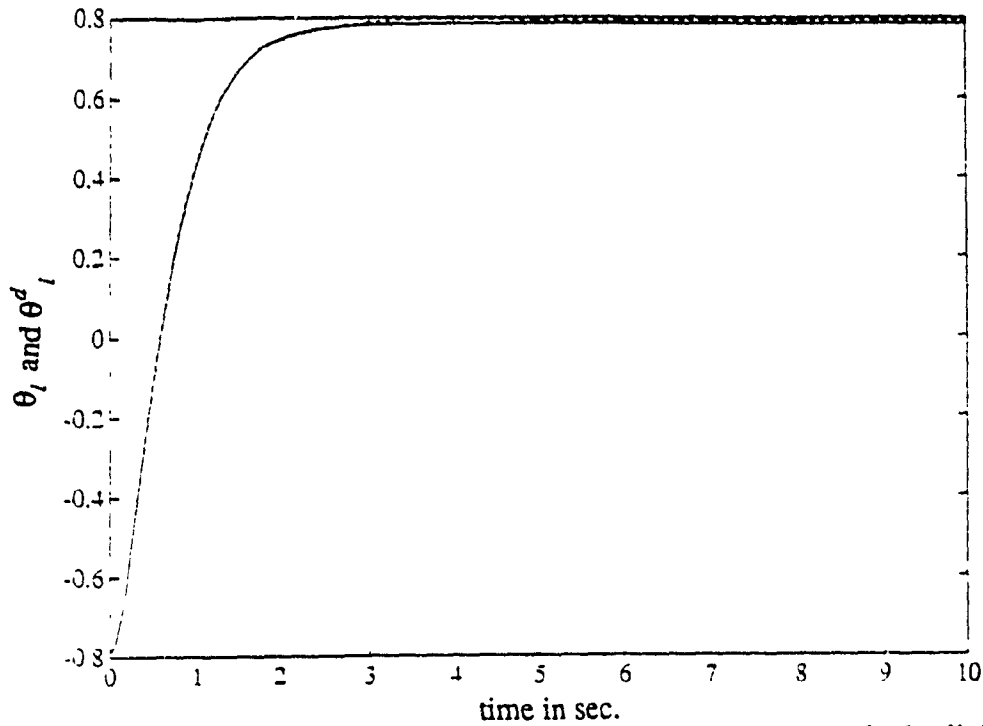


Figure 36. The position response of the full order system (single link flexible manipulator) using linear non-adaptive control of Seraji. The uncertainty in the parameters is 20%. The perturbation parameter is 0.1. — denotes the desired trajectory and - - denotes the actual trajectory.

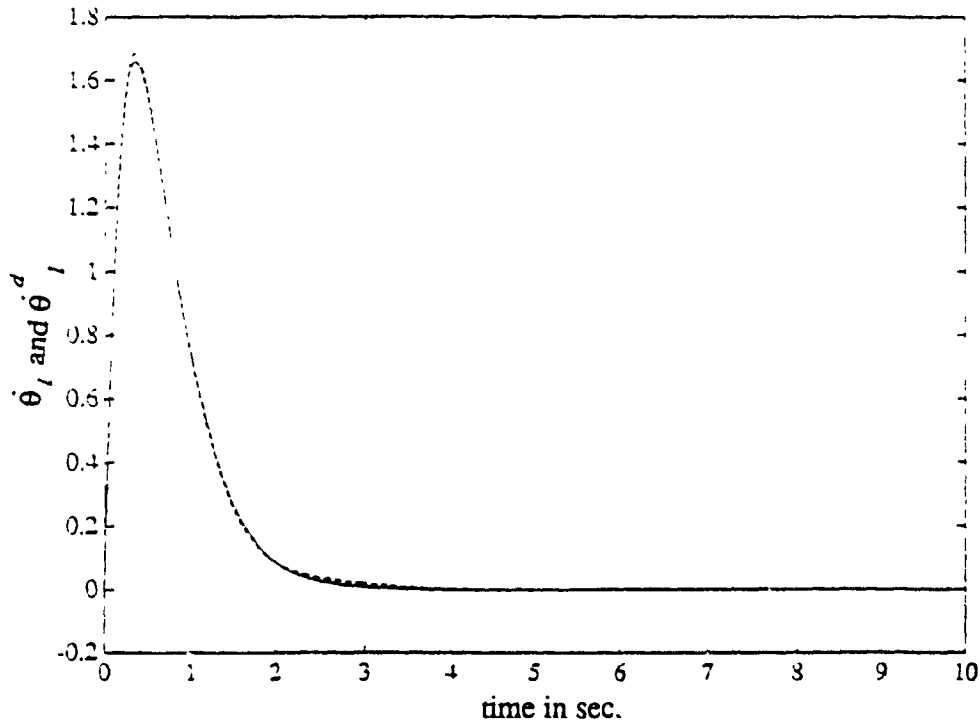


Figure 37. The position response of the full order system (single link flexible manipulator) using linear non-adaptive control of Seraji. The uncertainty in the parameters is 20%. The perturbation parameter is 0.1. — denotes the desired trajectory and - - denotes the actual trajectory.

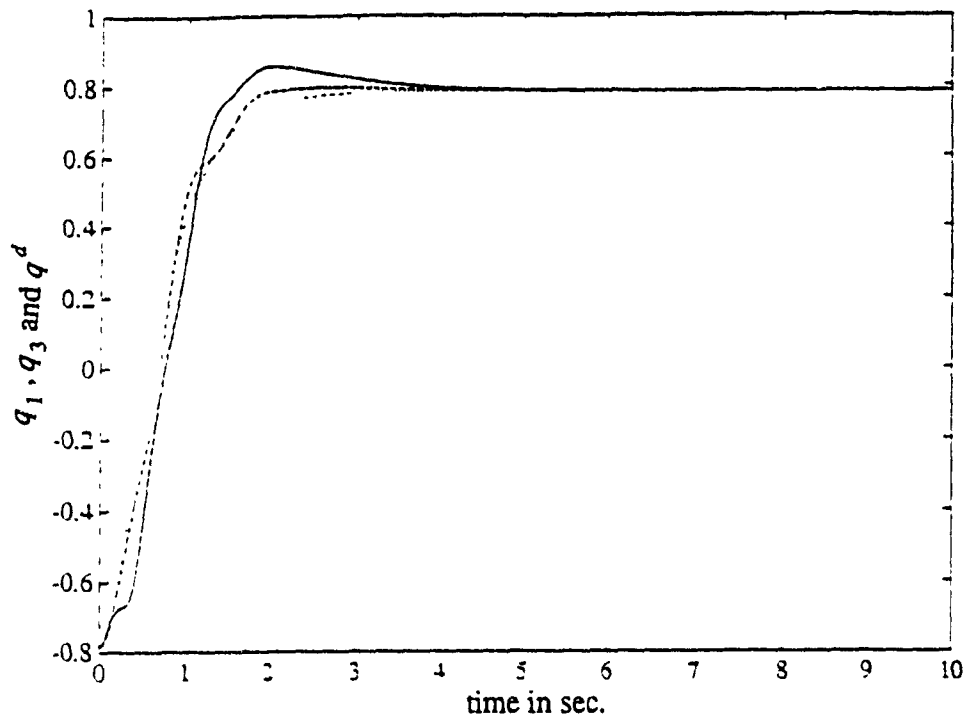


Figure 38. The position response of the full order system (two link flexible manipulator) using linear adaptive control of Seraji. The perturbation parameter is 0.1. — denotes the desired trajectory, - - denotes the response of the first link and ... denotes that of the second link.

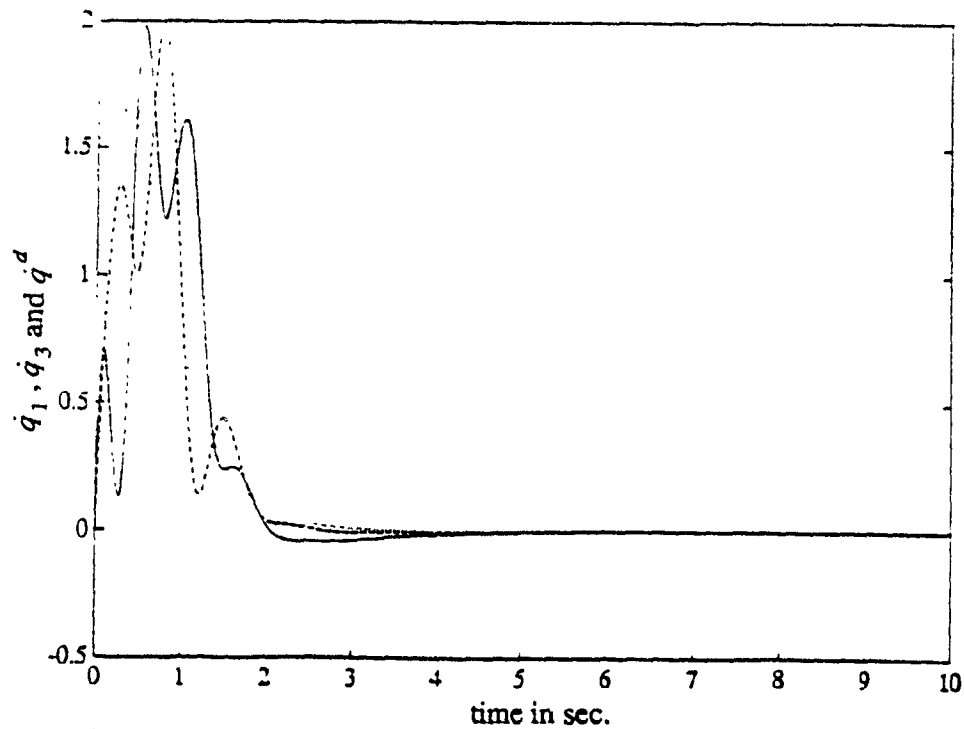


Figure 39. The velocity response of the full order system (two link flexible manipulator) using linear adaptive control of Seraji. The perturbation parameter is 0.2. — denotes the desired trajectory, - - denotes the response of the first link and ... denotes that of the second link.

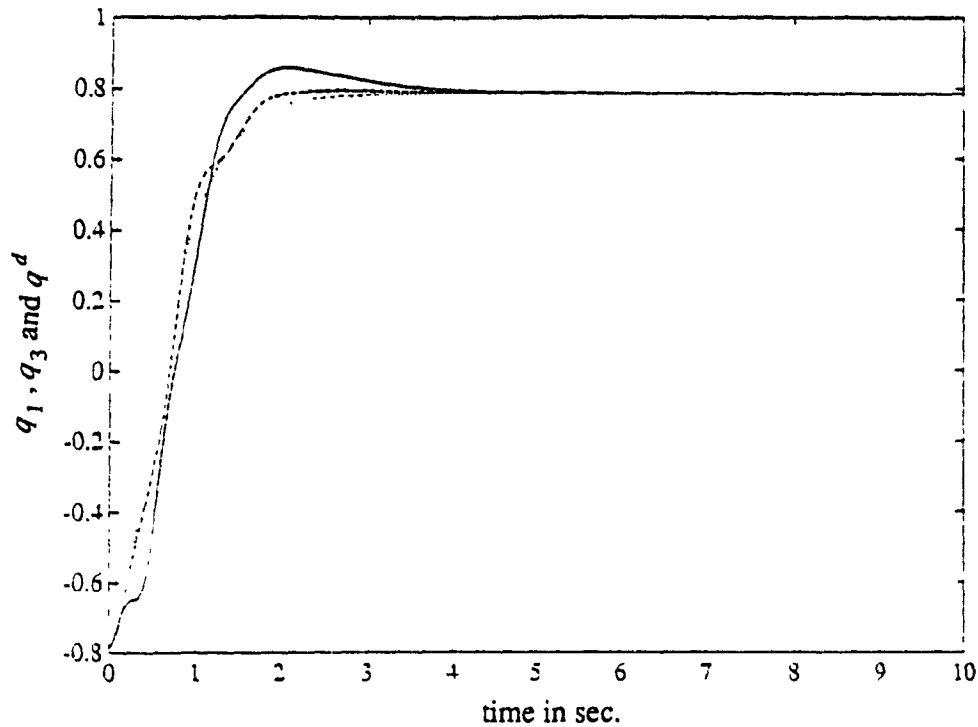


Figure 40. The position response of the full order system (two link flexible manipulator) using linear adaptive control of Seraji. The perturbation parameter is 0.2. — denotes the desired trajectory, - - denotes the response of the first link and ... denotes that of the second link.

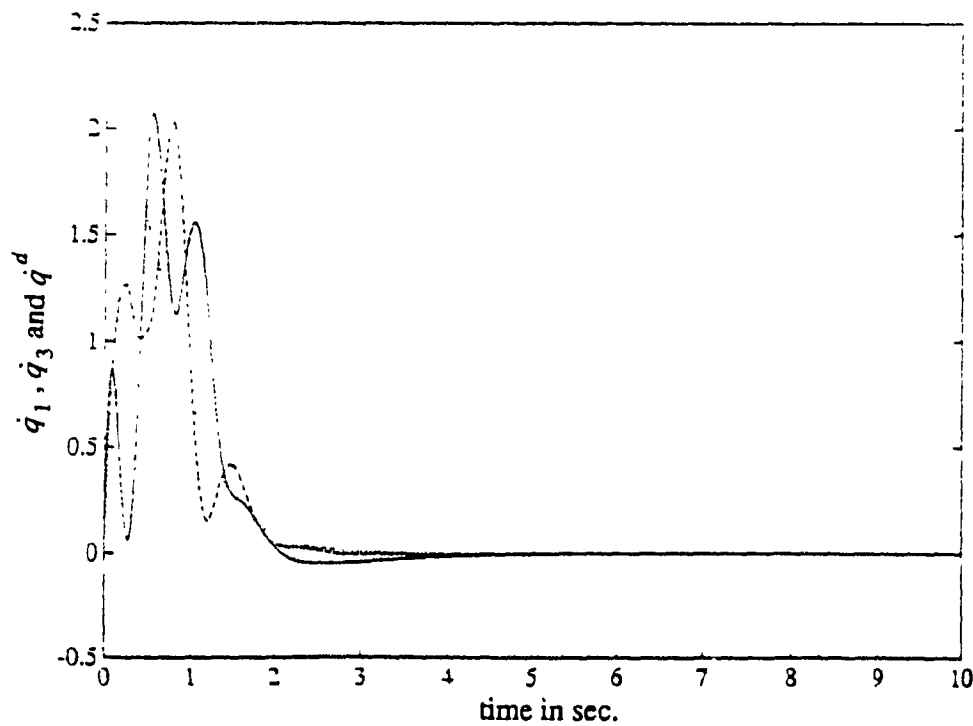


Figure 41. The velocity response of the full order system (two link flexible manipulator) using linear adaptive control of Seraji. The perturbation parameter is 0.2. — denotes the desired trajectory, - - denotes the response of the first link and ... denotes that of the second link.

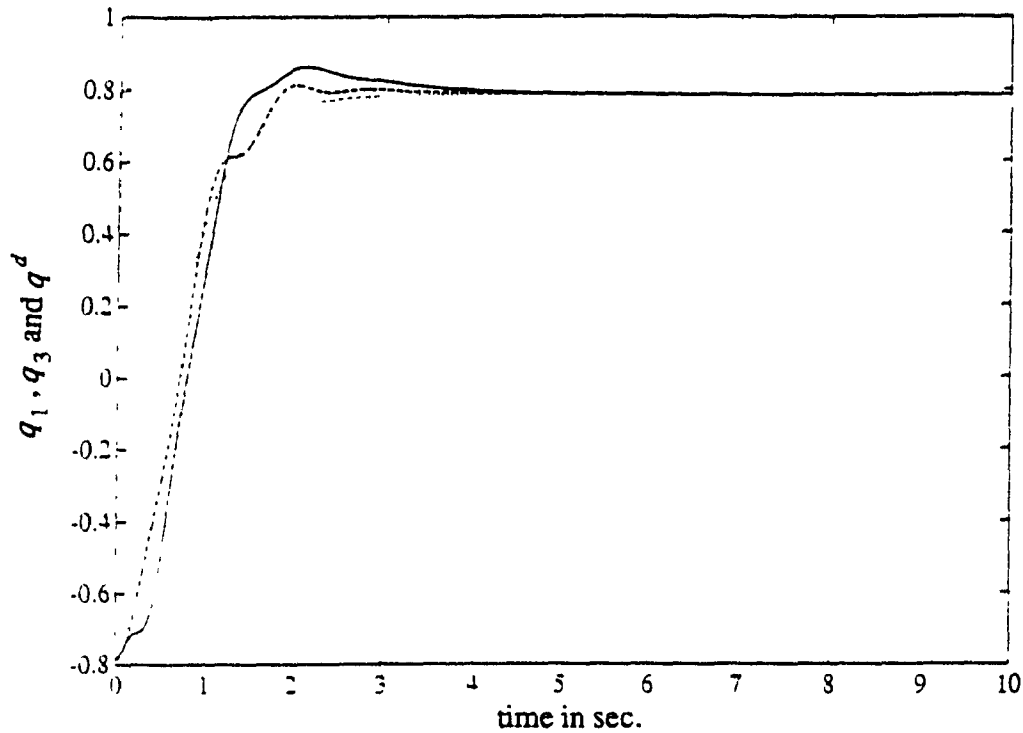


Figure 42. The position response of the full order system (two link flexible manipulator) using linear adaptive control of Seraji. The uncertainty in the parameters is 20%. The perturbation parameter is 0.1. — denotes the desired trajectory, - - denotes the response of the first link and ... denotes that of the second link.

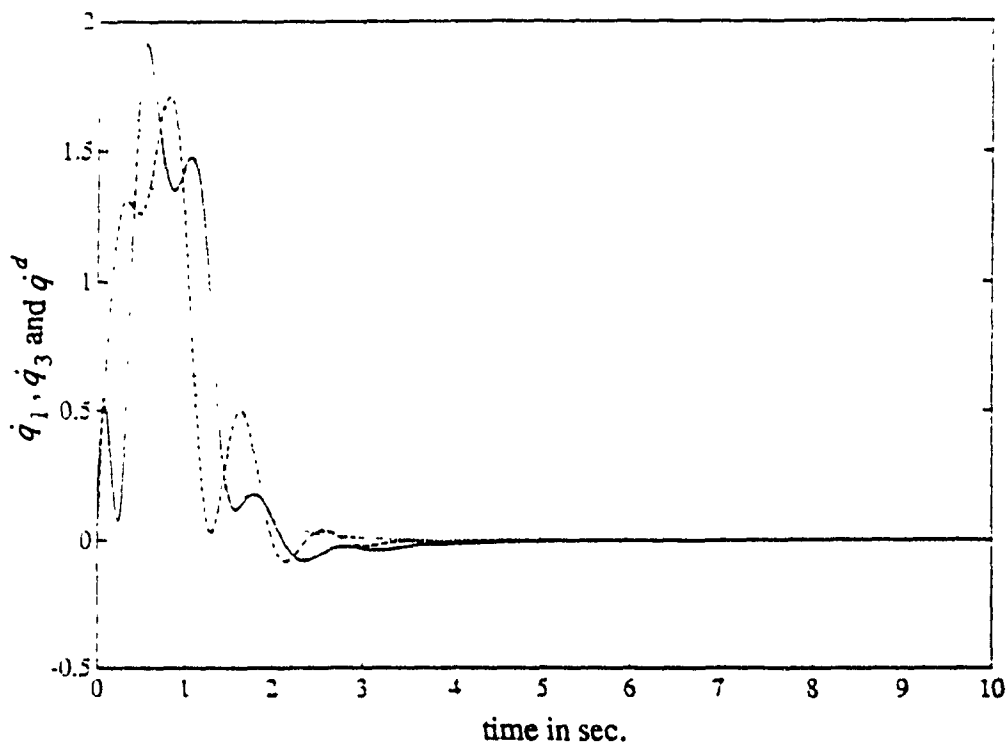


Figure 43. The velocity response of the full order system (two link flexible manipulator) using linear adaptive control of Seraji. The uncertainty in the parameters is 20%. The perturbation parameter is 0.1. — denotes the desired trajectory, - - denotes the response of the first link and ... denotes that of the second link.

5.c Comparison of Linear Control Methods

The main feature of the nonadaptive linear control scheme described in Section 3.a is its simplicity in being implemented in practice. However, when there is a mismatch between the robot model and the feedforward controller, particularly when all physical parameters of the manipulator cannot be measured accurately, the nonadaptive controller leads to a steady state error as shown in figure 13. This drawback is overcome by adapting the controller gains as described in Section 3.b and as shown in figure 16. With the update laws there are now additional differential equations to be solved, increasing the complexity of the system. As a direct consequence the time taken for numerical simulation is also increased.

Nonlinear Control Methods

Feedback Linearization Scheme

The "nominal" full order models of the single link flexible joint manipulator given by (2.19a)-(2.19d) and the two link flexible joint manipulator given by (2.24)-(2.25) were simulated with composite control laws. In the case of the single link flexible joint manipulator the slow component of the composite controller is given by (4.12) and the fast component by (4.13). For the two link flexible joint manipulator the slow component is given by (4.14) and the fast component by (4.15). On simulating the "nominal" full order models, the steady state position and velocity errors were reduced to zero as shown in figures 44 and 45. However when the uncertainty in the parameters of the system was assumed to be 20%, due to the mismatch in the controller and system parameters, the steady state position error did not converge to zero though the system remained stable as shown in figures 46 and 47. Figures 48 and 49 show the response of the two link flexible joint manipulator when ϵ was increased from its nominal value of 0.1.

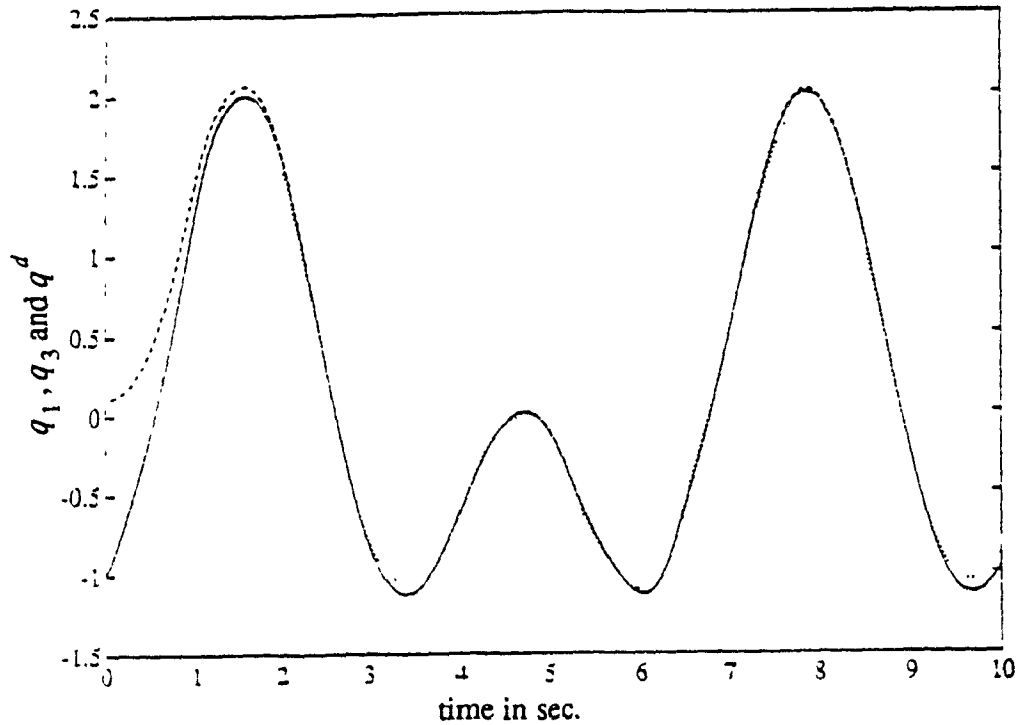


Figure 44. The position response of the full order system (two link flexible manipulator) using non-linear non-adaptive controller (feedback linearization). The perturbation parameter is 0.1. — denotes the desired trajectory, - - denotes the response of the first link and ... denotes that of the second link.

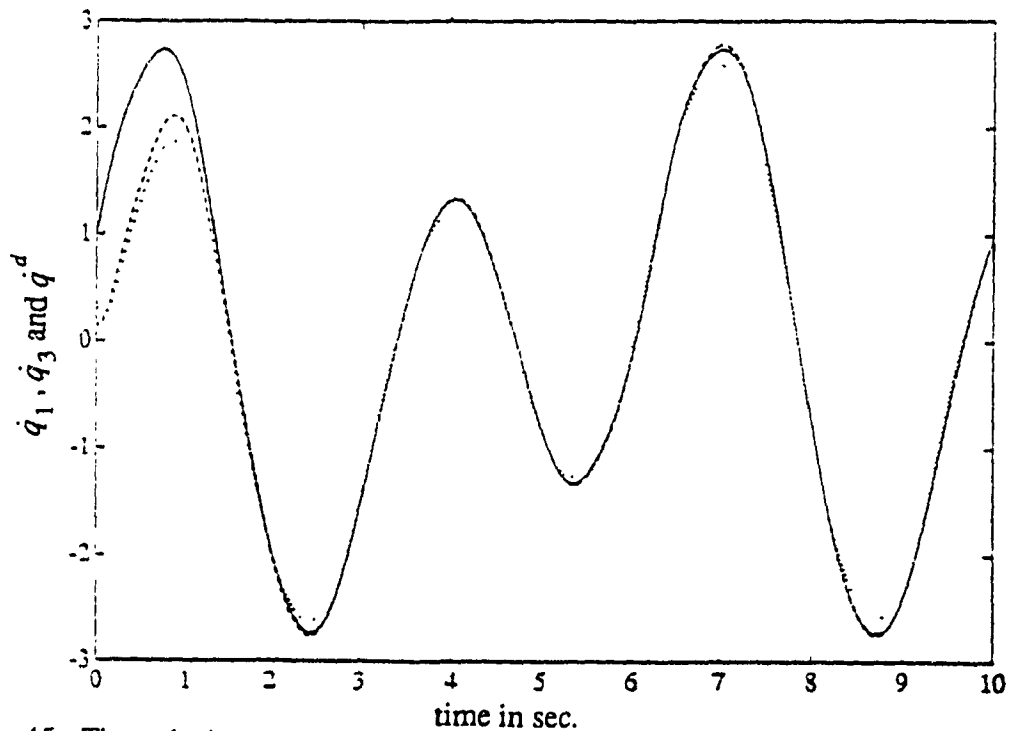


Figure 45. The velocity response of the full order system (two link flexible manipulator) using non-linear non-adaptive controller (feedback linearization). The perturbation parameter is 0.1. — denotes the desired trajectory, - - denotes the response of the first link and ... denotes that of the second link.

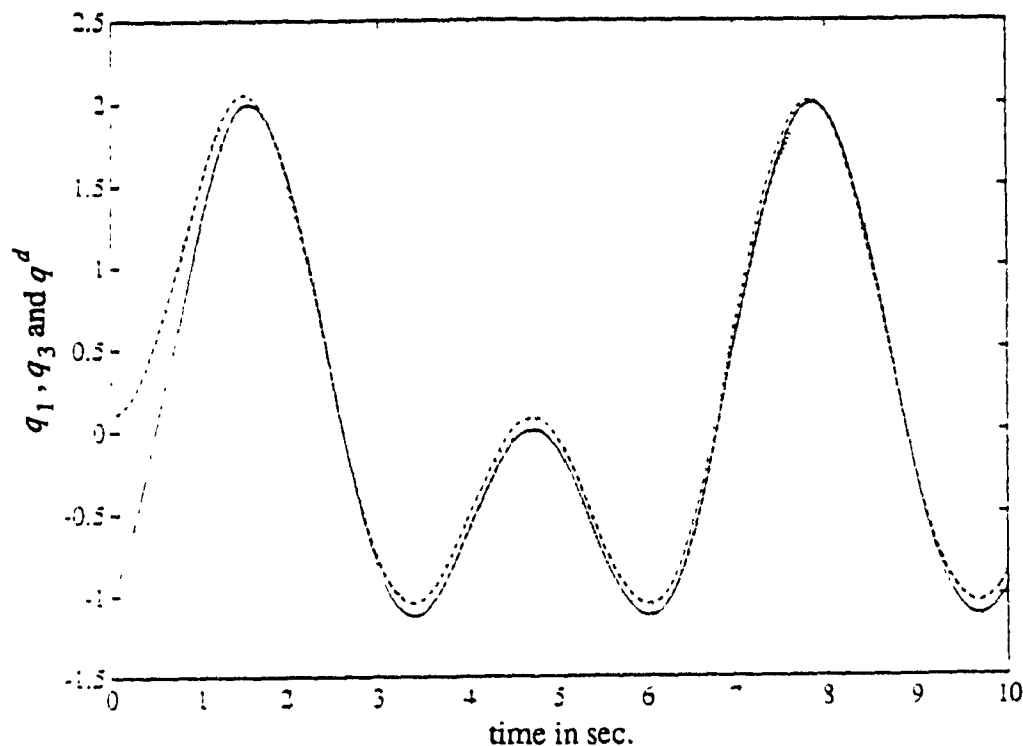


Figure 46. The position response of the full order system (two link flexible manipulator) using non-linear non-adaptive controller (feedback linearization). The perturbation parameter is 0.1. The uncertainty in the parameters is 20%. — denotes the desired trajectory, - - denotes the response of the first link and ... denotes that of the second link.

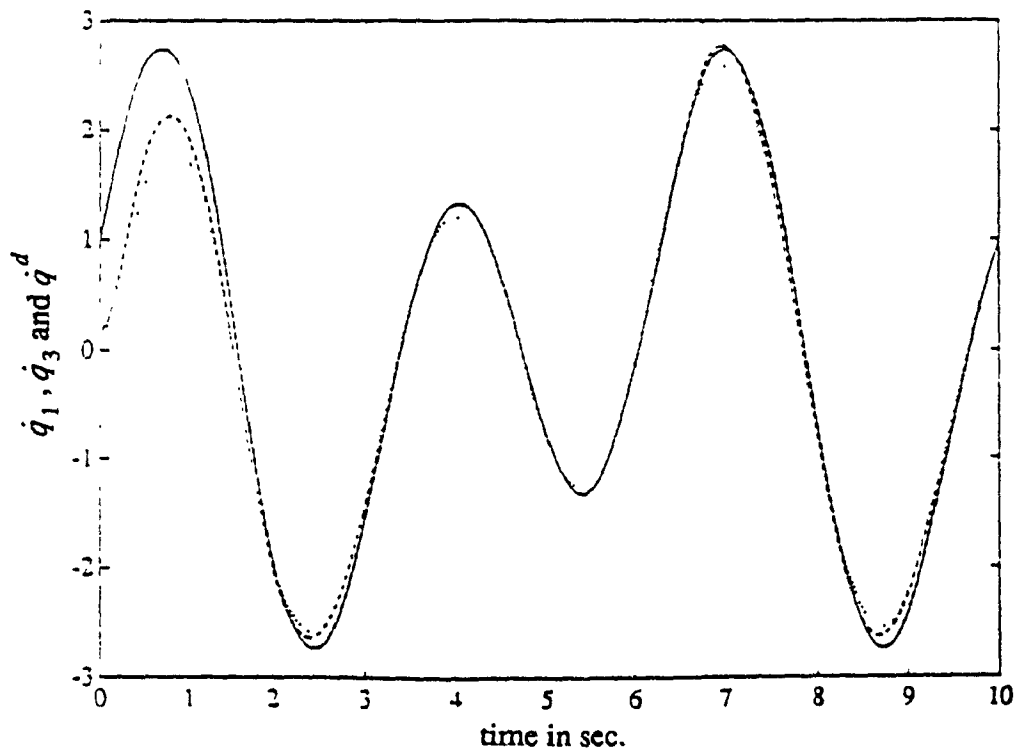


Figure 47. The velocity response of the full order system (two link flexible manipulator) using non-linear non-adaptive controller (feedback linearization). The perturbation parameter is 0.1. The uncertainty in the parameters is 20%. — denotes the desired trajectory, - - denotes the response of the first link and ... denotes that of the second link.

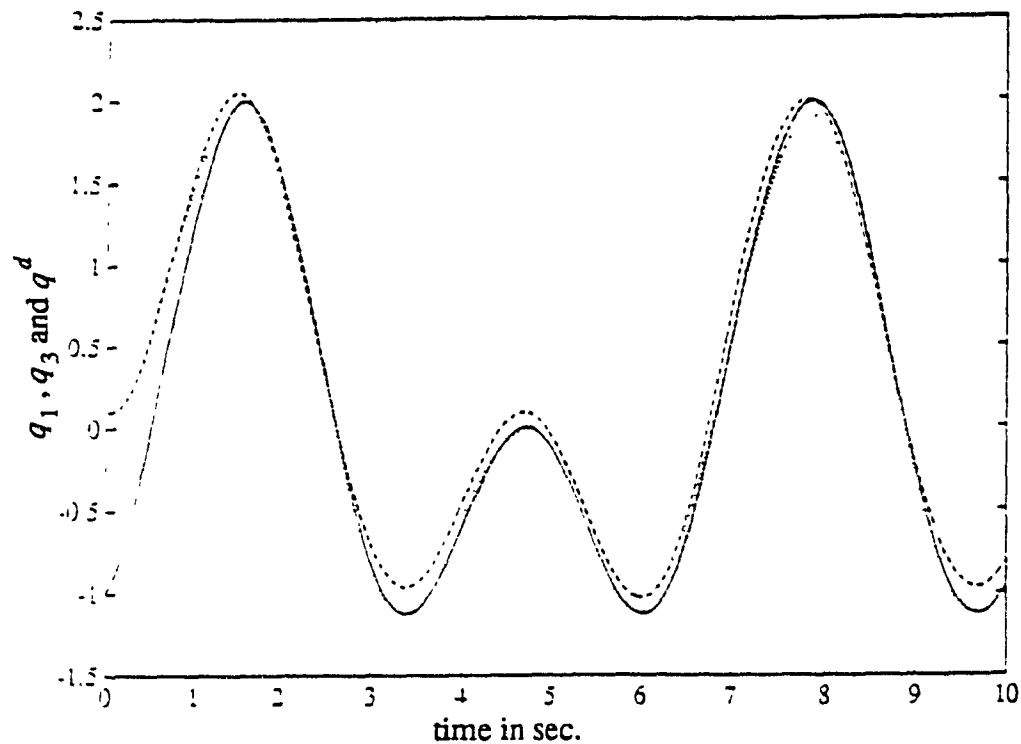


Figure 48. The position response of the full order system (two link flexible manipulator) using non-linear non-adaptive controller (feedback linearization). The perturbation parameter is 0.2. — denotes the desired trajectory, - - denotes the response of the first link and ... denotes that of the second link.

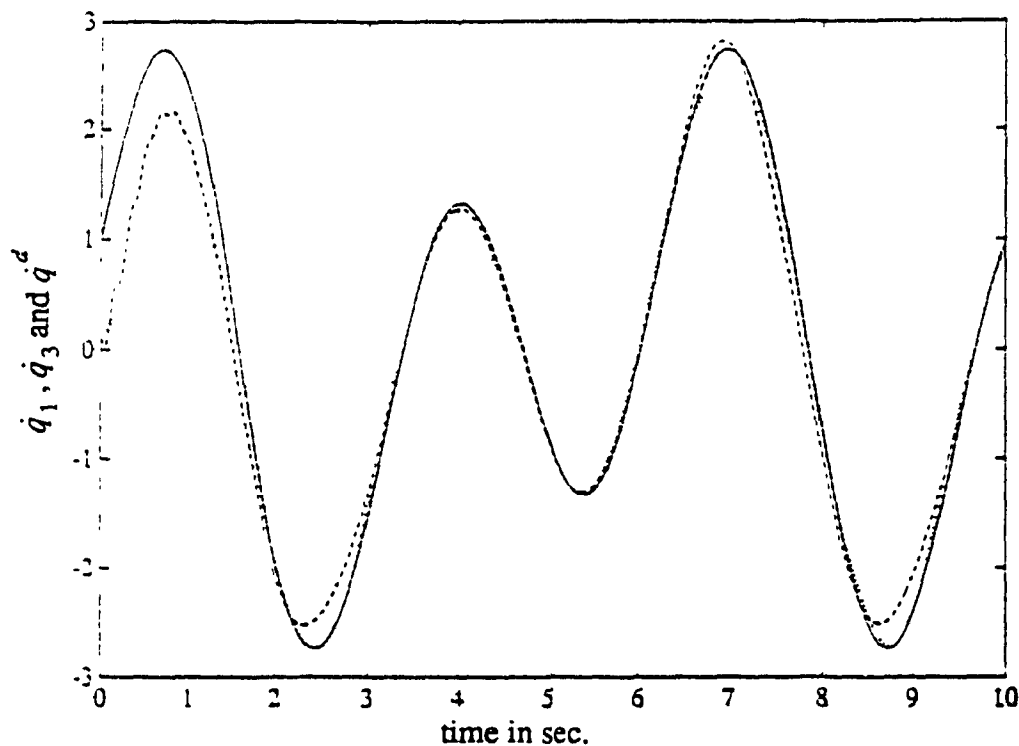


Figure 49. The velocity response of the full order system (two link flexible manipulator) using non-linear non-adaptive controller (feedback linearization). The perturbation parameter is 0.2. — denotes the desired trajectory, - - denotes the response of the first link and ... denotes that of the second link.

Passivity Based Control Methods

The composite control laws for the full order single link flexible manipulator are given by (4.32) (slow component) and (4.38) (fast component). For the two link flexible joint manipulator the slow component is given by (4.41) and the fast component by (4.43). The adaptive gains had to be reduced by nearly ten fold from their corresponding values for the reduced order model to ensure successful tracking. On application of these control laws to the "nominal" full order models, the steady state position and velocity errors were reduced to zero as shown in figures 50 and 51. Due to the adaptation process, even when the composite controller was applied to models whose parameter uncertainty was assumed to be 20%, the steady state position and velocity errors were reduced to zero as shown in figures 52 and 53. Figures 54 and 55 show the response of the two link flexible joint manipulator when ϵ was increased from its nominal value of 0.1.

Inverse Dynamics Method

In the case of the single link flexible joint manipulator, the slow component of the composite controller is given by (4.56) and the adaptive fast component was similarly obtained. For the two link flexible joint manipulator, the slow component of the composite controller is given by (4.58) and the fast component by (4.60). The adaptive gains had to be reduced by nearly ten fold from their corresponding values for the reduced order model to ensure successful tracking. As shown in figures 56 and 57, application of these control laws to the "nominal" full order models, resulted in very good tracking of the desired trajectory with zero steady state position and velocity errors. When the control laws were applied to full order models with 20% parameter uncertainty, the steady state position and velocity errors were still reduced to zero as shown in figures 58 and 59. Figures 60 and 61 show the response of the two link flexible joint manipulator when ϵ was increased from its nominal value of 0.1.

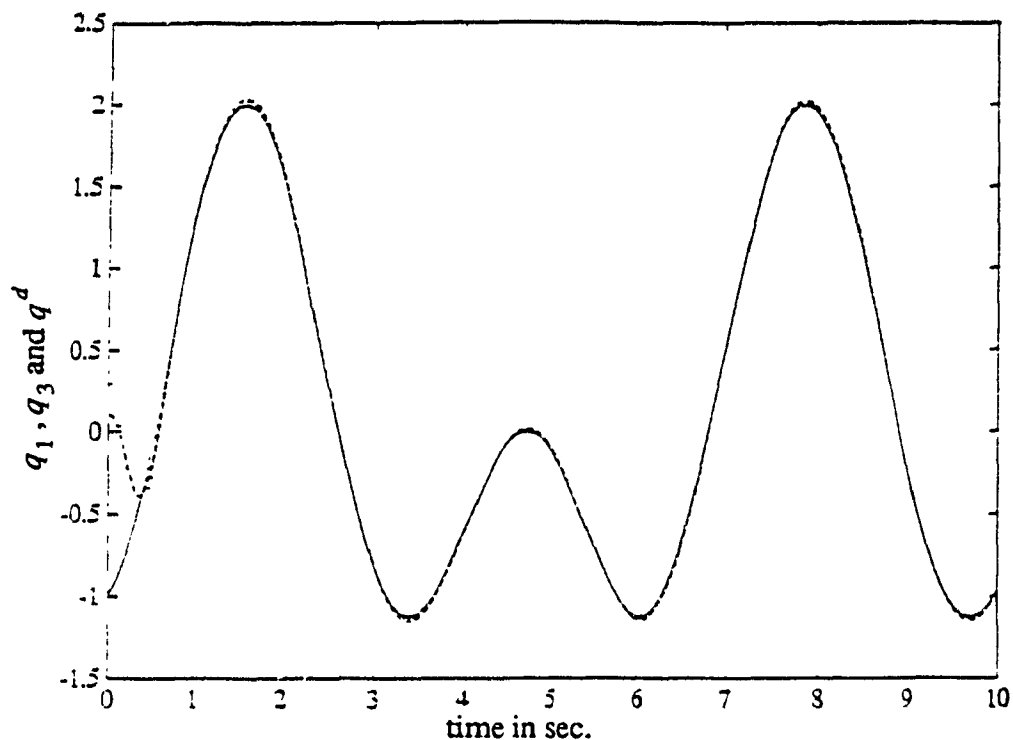


Figure 50. The position response of the full order system (two link flexible manipulator) using non-linear passive adaptive control of Slotine and Li. The perturbation parameter is 0.1. — denotes the desired trajectory, - - denotes the response of the first link and ... denotes that of the second link.

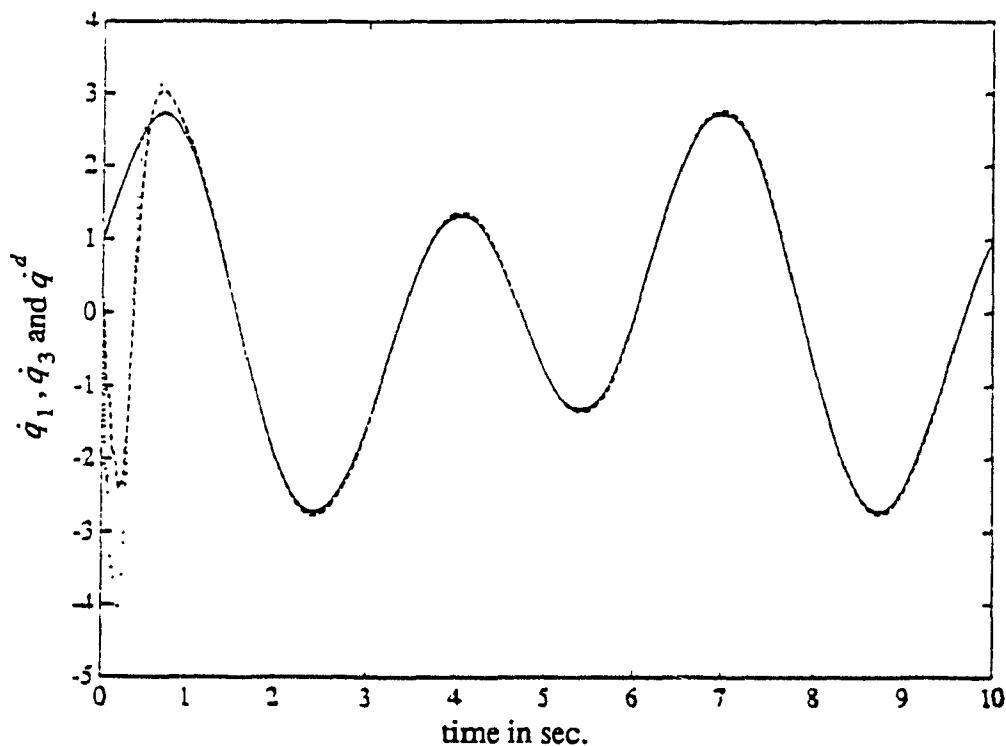


Figure 51. The velocity response of the full order system (two link flexible manipulator) using non-linear passive adaptive control of Slotine and Li. The perturbation parameter is 0.1. — denotes the desired trajectory, - - denotes the response of the first link and ... denotes that of the second link.

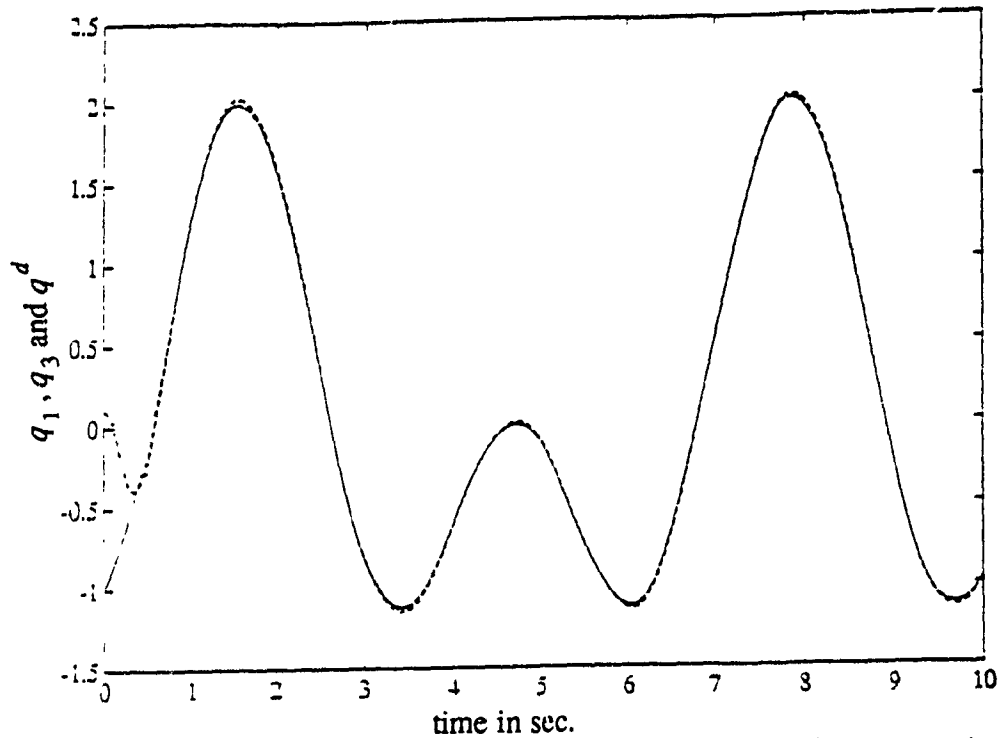


Figure 52. The position response of the full order system (two link flexible manipulator) using non-linear passive adaptive control of Slotine and Li. The perturbation parameter is 0.1. The uncertainty in the parameters is 20%. — denotes the desired trajectory, - - denotes the response of the first link and ... denotes that of the second link.

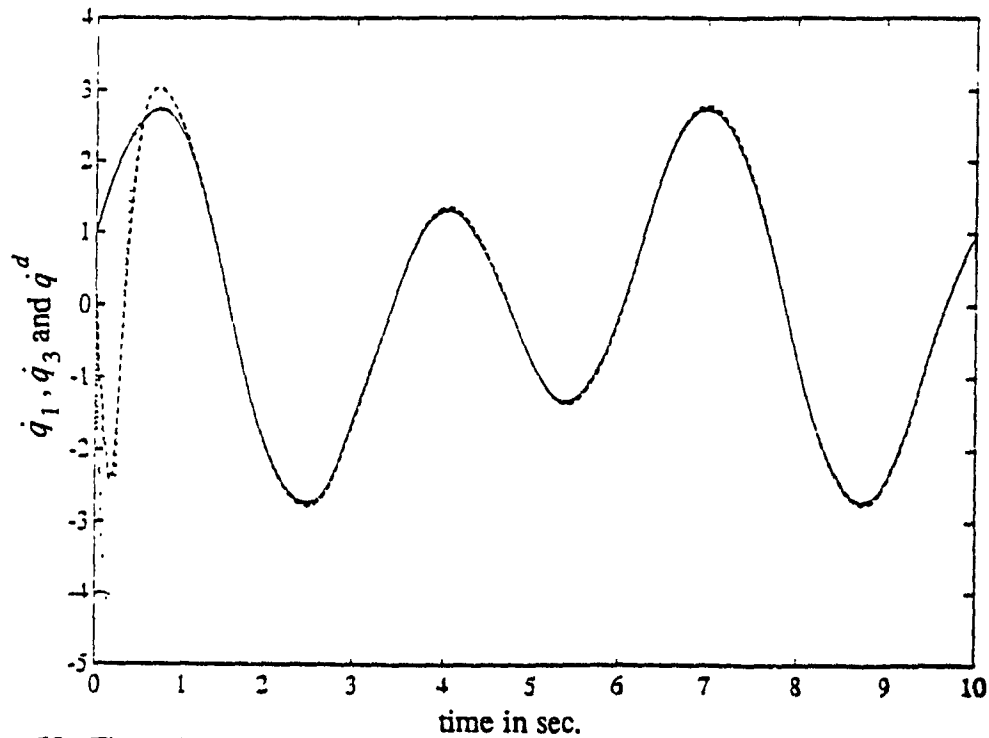


Figure 53. The velocity response of the full order system (two link flexible manipulator) using non-linear passive adaptive control of Slotine and Li. The perturbation parameter is 0.1. The uncertainty in the parameters is 20%. — denotes the desired trajectory, - - denotes the response of the first link and ... denotes that of the second link.

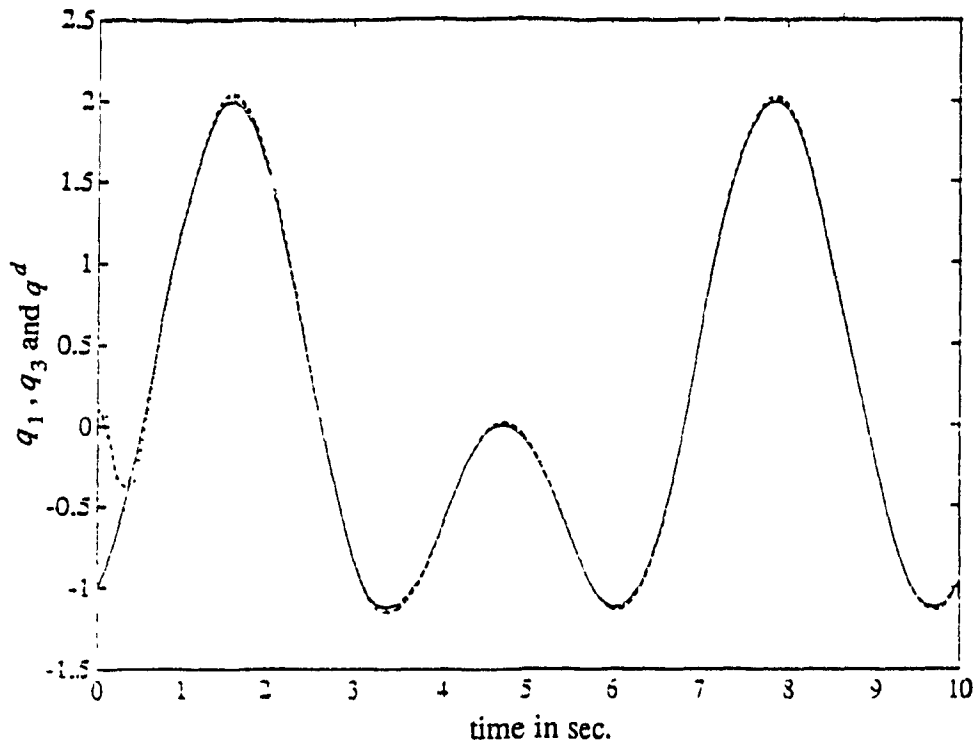


Figure 54. The position response of the full order system (two link flexible manipulator) using non-linear passive adaptive control of Slotine and Li. The perturbation parameter is 0.2. — denotes the desired trajectory, - - denotes the response of the first link and ... denotes that of the second link.

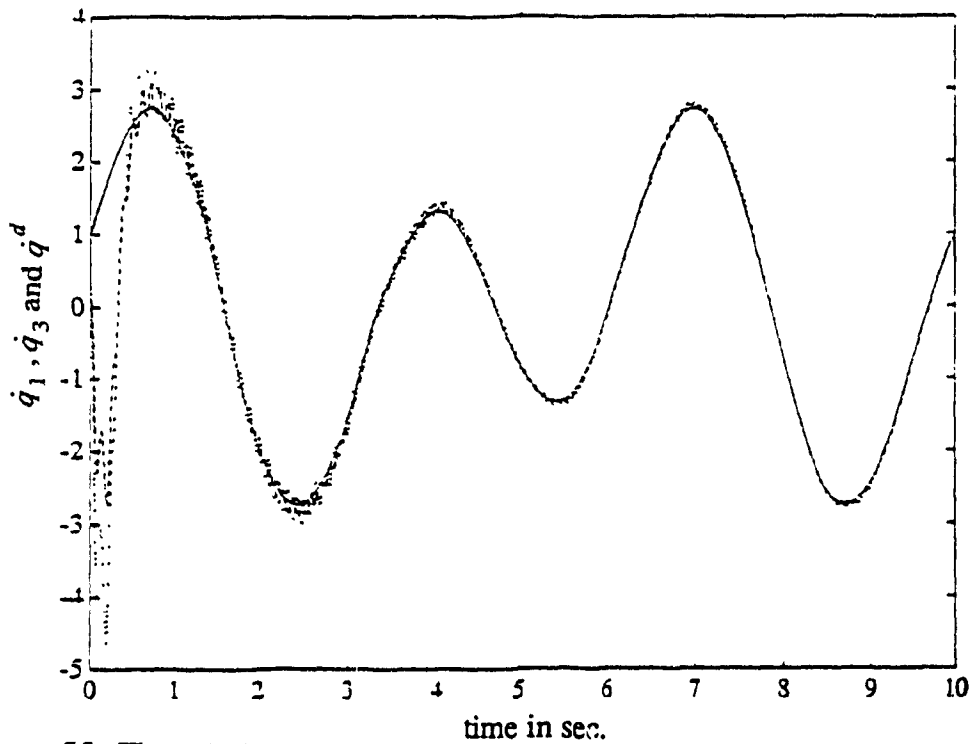


Figure 55. The velocity response of the full order system (two link flexible manipulator) using non-linear passive adaptive control of Slotine and Li. The perturbation parameter is 0.2. — denotes the desired trajectory, - - denotes the response of the first link and ... denotes that of the second link.

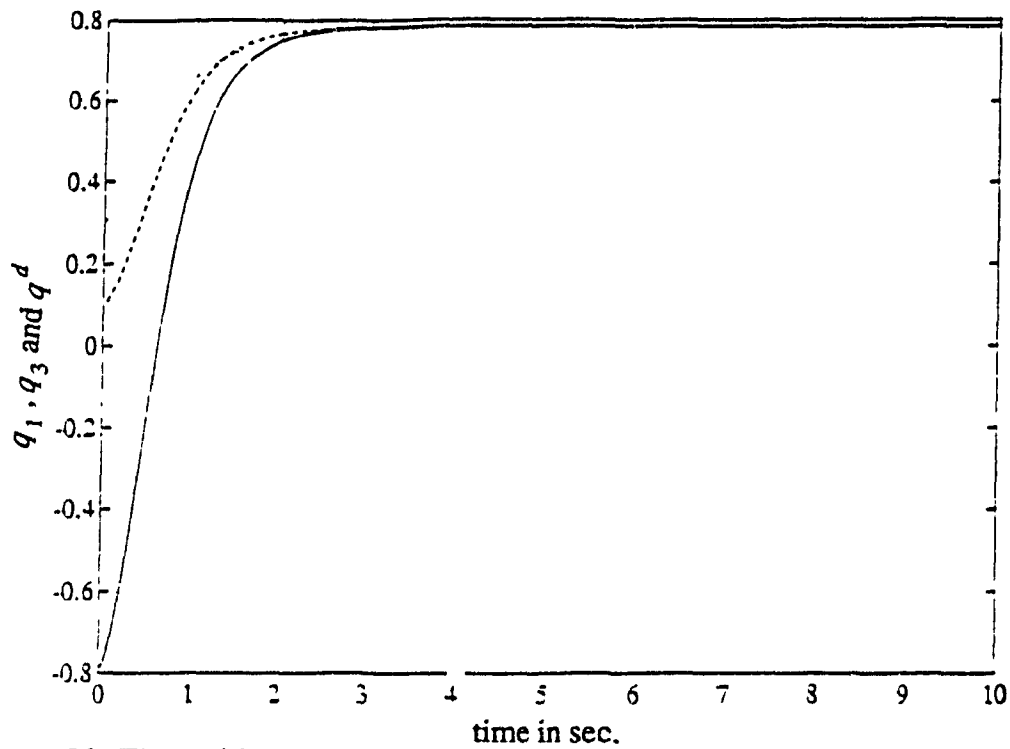


Figure 56. The position response of the full order system (two link flexible manipulator) using non-linear adaptive control of Craig et al. The perturbation parameter is 0.1. — denotes the desired trajectory, - - denotes the response of the first link and ... denotes that of the second link.

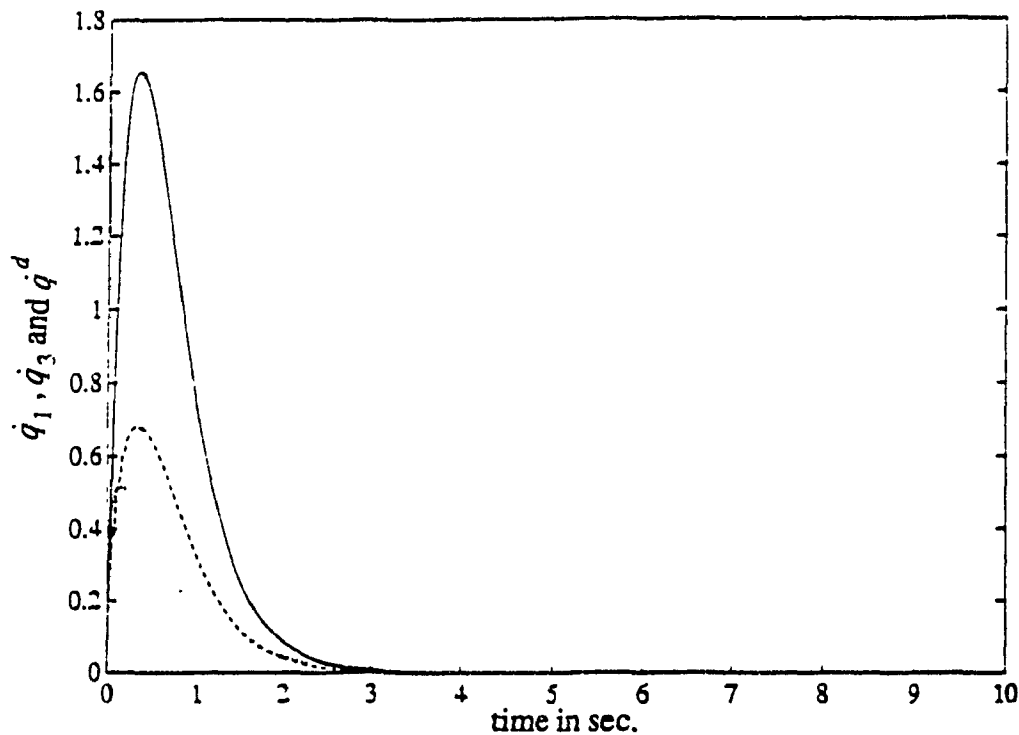


Figure 57. The velocity response of the full order system (two link flexible manipulator) using non-linear adaptive control of Craig et al. The perturbation parameter is 0.1. — denotes the desired trajectory, - - denotes the response of the first link and ... denotes that of the second link.

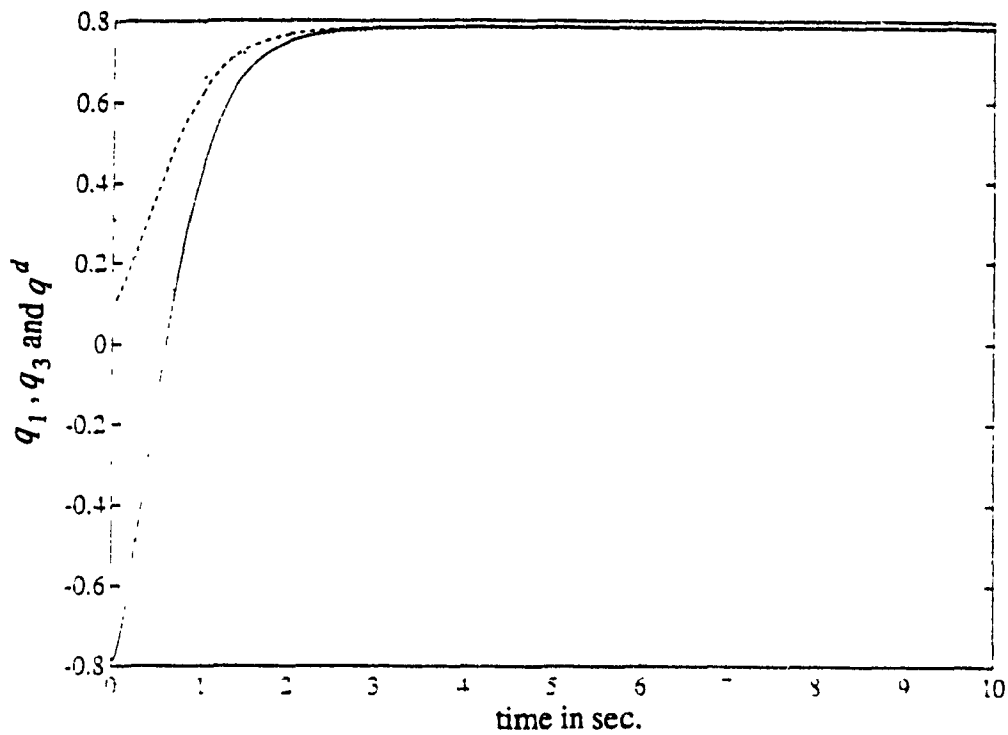


Figure 58. The position response of the full order system (two link flexible manipulator) using non-linear adaptive control of Craig et al. The uncertainty in the parameters is 20%. — denotes the desired trajectory, - - denotes the response of the first link and ... denotes that of the second link.

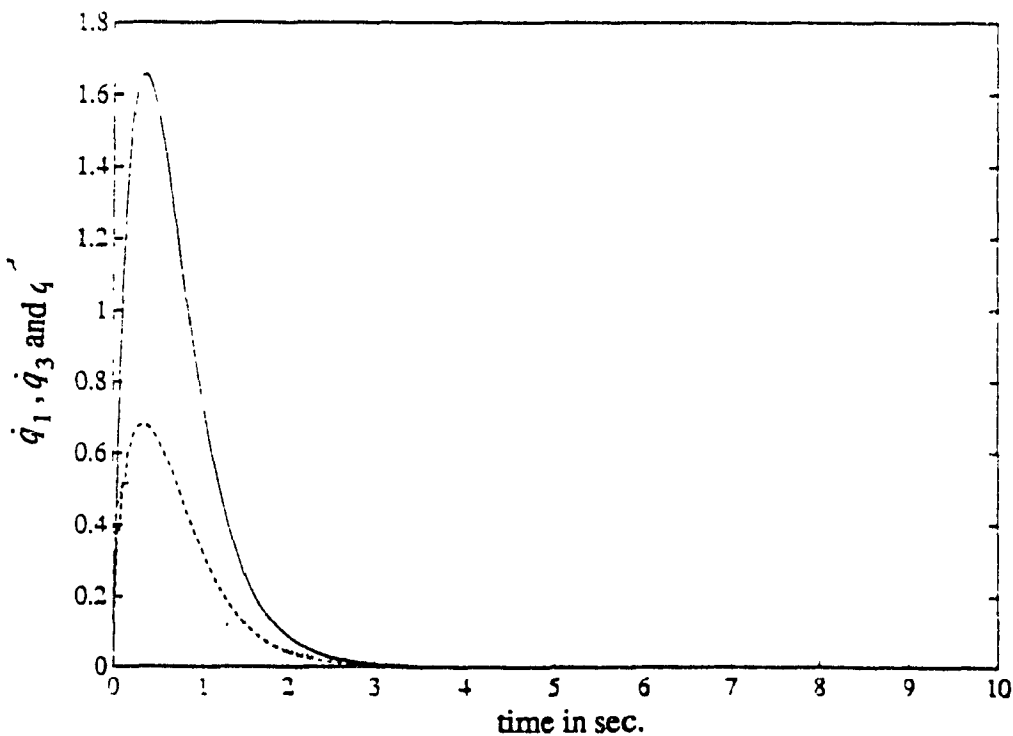


Figure 59. The velocity response of the full order system (two link flexible manipulator) using non-linear adaptive control of Craig et al. The uncertainty in the parameters is 20%. — denotes the desired trajectory, - - denotes the response of the first link and ... denotes that of the second link.

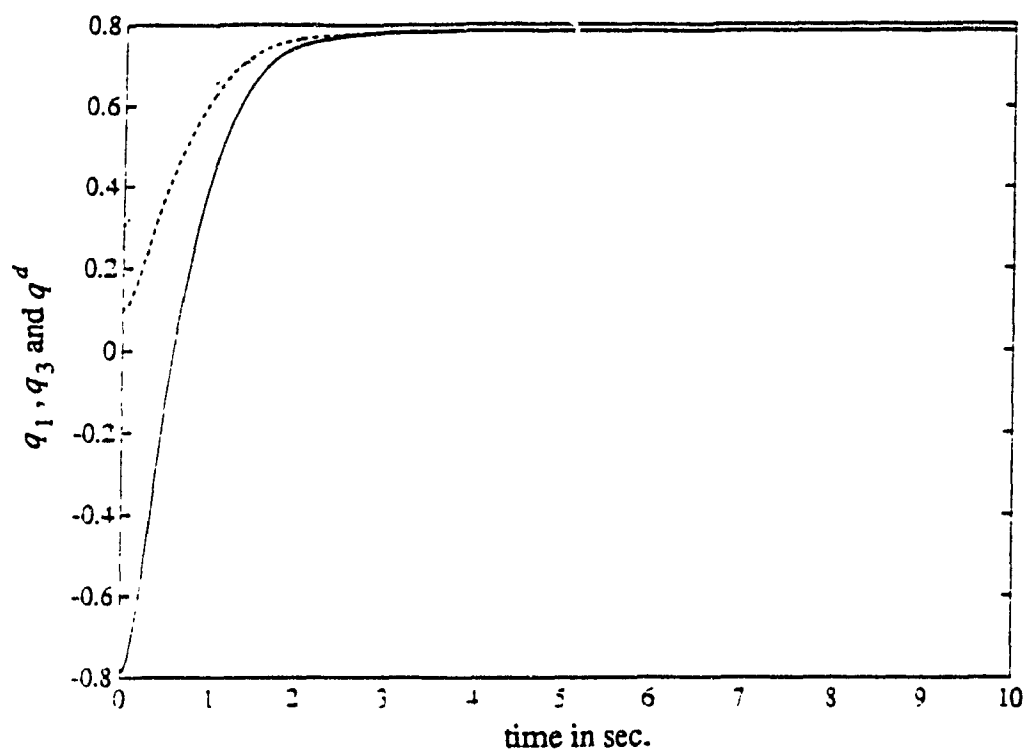


Figure 60. The position response of the full order system (two link flexible manipulator) using non-linear adaptive control of Craig et al. The perturbation parameter is 0.2. — denotes the desired trajectory, - - denotes the response of the first link and ... denotes that of the second link.

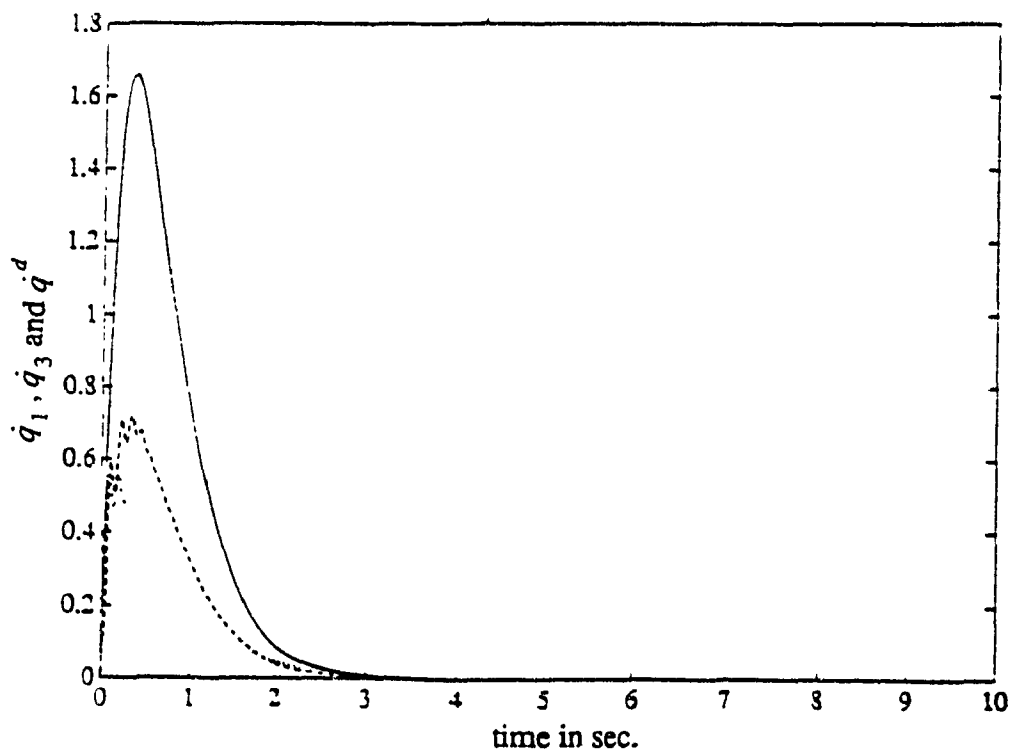


Figure 61. The velocity response of the full order system (two link flexible manipulator) using non-linear adaptive control of Craig et al. The perturbation parameter is 0.2. — denotes the desired trajectory, - - denotes the response of the first link and ... denotes that of the second link.

On application of either linear/ nonlinear, or nonadaptive/ adaptive control laws, the steady state error in the case of the exponential trajectory was reduced to zero after an initial transient period during which the fast variables converge to their quasi steady state values. However, in the case of the time varying sinusoidal trajectory the system tracked the desired trajectory during the linear portion but the error did not converge to zero when there was a change in sign of the slope. This error is more apparent in the case of nonadaptive control laws. The explanation for this behavior is dealt with in Chapter 6.

As ϵ was increased from its nominal value of 0.1 the system became unstable at a certain value of ϵ . This value of ϵ varied for the different control laws considered. Figure 62 shows the position response of the single link manipulator being controlled by Slotine and Li's scheme. At the same value of ϵ , the same system being controlled by Craig et al's scheme remains stable as shown in figure 63. Figure 55 shows the presence of oscillations at higher values of ϵ

Overall on the face of changes in ϵ and parameters, the nonlinear adaptive control techniques were found to perform better than nonlinear / linear nonadaptive and linear adaptive control schemes. Among the two nonlinear adaptive control techniques considered, Craig et al's scheme proved to be more robust to changes in ϵ and parameters than Slotine and Li's scheme.

The estimates of the parameters converged to constant values though not necessarily to their true values as shown in figure 64. This is due to the desired trajectory not being sufficiently rich enough to excite all the modes of the system[18].

5.d Comparison of Nonlinear Control Methods

Feedback linearization control schemes described in Section 4.a globally linearizes the nonlinear robot dynamics by employing nonlinear feedback thereby cancelling the nonlinearities and decoupling the robot dynamics whereas the linear control schemes

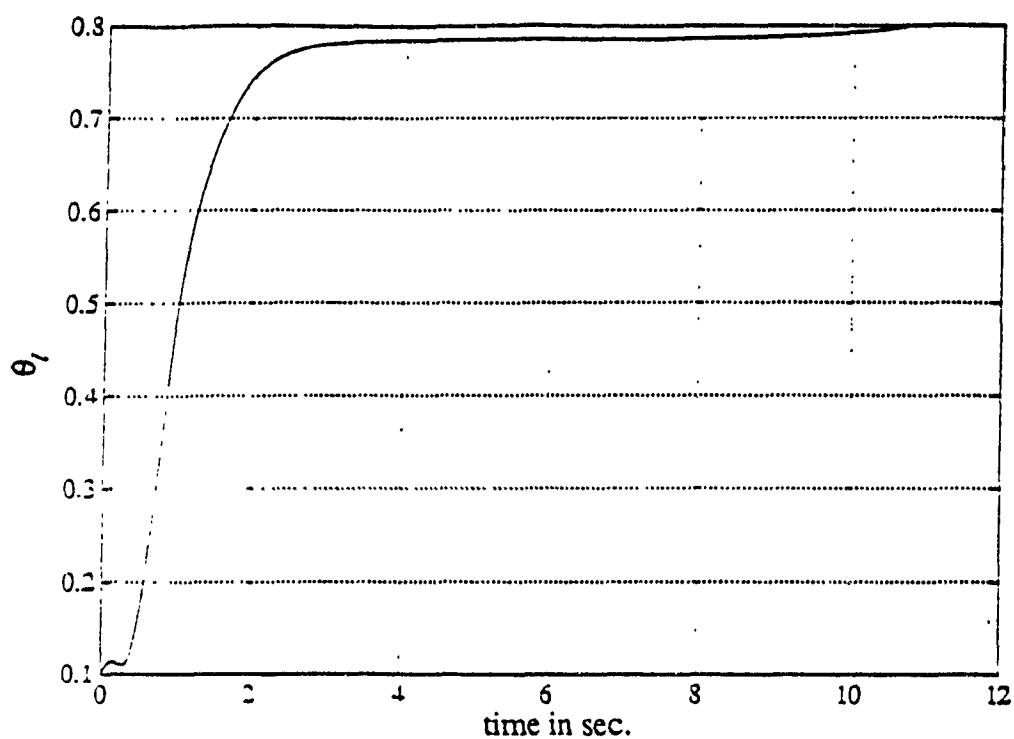


Figure 62. The position response of the full order system (single link flexible manipulator) using non-linear passive adaptive control of Slotine and Li. The perturbation parameter is 0.29.

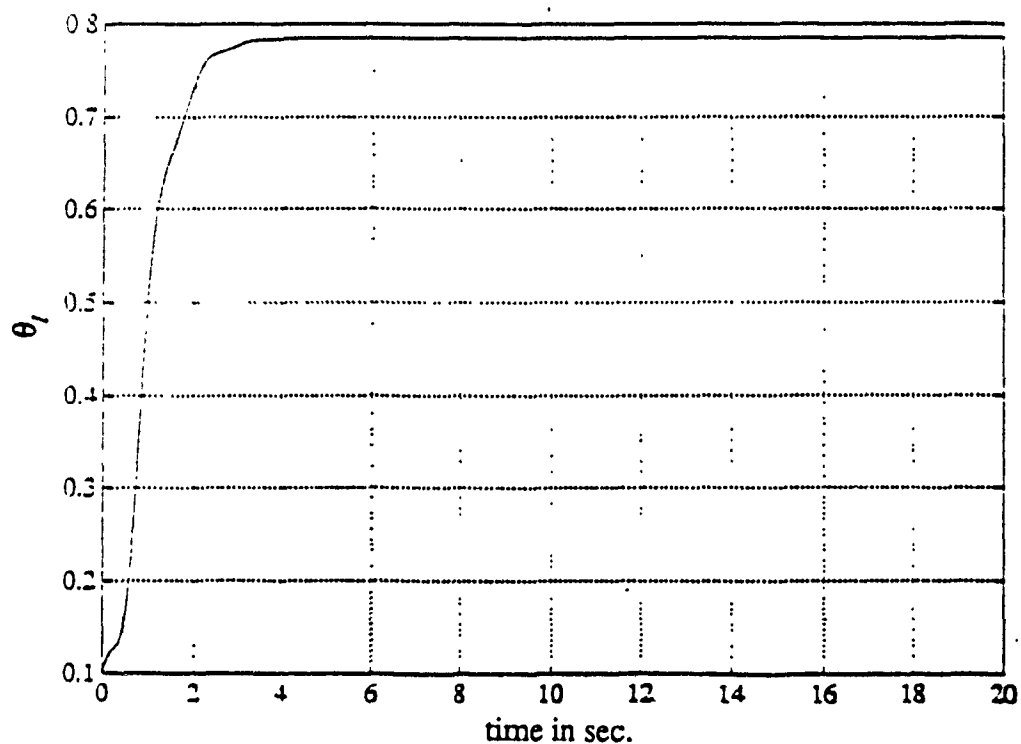


Figure 63. The position response of the full order system (single link flexible manipulator) using non-linear adaptive control of Craig et al. The perturbation parameter is 0.29.

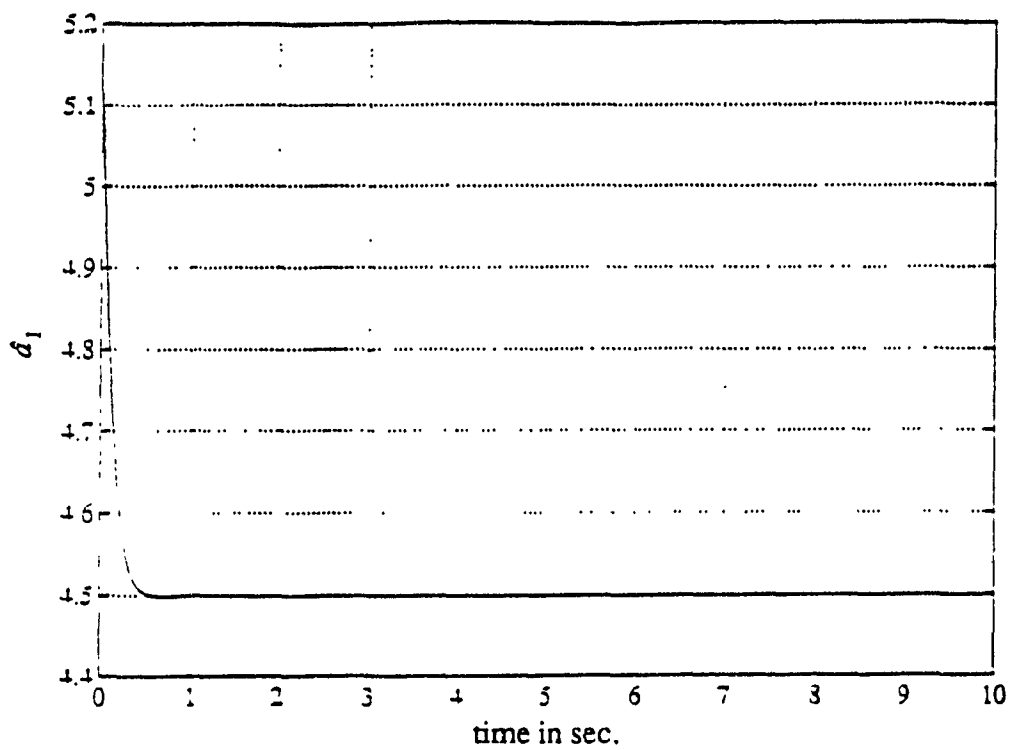


Figure 64. The response of one of the parameter estimates for the full order system (single link flexible manipulator) using non-linear passive adaptive control law of Slotine and Li.

described in Chapter 3 locally linearize the robot model about an operating point.

When the parameters are not known accurately, the controller leads to a steady state error in the nonadaptive feedback linearization scheme described in Section 4.a and as shown in figure 17. However, when an adaptive controller as described in Section 4.b or 4.c is used the steady state error is absent as shown in figures 21 and 25.

The update laws of the adaptive control scheme increase the complexity of the system and the amount of computation time required to implement the controller. However these do not make the methods impractical.

The passivity based control schemes described in Section 4.b does not lead to a linear system in the closed loop. The main advantage of this scheme over that of the adaptive inverse dynamics method described in Section 4.c is that it does not require measurement of acceleration or inversion of the inertia matrix.

It was found that when ϵ was increased from its nominal value, (in the case of the single link manipulator) the control law of Slotine and Li using a state feedback fast controller resulted in an unstable system at $\epsilon=0.29$ whereas Craig, Hsu and Sastry's at the same value of ϵ produced a stable system using the same feedback controller as shown in figures 62 and 63. This suggests that the adaptive inverse dynamics scheme of Craig, Hsu and Sastry is more robust to changes in elasticity than the passivity based scheme of Slotine and Li.

In the next chapter, we analyze the stability of the two nonlinear adaptive control schemes developed in Chapter 4.

Chapter 6

Stability Analysis of Adaptive Systems

In proving the stability of the reduced order system and deriving the adaptive laws, we made use of different Lyapunov functions. However, in most cases a state feedback controller was used to damp out the oscillations due to the fast dynamics. Since the fast subsystem and its controller is common to all the control schemes, the stability properties of the fast subsystem is first investigated.

The fast subsystem expressed in the slow time scale is given by (2.13a)-(2.13b) as

$$\varepsilon \dot{\eta}_1 = \eta_2 \quad (6.1a)$$

$$\varepsilon \dot{\eta}_2 = (-H_1 + H_2 + H_3 - H_4) \eta_1 + (H_2 - H_4) U^{*f}(\eta_1, \eta_2) \quad (6.1b)$$

where U^{*f} is the torque applied to the fast subsystem in order to stabilize the fast dynamics. With a state feedback fast control torque

$$U^f = K_{pf} \eta_1 + K_{vf} \eta_2 \quad (6.2)$$

the fast subsystem expressed in the fast time scale $\tau = t/\varepsilon$, is given by

$$\begin{aligned} \frac{d\eta_1}{d\tau} &= \eta_2 \\ \frac{d\eta_2}{d\tau} &= (-H_1 + H_2 + H_3 - H_4) \eta_1 + (H_2 - H_4) (K_{pf} \eta_1 + K_{vf} \eta_2) \end{aligned}$$

or equivalently

$$\frac{d\eta}{d\tau} = A_f \begin{bmatrix} \eta_1 \\ \eta_2 \end{bmatrix} \quad (6.3)$$

where $A_f = \begin{bmatrix} 0 & 1 \\ (-H_1 + H_2 + H_3 - H_4) + (H_2 - H_4)K_{pf} & (H_2 - H_4)K_{vf} \end{bmatrix}$ is a constant matrix, since

H_i 's are functions of the slow variables that are kept "frozen" in the fast time scale. We

choose the Lyapunov function candidate for the fast subsystem as

$$W(\eta) = \eta^T R_f \eta \quad (6.4)$$

where $\eta = \begin{bmatrix} \eta_1 \\ \eta_2 \end{bmatrix}$ and R_f is a positive definite matrix that satisfies the Lyapunov equation

$$A_f^T R_f + R_f A_f = -F, \quad (6.5)$$

for a given positive definite matrix F . The derivative of $W(\eta)$ along the trajectories of the fast subsystem is

$$\dot{W} = \eta^T [A_f^T R_f + R_f A_f] \eta \quad (6.6)$$

Substituting for $[A_f^T R_f + R_f A_f]$ from (6.5) we get

$$\dot{W} = -\eta^T F \eta < 0. \quad (6.7)$$

As long as the desired trajectories for the fast variables are bounded, the tracking error must converge to zero, i.e. $\eta \rightarrow 0$ as $t \rightarrow \infty$. Now let us consider the Lyapunov function of the slow subsystem. Since the non linear adaptive control methods considered in Chapter 4, makes use of different Lyapunov functions to prove stability of the reduced order models, we will consider each scheme separately.

6.a Slotine and Li's Scheme

The Lyapunov function of the slow subsystem is given by (4.25). It can be rewritten as

$$V(q, \tilde{P}_s) = \frac{1}{2} \begin{bmatrix} \tilde{P}_s & S_s \end{bmatrix} \begin{bmatrix} \Gamma_s^{-1} & 0 \\ 0 & M_r \end{bmatrix} \begin{bmatrix} \tilde{P}_s \\ S_s \end{bmatrix}$$

or equivalently as

$$V(H_s) = \frac{1}{2} H_s^T Q_s H_s \quad (6.8)$$

where $H_s = \begin{bmatrix} \tilde{P}_s \\ S_s \end{bmatrix}$ and $Q_s = \begin{bmatrix} \Gamma_s^{-1} & 0 \\ 0 & M_r \end{bmatrix}$.

Hence

$$\begin{aligned}\nabla_{H_s} V(H_s) &= \frac{1}{2} [H_s^T Q_s + Q_s H_s] \\ &= \frac{1}{2} [Q_s^T + Q_s] H_s.\end{aligned}\quad (6.9)$$

Equation (6.9) will be used later when evaluating the interconnection conditions.

Now, we consider the stability of the full order system. Since both the reduced order slow and fast subsystems have been stabilized by design, intuitively it follows from the results in [11] and [12] that for sufficiently small perturbation parameter ϵ , the full order system remains stable too. To prove this, the quadratic-type Lyapunov function candidate proposed in [12] is considered here.

$$v(q, \tilde{P}_s, \eta) = (1-d) V(q, \tilde{P}_s) + d W(\eta)$$

where V is the Lyapunov function for the slow subsystem (4.25), W is the Lyapunov function for the fast subsystem (6.4), \tilde{P}_s represents the time varying estimation error of the parameters in the slow subsystem, and d is a positive number chosen as $0 < d < 1$.

Computing \dot{v} along the trajectory of the full order system we have

$$\dot{v}(H_s, \eta) = (1-d)[\nabla_{H_s} V(H_s)]^T f(q, \eta, \epsilon) + \frac{d}{\epsilon} [\nabla_{\eta} W(\eta)]^T g(q, \eta, \epsilon).$$

Adding and subtracting $(1-d)[\nabla_{H_s} V(H_s)]^T f_r(q, \eta=0, \epsilon=0)$ and $\frac{d}{\epsilon} [\nabla_{\eta} W(\eta)]^T g_r(\eta, \epsilon)$ we get

$$\begin{aligned}\dot{v} &= (1-d)[\nabla_{H_s} V(H_s)]^T f_r(q, \eta=0, \epsilon=0) + (1-d)[\nabla_{H_s} V(H_s)]^T [f(q, \eta, \epsilon) - f_r(q, \eta=0, \epsilon=0)] \\ &\quad + \frac{d}{\epsilon} [\nabla_{\eta} W(\eta)]^T g_r(\eta, \epsilon) + \frac{d}{\epsilon} [\nabla_{\eta} W(\eta)]^T [g(q, \eta, \epsilon) - g_r(\eta, \epsilon)].\end{aligned}$$

The above algebraic manipulation makes it easier to determine \dot{v} , since the first term is computed over the trajectories of the reduced order rigid model with the slow adaptation law and the third term is computed over the trajectories of the fast subsystem. Consequently, the first term is reduced to $-(1-d)S_s^T K_{ds} S_s$ and the third term is reduced

to $-\frac{d}{\epsilon}\eta^T F \eta$. To simplify the second and fourth terms in \dot{v} we need to assume the following interconnection conditions.

Interconnection Conditions

The first interconnection condition involves the relationship between the full order system and the reduced order slow subsystem. We have the full order system given by (2.5). Using the transformation $Z = Z_1^{*qss}$ and substituting for Z_1^* in terms of η_1 and Z_1^{*qss} we get

$$\ddot{q} = -(H_1 h_1 + H_2 h_2) + (H_2 - H_1) \left[\eta_1 + (-H_1 + H_2 + H_3 - H_4)^{-1} \left[((H_1 - H_3)h_1 + (H_2 - H_4)h_2) - (H_2 - H_4)U^{*s} \right] \right] + H_2 U^*$$

which on rearrangement yields

$$\begin{aligned} f(q, \eta, \epsilon) = \ddot{q} = & \left[-(H_2 - H_1)(-H_1 + H_2 + H_3 - H_4)^{-1}(H_2 - H_4) + H_2 \right] U^{*s} \\ & + \left[(H_2 - H_1)(-H_1 + H_2 + H_3 - H_4)^{-1}(H_1 - H_3) - H_1 \right] h_1 \\ & + \left[(H_2 - H_1)(-H_1 + H_2 + H_3 - H_4)^{-1}(H_2 - H_4) - H_2 \right] h_2 + (H_2 - H_1)\eta_1 + H_2 U^{*f}. \end{aligned} \quad (6.10)$$

The reduced order slow subsystem f_r is given by (2.8b). From the expressions of $f(q, \eta, \epsilon)$ and $f_r(q, \eta=0, \epsilon=0)$, we get

$$f - f_r = \begin{bmatrix} 0 \\ (H_2 - H_1) \end{bmatrix} \eta_1 + \begin{bmatrix} 0 \\ H_2 U^{*f} \end{bmatrix}. \quad (6.11)$$

Combining (6.9) and (6.11) we obtain

$$\begin{aligned} [\nabla_{H_s} V(H_s)]^T (f - f_r) &= \frac{1}{2} \left[(Q_s^T + Q_s)H_s \right]^T (f - f_r) \\ &= S_s M_r \left[(H_2 - H_1)\eta_1 + H_2 U^{*f} \right]. \end{aligned} \quad (6.12)$$

The second interconnection condition involves the relationship between the fast part of the full order system and the fast subsystem. We have the full order system given

by (2.6) or equivalently in the configuration space by (2.9c)-(2.9d). Substituting for Z_1^* and Z_2^* from (2.11) in (2.9c)-(2.9d) we have

$$\begin{aligned} \epsilon(\dot{\eta}_1 + \dot{Z}_1^{*qss}) &= Z_2^* \\ \epsilon\dot{\eta}_2 &= -((H_1 - H_3)h_1 + (H_2 - H_4)h_2) + (-H_1 + H_2 + H_3 - H_4)(\eta_1 + Z_1^{*qss}) + (H_2 - H_4)U^* \end{aligned} \quad (6.13)$$

Substituting for Z_1^{*qss} in (6.13) and on algebraic manipulation we get

$$\begin{aligned} \epsilon\dot{\eta}_1 &= \eta_2 - \epsilon\dot{Z}_1^{*qss} \\ \epsilon\dot{\eta}_2 &= (-H_1 + H_2 + H_3 - H_4)\eta_1 + (H_2 - H_4)U^{*f} \end{aligned} \quad (6.14)$$

or equivalently

$$g(q, \eta) = \epsilon\dot{\eta} = \begin{bmatrix} 0 & 1 \\ (-H_1 + H_2 + H_3 - H_4) & 0 \end{bmatrix} \eta + \begin{bmatrix} 0 \\ H_2 - H_4 \end{bmatrix} U^{*f} - \begin{bmatrix} 1 \\ 0 \end{bmatrix} \dot{Z}_1^{*qss}. \quad (6.15)$$

The fast subsystem is given by (2.13a)-(2.13b). This can be rewritten as

$$g_r(\eta) = \epsilon\dot{\eta} = \begin{bmatrix} 0 & 1 \\ (-H_1 + H_2 + H_3 - H_4) & 0 \end{bmatrix} \eta + \begin{bmatrix} 0 \\ H_2 - H_4 \end{bmatrix} U^{*f}. \quad (6.16)$$

From (6.15) and (6.16) we get

$$g(q, \eta) - g_r(\eta) = \begin{bmatrix} -\epsilon\dot{Z}_1^{*qss} \\ 0 \end{bmatrix}. \quad (6.17)$$

We have Z_1^{*qss} as

$$\begin{aligned} Z_1^{*qss} &= (-H_1 + H_2 + H_3 - H_4)^{-1} \left[((H_1 - H_3)h_1 + (H_2 - H_4)h_2) + (H_2 - H_4)U^{*f} \right] \\ &= Z_1^{*qss}(\bar{q}, S_s, \bar{P}_s, q_d, \dot{q}_d, \ddot{q}_d) \end{aligned} \quad (6.18)$$

and therefore

$$\begin{aligned} \dot{Z}_1^{*qss} &= \frac{dZ_1^{*qss}}{dt} = \frac{\partial Z_1^{*qss}}{\partial \bar{q}} \dot{\bar{q}} + \frac{\partial Z_1^{*qss}}{\partial S_s} \dot{S}_s + \frac{\partial Z_1^{*qss}}{\partial \bar{P}_s} \dot{\bar{P}}_s + \\ &\quad \frac{\partial Z_1^{*qss}}{\partial q_d} \dot{q}_d + \frac{\partial Z_1^{*qss}}{\partial \dot{q}_d} \ddot{q}_d + \frac{\partial Z_1^{*qss}}{\partial \ddot{q}_d} \dddot{q}_d. \end{aligned} \quad (6.19)$$

Let

$$p(t) = \frac{\partial Z_1^{*qss}}{\partial q_d} \dot{q}_d + \frac{\partial Z_1^{*qss}}{\partial \dot{q}_d} \ddot{q}_d + \frac{\partial Z_1^{*qss}}{\partial \ddot{q}_d} \dddot{q}_d. \quad (6.20)$$

Then

$$\dot{Z}_1^{*qss} = p(t) + \frac{\partial Z_1^{*qss}}{\partial \bar{q}} \dot{\bar{q}} + \frac{\partial Z_1^{*qss}}{\partial S_s} \dot{S}_s + \frac{\partial Z_1^{*qss}}{\partial \bar{P}_s} \dot{\bar{P}}_s. \quad (6.21)$$

From (4.19), (4.21) and (4.22) we have

$$\dot{\bar{q}} = S_s - \Lambda_s \bar{q}. \quad (6.22)$$

Substituting for $\dot{\bar{q}}$, \dot{S}_s and $\dot{\bar{P}}_s$ from (6.22), (4.24) and (4.29) respectively, we get

$$\begin{aligned} \dot{Z}_1^{*qss} = p(t) + \frac{\partial Z_1^{*qss}}{\partial \bar{q}} (S_s - \Lambda_s \bar{q}) + \frac{\partial Z_1^{*qss}}{\partial \bar{P}_s} (-\Gamma_s Y_s^T S_s) + \\ \frac{\partial Z_1^{*qss}}{\partial S_s} \left[\frac{Y \bar{P}_s}{M_r} - \frac{(C_r + K_{ds}) S_s}{M_r} \right]. \end{aligned} \quad (6.23)$$

On rearranging we get,

$$\begin{aligned} \dot{Z}_1^{*qss} = p(t) + \left[\frac{\partial Z_1^{*qss}}{\partial \bar{q}} - \Gamma_s Y_s^T \frac{\partial Z_1^{*qss}}{\partial \bar{P}_s} - \frac{(C_r + K_{ds})}{M_r} \frac{\partial Z_1^{*qss}}{\partial S_s} \right] S_s + \\ \frac{\partial Z_1^{*qss}}{\partial \bar{q}} (-\Lambda_s \bar{q}) + \frac{\partial Z_1^{*qss}}{\partial S_s} \frac{Y \bar{P}_s}{M_r}. \end{aligned} \quad (6.24)$$

Let

$$\left| \left| p(t) \right| \right| \leq K_1(t) \quad (6.25)$$

$$\begin{aligned} \left| \left| \left[\frac{\partial Z_1^{*qss}}{\partial \bar{q}} - \Gamma_s Y_s^T \frac{\partial Z_1^{*qss}}{\partial \bar{P}_s} - \frac{(C_r + K_{ds})}{M_r} \frac{\partial Z_1^{*qss}}{\partial S_s} \right] S_s + \frac{\partial Z_1^{*qss}}{\partial \bar{q}} (-\Lambda_s \bar{q}) + \frac{\partial Z_1^{*qss}}{\partial S_s} \frac{Y \bar{P}_s}{M_r} \right| \right| \\ \leq \left[K_2(t) S_s + K_3(t) \bar{q} + K_4(t) \bar{P}_s \right] \end{aligned} \quad (6.26)$$

From (6.17), (6.24), (6.25) and (6.26) it follows that

$$g - g_r = \begin{bmatrix} -\epsilon(K_1(t) + K_2(t) S_s + K_3(t) \bar{q} + K_4(t) \bar{P}_s) \\ 0 \end{bmatrix}. \quad (6.27)$$

Combining (6.6) and (6.27) we obtain

$$[\nabla_{\eta} W(\eta)]^T (g - g_r) = -2\eta R_f \varepsilon \left[K_1(t) + K_2(t)S_s + K_3(t)\bar{q} + K_4(t)\bar{P}_s \right]. \quad (6.28)$$

We now make the following assumptions:

- 1) The Lyapunov function of the slow subsystem is such that

$$[\nabla_{H_s} V(H_s)] f_r = -S_s^T K_{ds} S_s \leq -\alpha_1 \Psi^2(q), \quad \alpha_1 > 0$$

where $\Psi(q)$ is a scalar-valued function of q that vanishes at $q=0$ and is non zero for all other q in the domain of interest.

- 2) The Lyapunov function of the fast subsystem is such that

$$\left[\nabla_{\eta} W(\eta) \right] g_r = -\eta^T F \eta \leq -\alpha_2 \Phi^2(\eta), \quad \alpha_2 > 0$$

where $\Phi(\eta)$ is a scalar-valued function that vanishes at $\eta=0$ and is non zero for all other η in the domain of interest.

- 3) The following inequalities hold

$$\begin{aligned} \text{a) } [\nabla_{H_s} V(H_s)]^T \left[f(q, \eta, \varepsilon) - f_r(q, \eta=0, \varepsilon=0) \right] &= S_s^T M_r \left[(H_2 - H_1)\eta_1 + H_2 U^{*f} \right] \\ &\leq \beta_1 \Psi(q) \Phi(\eta) \end{aligned}$$

$$\begin{aligned} \text{b) } [\nabla_{\eta} W(\eta)]^T \left[g(q, \eta, \varepsilon) - g_r(\eta, \varepsilon) \right] &= -2\eta R_f \varepsilon \left[K_1(t) + K_2(t)S_s + K_3(t)\bar{q} + K_4(t)\bar{P}_s \right] \\ &\leq \varepsilon K_5 \Psi(q) \Phi(\eta) + \varepsilon \Phi(\eta) \left[K_1(t) + K_4(t)\bar{P}_s \right] \end{aligned}$$

where the constants β_1, β_2 and K_5 are non negative.

With the above assumptions \dot{v} is reduced to

$$\begin{aligned} \dot{v} &= -(1-d)\alpha_1 \Psi^2 - \frac{d}{\varepsilon} \alpha_2 \Phi^2 + (1-d)\beta_1 \Psi \Phi + \frac{d}{\varepsilon} \left[\varepsilon K_5 \Psi \Phi + \varepsilon \Phi (K_1(t) + K_4(t)\bar{P}_s) \right] \\ &= - \begin{bmatrix} \Psi(q) \\ \Phi(\eta) \end{bmatrix}^T T \begin{bmatrix} \Psi(q) \\ \Phi(\eta) \end{bmatrix} + \mu(t) \end{aligned}$$

where

$$T = \begin{bmatrix} (1-d)\alpha_1 & -(1-d)\frac{\beta_1}{2} - \frac{dK_5}{2} \\ -(1-d)\frac{\beta_1}{2} - \frac{dK_5}{2} & d\frac{\alpha_2}{\epsilon} \end{bmatrix}, \quad \mu(t) = d \Phi [K_1(t) + K_4(t)\bar{P}_s]. \quad (6.29)$$

The expression for \dot{v} consists of a quadratic term and $\mu(t)$. For $d < 1$ and an upper bound for ϵ_{pd} such that $\epsilon_{pd} > \epsilon$, T is positive definite where

$$\epsilon_{pd}(d) = \frac{\alpha_1 \alpha_2}{\frac{[\beta_1(1-d) + dK_5]^2}{4d(1-d)}}.$$

The maximum value $\epsilon_{pd}(d)$ is obtained by differentiating $\epsilon_{pd}(d)$ with respect to d .

The maximum value $\epsilon_{pd}(d)$ occurs at $d_{\max} = \frac{\beta_1}{K_5 + \beta_1}$ and found to be $\epsilon_{\max} = \frac{\alpha_1 \alpha_2}{K_5 + \beta_1}$.

Figure 65 shows the upper bounds of ϵ . Since $\mu(t)$ is a function of the desired trajectory and its derivatives, the following scenario arises:

The desired trajectory is three times continuously differentiable with bounded derivatives. This follows from (6.20) where $p(t)$ is a function of all the first three derivatives of the desired trajectory. It implies that $K_1(t)$ and hence $\mu(t)$ is a bounded function of time.

Let us assume that the maximum value $\mu(t)$ is μ_m . Therefore $\mu(t) \leq \mu_m$. Let $B = B_q \times B_{\bar{P}_s} \times B_{\eta} \subset R^n \times R^m \times R^n$, i.e. $B \subset R^{2n+m}$. Define the set $b = \{(q, \bar{P}_s, \eta) : (q, \bar{P}_s, \eta) \in B\} \subset R^{2n+m}$. b is a prism containing the origin and extending along $\|q\|$, $\|\bar{P}_s\|$ and $\|\eta\|$. Let us also define the following regions with $\epsilon < \epsilon_{\max}$:

$$(a) \quad R_{\mu_m} = \{(q, \bar{P}_s, \eta) \in b; \begin{bmatrix} \Psi(q) \\ \Phi(\eta) \end{bmatrix}^T T \begin{bmatrix} \Psi(q) \\ \Phi(\eta) \end{bmatrix} \leq \mu_m\}$$

and

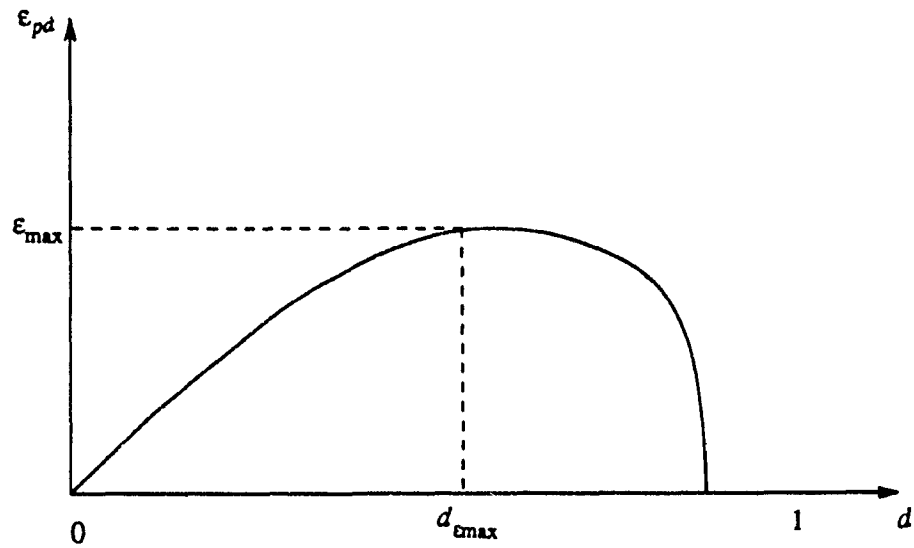


Figure 65. Upper bounds of ϵ

$$(b) \quad R_{\mu_m}^0 = \{(q, \tilde{P}_s, \eta) \in b; \begin{bmatrix} \Psi(q) \\ \Phi(\eta) \end{bmatrix}^T T \begin{bmatrix} \Psi(q) \\ \Phi(\eta) \end{bmatrix} > \mu_m\}.$$

The first set R_{μ_m} is a subset of b with an elliptic cross section defined by

$$(1-d)\alpha_1 \Psi^2 - \left[(1-d)\beta_1 + dK_s \right] \Psi \Phi + d \frac{\alpha_2}{\varepsilon} \Phi^2 \leq \mu_m.$$

Figures 66 and 67 show the regions b , $R_{\mu_m}^0$ and R_{μ_m} . It is obvious that in $R_{\mu_m}^0$, $\dot{v} \leq 0$ whereas in R_{μ_m} , \dot{v} can either be positive or negative. Let us define a region I where $v(q, \eta, \tilde{P}_s)$ has maximum value C , i.e. $v(q, \eta, \tilde{P}_s) = (1-d)V(q, \tilde{P}_s) + dW(\eta) \leq C$. If initially $(q(t=0), \eta(t=0), \tilde{P}_s(t=0)) \in I \cap R_{\mu_m}^0$ where $\dot{v} \leq 0$, subsequently as long as $(q(t), \eta(t), \tilde{P}_s(t))$ lies inside $R_{\mu_m}^0$, it either moves to a lower level such that $v \leq C_1 \leq C$ or remains at the same level. Therefore the full order system is stable in the sense of Lyapunov. However, if it converges to R_{μ_m} , where \dot{v} has unknown sign, two possible situations can arise. It is quite possible that \tilde{P}_s could grow such that $(q(t), \eta(t), \tilde{P}_s(t))$ is still in R_{μ_m} , however \tilde{P}_s leaves the domain b to infinity leading to instability due to parameter drift. It is also possible that once in R_{μ_m} , $(q(t), \eta(t), \tilde{P}_s(t))$ are such that they cross the boundary of region R_{μ_m} and reach the boundary of region $R_{\mu_m}^0$, where \dot{v} is negative semi definite. Once in $R_{\mu_m}^0$, v could move to a lower level, during the course of which $(q(t), \eta(t), \tilde{P}_s(t))$ could converge to R_{μ_m} . This process could occur many times leading to a phenomenon similar to limit cycles. This shows that tracking of time varying desired trajectories could be non robust in the sense that certain desired signals are not guaranteed to result in error free tracking.

If instead of a state feedback fast controller, an adaptive fast controller had been used to damp out the fast oscillations a parameter estimation error term \tilde{P}_f will appear in $\mu(t)$ affecting the stability.

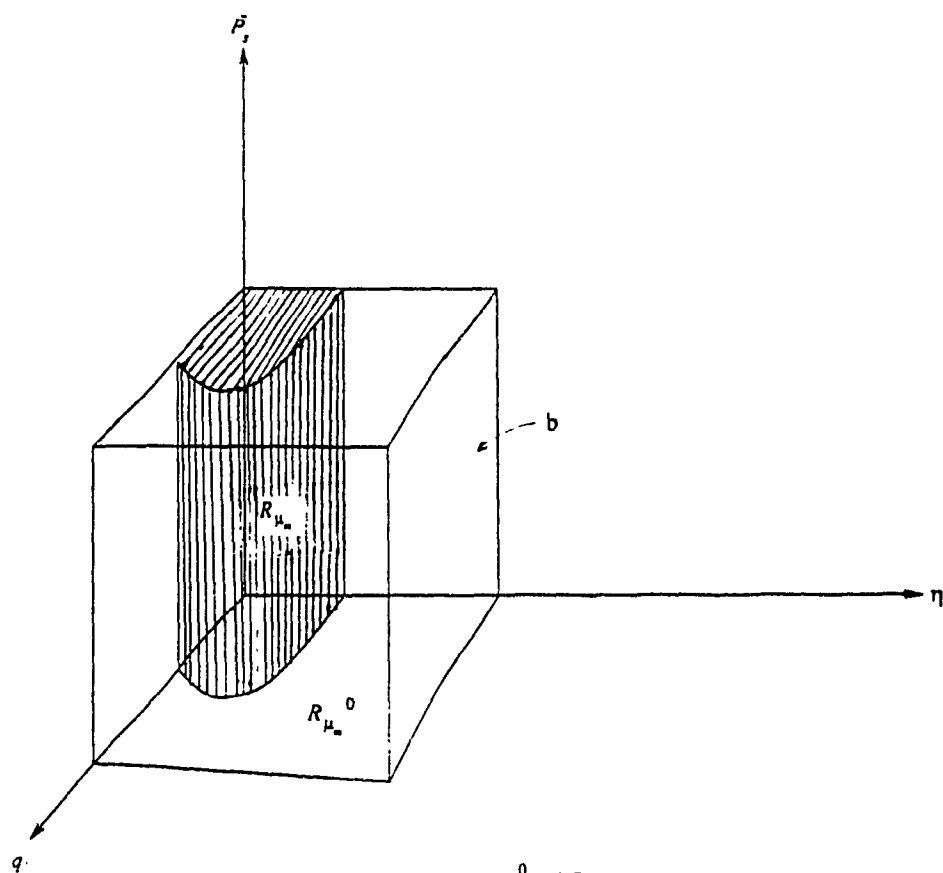


Figure 66. Region b , $R_{\mu_m}^0$ and R_{μ_m}

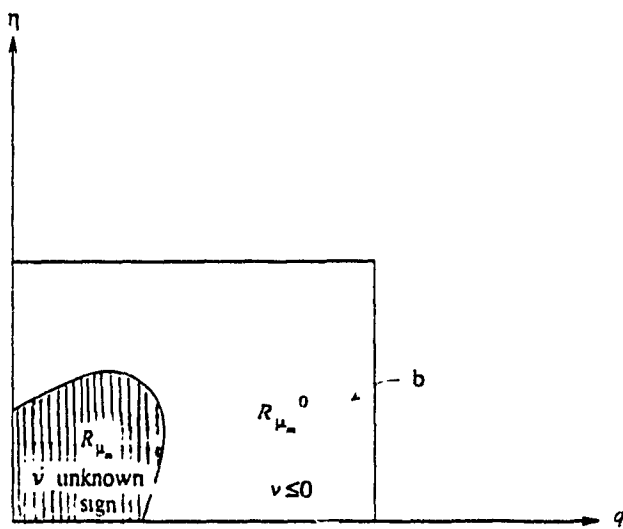


Figure 67. Cross section of figure 66 showing Region b , $R_{\mu_m}^0$ and R_{μ_m} .

Now let us consider the stability of the full order system, controlled by Craig, Hsu and Sastry's scheme.

6.b Craig, Hsu & Sastry's Scheme

Proceeding similarly, the stability of the full order system controlled by Craig et al's control law can also be proved. The Lyapunov function of the slow subsystem is given by (4.49). It can be rewritten as

$$V(H_{sc}) = \frac{1}{2} H_{sc}^T Q_{sc} H_{sc}$$

$$\text{where } H_{sc} = \begin{bmatrix} \tilde{P}_s \\ \underline{X} \end{bmatrix} \text{ and } Q_{sc} = \begin{bmatrix} \Gamma^{-1} & 0 \\ 0 & \rho \end{bmatrix}.$$

Hence

$$\nabla_{H_{sc}} V(H_{sc}) = \frac{1}{2} [Q_{sc}^T + Q_{sc}] H_{sc} \quad (6.30)$$

Equation (6.30) will be used later when evaluating the interconnection conditions.

The Lyapunov function candidate of the fast subsystem is unchanged from (6.4). The first interconnection condition involving the relationship between the slow part of the full order system and the reduced order slow subsystem is unchanged from (6.11). Combining (6.30) and (6.11) we obtain

$$[\nabla_{H_{sc}} V(H_{sc})]^T (f - f_r) = \frac{1}{2} [(Q_{sc}^T + Q_{sc}) H_{sc}]^T (f - f_r) \quad (6.31)$$

$$= \underline{X} \rho [(H_2 - H_1) \eta_1 + H_2 U^{*f}] \quad (6.32)$$

The second interconnection condition involving the relationship between the fast part of the full order system and the reduced order fast subsystem is unchanged from (6.17). However in Z_1^{*qss} the term U^{*f} is given by (4.44). Hence $Z_1^{*qss} = Z_1^{*qss}(\tilde{P}_s, q_d, \dot{q}_d, \ddot{q}_d, \dot{E}, \ddot{E})$ and therefore

$$\begin{aligned} \dot{Z}_1^{*qss} &= \frac{dZ_1^{*qss}}{dt} = \frac{\partial Z_1^{*qss}}{\partial \bar{P}_s} \dot{\bar{P}}_s + \frac{\partial Z_1^{*qss}}{\partial E} \dot{E} + \frac{\partial Z_1^{*qss}}{\partial \dot{E}} \ddot{E} + \\ &\quad \frac{\partial Z_1^{*qss}}{\partial q_d} \dot{q}_d + \frac{\partial Z_1^{*qss}}{\partial \dot{q}_d} \ddot{q}_d + \frac{\partial Z_1^{*qss}}{\partial \ddot{q}_d} \dddot{q}_d \end{aligned} \quad (6.33)$$

Letting

$$p(t) = \frac{\partial Z_1^{*qss}}{\partial q_d} \dot{q}_d + \frac{\partial Z_1^{*qss}}{\partial \dot{q}_d} \ddot{q}_d + \frac{\partial Z_1^{*qss}}{\partial \ddot{q}_d} \dddot{q}_d$$

as in (6.20), \dot{Z}_1^{*qss} reduces to

$$\dot{Z}_1^{*qss} = p(t) + \frac{\partial Z_1^{*qss}}{\partial \bar{P}_s} \dot{\bar{P}}_s + \frac{\partial Z_1^{*qss}}{\partial E} \dot{E} + \frac{\partial Z_1^{*qss}}{\partial \dot{E}} \ddot{E} \quad (6.34)$$

Substituting for \dot{E} , \ddot{E} and $\dot{\bar{P}}_s$ from (4.54) and (4.48) respectively, we get

$$\dot{Z}_1^{*qss} = p(t) + \left[-\Gamma Y^T \hat{M}_r^{-1} \frac{\partial Z_1^{*qss}}{\partial \bar{P}_s} + A \frac{\partial Z_1^{*qss}}{\partial \underline{X}} \right] \underline{X} + B \hat{M}_r^{-1} Y \bar{P}_s \frac{\partial Z_1^{*qss}}{\partial \underline{X}} \quad (6.35)$$

Let

$$\left| \left| p(t) \right| \right| \leq K_1(t) \quad (6.36)$$

and

$$\begin{aligned} &\left| \left| \left[-\Gamma Y^T \hat{M}_r^{-1} \underline{X} \frac{\partial Z_1^{*qss}}{\partial \bar{P}_s} + A \frac{\partial Z_1^{*qss}}{\partial \underline{X}} \right] \underline{X} + B \hat{M}_r^{-1} Y \bar{P}_s \frac{\partial Z_1^{*qss}}{\partial \underline{X}} \right| \right| \\ &\leq K_2(t) \underline{X} + K_4(t) \bar{P}_s \end{aligned} \quad (6.37)$$

From (6.17), (6.35), (6.36) and (6.37) it follows that

$$g - g_r = \begin{bmatrix} -\epsilon(K_1(t) + K_2(t)\underline{X} + K_4(t)\bar{P}_s) \\ 0 \end{bmatrix}. \quad (6.38)$$

Combining (6.6) and (6.38) we obtain

$$[\nabla_{\eta} W(\eta)]^T (g - g_r) = -2\eta R_f \epsilon \left[K_1(t) + K_2(t)\underline{X} + K_4(t)\bar{P}_s \right]. \quad (6.39)$$

We now make the following assumptions:

- 1) The Lyapunov function of the slow subsystem is such that

$$[\nabla_{H_{sc}} V(H_{sc})] f_r = -\underline{X}^T Q \underline{X} \leq -\alpha_1 \Psi^2(\underline{X}), \quad \alpha_1 > 0$$

where $\Psi(\underline{X})$ is a scalar-valued function of \underline{x} that vanishes at $\underline{x}=0$ and is non zero for all other \underline{x} in the domain of interest.

- 2) The Lyapunov function of the fast subsystem is such that

$$[\nabla_{\eta} W(\eta)] g_r = -\eta^T F \eta \leq -\alpha_2 \Phi^2(\eta), \quad \alpha_2 > 0$$

where $\Phi(\eta)$ is a scalar-valued function that vanishes at $\eta=0$ and is non zero for all other η in the domain of interest.

- 3) The following inequalities hold

$$a) [\nabla_{H_{sc}} V(H_{sc})]^T [f(q, \eta, \varepsilon) - f_r(q, \eta=0, \varepsilon=0)] = \underline{X} \rho(H_2 - H_1) \eta_1 \leq \beta_1 \Psi(\underline{X}) \Phi(\eta)$$

$$b) [\nabla_{\eta} W(\eta)]^T [g(q, \eta, \varepsilon) - g_r(\eta, \varepsilon)] = -2 \eta R_f \varepsilon [K_1(t) + K_2(t) \underline{X} + K_4(t) \tilde{P}_s]$$

$$\leq \varepsilon K_5 \Psi(x) \Phi(\eta) + \varepsilon \Phi(\eta) [K_1(t) + K_4(t) \tilde{P}_s]$$

where the constants β_1 , β_2 and K_5 are non negative.

With the above assumptions \dot{v} is reduced to

$$\begin{aligned} \dot{v} &= -(1-d)\alpha_1 \Psi^2 - \frac{d}{\varepsilon} \alpha_2 \Phi^2 + (1-d)\beta_1 \Psi \Phi + \frac{d}{\varepsilon} [\varepsilon K_5 \Psi \Phi + \varepsilon \Phi (K_1(t) + K_4(t) \tilde{P}_s)] \\ &= - \begin{bmatrix} \Psi(q) \\ \Phi(\eta) \end{bmatrix}^T T \begin{bmatrix} \Psi(q) \\ \Phi(\eta) \end{bmatrix} + \mu(t) \end{aligned}$$

where

$$T = \begin{bmatrix} (1-d)\alpha_1 & -(1-d)\frac{\beta_1}{2} - \frac{dK_5}{2} \\ -(1-d)\frac{\beta_1}{2} - \frac{dK_5}{2} & \frac{\alpha_2}{\varepsilon} \end{bmatrix}, \quad \mu(t) = d \Phi [K_1(t) + K_4(t) \tilde{P}_s]$$

For $d < 1$, and an upper bound for ϵ_{pd} such that $\epsilon_{pd} > \epsilon$, T is positive definite where

$$\epsilon_{pd}(d) = \frac{\alpha_1 \alpha_2}{\frac{[\beta_1(1-d) + dK_5]^2}{4d(1-d)}}$$

Since both Craig et al's scheme and Slotine and Li's scheme make use of similar Lyapunov functions, both the methods result in similar T and $\mu(t)$ with the constants K_1 , taking different values. Hence following in identical fashion as in the case of Slotine and Li, the regions R_{μ_n} and $R_{\mu_n}^0$ could be defined and stability analyzed.

The error in tracking is a measure of the distance from the origin to the farthest point on the boundary of R_{μ_n} and $R_{\mu_n}^0$. Hence the stability to a certain extent is associated with the size of region R_{μ_n} where \dot{v} has unknown sign. Numerical simulations suggest that the region R_{μ_n} in the case of the full order system being controlled by Craig et al's scheme is smaller in size than that obtained with Slotine and Li's algorithm.

Chapter 7

Conclusions and Directions for Future Work

7.a Conclusions

This thesis deals with the problem of controlling flexible joint robot manipulators. The main contribution of the research described in this thesis have been to provide a reliable technique to maintain closed loop stability and achieve tracking of a desired trajectory in the presence of unmodeled dynamics and parameter variations.

The concept of a singular perturbation has been utilized to construct control schemes for flexible manipulators. The control scheme takes the form of a composite controller, consisting of a fast control designed to damp the fast elastic oscillations and the rigid control designed by neglecting the elasticity. Once the fast elastic oscillations have been cancelled by the fast controller, the resulting slow part of the system is close to the dynamics of the rigid robot, which can be controlled by any technique.

Comparisons between linear/ nonlinear, adaptive/ nonadaptive control schemes were made. Simulations were carried out in the case of a single link and two link flexible joint manipulators. The gains of the adaptive controller have to be tuned in order to achieve error free tracking and stability.

Initially the fast controller was designed using adaptive control as the slow controller. Simulations carried out in the case of a single link flexible joint manipulator suggest that a composite controller employing a simple feedback fast controller is less susceptible to changes in the perturbation parameter than a composite controller with an adaptive fast controller. Hence, for the two link flexible joint robot manipulator, a feedback fast controller was used to damp out the fast oscillations. In order to make the damping more efficient, both position and velocity feedback were utilized.

The simulations suggest that the nonlinear control schemes performed better than the linear control schemes. This can be explained by the fact that the nonlinear control methods achieves global linearization whereas the linear control methods achieve local linearization. Among the nonlinear control schemes Craig et al's algorithm was found to be more robust to changes in the perturbation parameter than that of Slotine and Li.

In chapter 6, sufficient conditions for the stability of flexible joint robot manipulators controlled by composite adaptive controller have been given. In analyzing the stability of the full order system, we define two regions, viz. $R_{\mu_m}^0$ and R_{μ_m} . In $R_{\mu_m}^0$, $\dot{v} \leq 0$ whereas in R_{μ_m} , \dot{v} has unknown sign. If the values of q , η and \tilde{P}_s are such that $(q(t), \eta(t), \tilde{P}_s(t))$ lies inside $R_{\mu_m}^0$ where \dot{v} is negative semi definite, the full order system is stable in the sense of Lyapunov. However, if it converges to R_{μ_m} where \dot{v} has unknown sign, it is quite possible that \tilde{P}_s could grow such that $(q(t), \eta(t), \tilde{P}_s(t))$ is still in R_{μ_m} , and \tilde{P}_s leaves the domain b to infinity leading to instability due to parameter drift. It is also possible that $(q(t), \eta(t), \tilde{P}_s(t))$ are such, they cross the boundary of regions R_{μ_m} and $R_{\mu_m}^0$, a process that could occur several times giving rise to a phenomenon similar to limit cycles. Thus the tracking of time varying desired trajectories could be non robust.

7.b Suggestions for Future Work

The ideas in this thesis can be extended in the following directions:

- (1) The composite controller can be implemented on a practical robot.
- (2) Craig et al's scheme requires the measurement of joint acceleration. The acceleration could be estimated from the velocity information already available. This is bound to add noise to the system. Hence the scheme has to be made robust to noise

and external disturbances.

- (3) Stability analysis could be extended to prove why the control scheme of Craig et al is more robust to changes in the perturbation parameter than that of Slotine and Li.
- (4) It could be investigated under what conditions a feedback fast controller is more effective in damping out the fast oscillations than an adaptive fast controller.

REFERENCES

- [1] J. J. E. Slotine and W. Li, "Adaptive Manipulator control : A case study", IEEE transactions on Automatic control, vol- AC 33, No 11, pp. 995-1003 Nov. 1988
- [2] J. J. E. Slotine and W. Li, "On the adaptive control of Robot Manipulators", The International Journal of Robotics Research, vol. 6, No 3, pp. 49-59, Fall 1987.
- [3] J. J. Craig, "Introduction to Robotics - Mechanics & control", Addison - Wesley Publishing Company, 1989.
- [4] J. J. Craig, P. Hsu and S. S. Sastry, "Adaptive control of Mechanical Manipulators", The International Journal of Robotics Research, vol. 6, No 2, pp. 16-28, Summer 1987.
- [5] M. W. Spong and M. Vidyasagar, "Robot Dynamics & Control", John Wiley & sons, 1989.
- [6] M. W. Spong, K. Khorasani and P. V. Kokotovic, "A slow manifold approach to the feedback control of flexible robots", IEEE Journal of Robotics & Automation, vol. RA-3, No 4, pp. 291-302, August 1987.
- [7] F. Ghorbel, J. Y. Hung and M. W. Spong, " Adaptive control of Flexible Joint Manipulators", IEEE control systems Magazine, pp. 9-13, December 1989
- [8] K. Khorasani, "Adaptive Control of Flexible Joint Robots", Proceedings of 1991 IEEE International Conference on Robotics and Automation, California, April 1991.
- [9] M. W. Spong , " Modeling and Control of Elastic Joint Robots", Transactions of ASME, Journal of Dynamic Systems, Measurement and Control, vol 109, pp. 310-319, December 1987.
- [10] R. Ortega and M. W. Spong, "Adaptive Motion Control of Rigid Robots: A

Tutorial", Proceedings of the 27th Conference on Decision and Control, Austin, Texas, December 88.

- [11] A. Saberi and H. Khalil, " Quadratic -type Lyapunov functions for Singularly Perturbed Systems", IEEE Transactions on Automatic Control, vol. AC 29, No 6, pp. 542-550, June 1984.
- [12] K. Khorasani and M. A. Pai, " Asymptotic Stability of Nonlinear Singularly Perturbed Systems using Higher Order Corrections", Automatica, vol. 21. No 6, pp. 717-727, 1985.
- [13] G. Cesareoa and R. Marino, "On the Controllability properties of Elastic Robots", Sixth Int. Conf. on Analysis and Optimization of systems, INRIA, Nice 84.
- [14] L. M. Sweet and M. C. Good, " Redefinition of the Robot Motion Control Problem: Effects of Plant Dynamics, Drive System Constraints, and user Requirements" , Proceedings of the 23rd IEEE Conference on Decision and Control, Las Vegas, November 1984.
- [15] H. Seraji, " Linear Multivariable control of Robot Manipulators" , Proceedings of IEEE International Conference on Robotics and Automation, San Francisco, pp. 565-571, 1986.
- [16] H. Seraji, " A new approach to Adaptive control of manipulator. ", Transactions of the ASME, Journal of Dynamic Systems, Measurement and Control, vol. 109, pp. 193-202, September 1987.
- [17] P. A. Ioannou and P. V. Kokotovic, " Adaptive Systems with Reduced models", Springer- Verlag, 1983.
- [18] K. S. Narendra and A. M. Annaswamy, " Stable Adaptive Systems", Prentice Hall, 1989.

- [19] R. E. O' Malley, " Introduction to Singular Perturbations", Academic Press, 1974.
- [20] P. M. Taylor, "Robotic Control", Macmillan Education, 1990.
- [21] F. Ghorbel and M. W. Spong, "Stability Analysis of Adaptively Controlled Flexible Joint Manipulators", Univ. of Illinois at Urbana- Champaign technical report, 1990.
- [22] P. V. Kokotovic and H. K. Khalil (Ed.), " Singular Perturbation in Systems and Control", IEEE Press, 1986.
- [23] J. J. Craig, " Adaptive control of Mechanical Manipulators", Addison-Wesley, 1988.
- [24] R. Marino and P. V. Kokotovic, "A Geometric Approach to Non Linear Singularly Perturbed Control Schemes", Automatica, vol. 24, No. 1, pp. 31-41, 1988.
- [25] M. W. Spong and R. Ortega, "On Adaptive Inverse Dynamic Control of Rigid Robots", IEEE Transactions on Automatic Control, vol. 35, No 1, January 1990.
- [26] K. Khorasani and P. V. Kokotovic, "A Corrective Feedback Design for Nonlinear Systems with Fast Actuators", IEEE Transactions on Automatic Control, vol. 31, No 1, January 1986.
- [27] K. Khorasani, "Nonlinear Feedback Control of Flexible Joint Manipulators: A Single Link Case Study", IEEE Transactions on Automatic Control, vol. 35, No 10, October 1990.
- [28] M. W. Spong, R. Ortega and R. Kelly, "Comments on Adaptive Manipulator Control: A Case Study", IEEE Transactions on Automatic Control, vol. 35, No 6, June 1990.
- [29] C. Abdallah, D. Dawson, P. Dorato and M. Jamshidi, "Survey of Robust Control for Rigid Robots", IEEE control systems Magazine, pp. 24-30, February 1991.
- [30] K. J. Astrom and B. Wittenmark, "Adaptive Control", Addison-Wesley Publishing Company, 1989.